

Characterizing the Role of Magnetic Cues Underlying Spatial Behavior

Michael Scott Painter

Dissertation submitted to the faculty of the Virginia Polytechnic Institute and State University in partial fulfillment of the requirements for the degree of

Doctor of Philosophy

In

Biological Sciences

John B. Phillips

Chris R. Anderson

Richard D. Fell

Brent D. Opell

Kendra B. Sewall

December 13, 2016
Blacksburg, Virginia

Keywords: Magnetoreception, Compass, Orientation, Navigation, Magnetic Field, Sensory Ecology, Radical Pair, Magnetite, *Drosophila*, *Vulpes vulpes*, Mammal, Rodent

Characterizing the Role of Magnetic Cues Underlying Spatial Behavior

Michael Scott Painter

ABSTRACT

In the 50+ years since the discovery of magnetic compass orientation by migratory songbirds, evidence for the use of magnetic cues has been obtained for a range of taxonomic groups, including several classes of vertebrate and invertebrate taxa. Surprisingly, however, the biophysical mechanisms and biological substrate that underlie magnetic sensing are still not fully understood. Moreover, while use of magnetic cues for compass orientation is intuitive, the functional significance of other forms of behavioral responses mediated by magnetic cues, such as spontaneous magnetic alignment, is less clear. The following research was carried out to investigate the mechanisms underlying magnetic orientation in vertebrates and invertebrates. This involved the modification of existing experimental systems to characterize responses to magnetic cues in laboratory animals (flies, mice) and the development of novel techniques for studying the role of magnetic cues in the spatial behavior of free-living animals (red foxes). Chapter II examines magnetic orientation in wild-type *Drosophila melanogaster* larvae. We show that three strains of larvae reared under non-directional ultraviolet (UV) light exhibit quadramodal spontaneous orientation along the anti-cardinal compass directions (i.e. northeast, southeast, southwest, northwest) when tested in a radially symmetrical environment under UV light. Double-blind experiments cancelling the horizontal component of the magnetic field confirmed that the response is dependent on magnetic cues rather than non-magnetic features of the test environment. Furthermore, we argue that the larval quadramodal pattern of response is consistent with properties of magnetic compass orientation observed in previous studies of adult *Drosophila* and laboratory mice, both of which have been proposed to be mediated by a light-dependent magnetic compass mechanism. Chapter III explores the use of novel biologging techniques to collect behavioral and spatial data from free-roaming mammals. Specifically, a previous observational study of free-roaming red foxes found a 4-fold increase in the success of

predatory ‘mousing’ attacks when foxes were facing ~north-northeast, consistent with magnetic alignment responses reported for a range of terrestrial animals. The authors propose that the magnetic field may be used to increase accuracy of mousing attacks. Using tri-axial accelerometer and magnetometer bio-loggers fitted to semi-domesticated red foxes, we created ‘magnetic ethograms’ from behavioral and magnetic machine learning algorithms ‘trained’ to identify three discrete behaviors (i.e. foraging, trotting, and mousing-like jumps) from raw accelerometer signatures and to classify the magnetic headings of mousing-like jumps into 45° sectors from raw magnetometer data. The classifier’s ability to accurately identify behaviors from a separate fox not used to train the algorithm suggests that these techniques can be used in future experiments to obtain reliable magnetic ethograms for free-roaming foxes. We also developed the first radio-frequency emitting collar that broadcasts in the low MHz frequency range shown to disrupt magnetic compass responses in a host of animals. The radio-frequency collars coupled with biologgers will provide a powerful tool to characterize magnetic alignment responses in predatory red foxes and can be adapted for use in studies of magnetic alignment and magnetic compass orientation in other free-roaming mammals. Chapter 3 discusses findings from a magnetic nest building assay involving male laboratory mice. Mice trained to position nests in one of four directions relative to the magnetic field exhibited both learned magnetic compass responses and fixed magnetic nest positioning orientation consistent with northeast-southwest spontaneous magnetic alignment behavior previously reported for wild mice and bank voles. This is the first mammalian assay in which both learned magnetic compass orientation and spontaneous magnetic alignment were exhibited in the same species, and suggests that the use of magnetic cues in rodents may be more flexible than previously realized.

Characterizing the Role of Magnetic Cues Underlying Spatial Behavior

Michael Scott Painter

GENERAL AUDIENCE ABSTRACT

A variety of animals have been shown to use the Earth's magnetic field to help guide diverse spatial behaviors, however, the underlying sensory mechanisms mediating this sense remain elusive. Evidence for two distinct sensory mechanisms has come from behavioral studies involving a wide range of organisms, including migratory birds, newts, mole rats, mice, and several classes of invertebrates. The following research was carried out to determine the underlying sensory mechanisms mediating magnetic sensing in larval fruit flies. Properties consistent with a light-dependent, photoreceptor-based mechanism were found to underlie innate magnetic alignment behavior in larval flies, similar to the proposed compass mechanism thought to mediate compass responses in migratory birds and newts. A reanalysis of two previous studies of learned magnetic compass responses in adult fruit flies and laboratory mice show similar behaviors when compared to that of larval flies, suggesting a common underlying light-dependent magnetic mechanism across these groups. Furthermore, we provide evidence for learned magnetic compass responses in laboratory mice, where the orientation of individuals appears to be dependent on properties of the local environment (e.g. electromagnetic, temperature, humidity) in training and testing. These data suggest that the use of magnetic cues in mammals is context-dependent and more flexible than previously recognized. We have also developed new technologies for studies of magnetic orientation in free-roaming animals. Specifically, bio-logging devices containing tri-axial accelerometer and magnetometer sensors were used to create 'magnetic ethograms', where the behavior and magnetic alignment of an animal can be reliably and accurately extracted from raw sensor data. We also discuss possible field experiments that can be performed to provide a specific test of the underlying sensory mechanism mediating magnetic behavior in free-roaming animals. This work will likely be of interest to a broad range of disciplines including sensory ecology, ethology, quantum chemistry, biophysics, wildlife management, and conservation.

Dedication

This work is dedicated to the family, friends, collaborators, students, flies, foxes, mice, and trout that have helped me grow and learn, resulting in the following dissertation.

Table of Contents

Abstract.....	ii
General Audience Abstract.....	iv
Dedication.....	v
Table of Contents.....	vi
List of Figures.....	x
List of Tables and Supplemental Material.....	xiii
Attributions.....	xv
Chapter I. Introduction to Magnetoreception.....	1
Figures.....	28
Literature Cited.....	42
Chapter II. Spontaneous magnetic orientation in larval <i>Drosophila</i> shares properties with learned magnetic compass responses in adult flies and mice.....	50
Abstract.....	50
Introduction.....	50
Materials and Methods.....	54
Stocks.....	54
Rearing Vials.....	54
Rearing and Testing Enclosure.....	55
Rearing.....	55
Testing.....	56
Double-Blind Horizontal Cancelled Field Experiment.....	58
Reanalysis of Adult <i>Drosophila</i> Data.....	59

Training.....	59
Testing.....	59
Reanalysis of C57BL/6 Trained Magnetic Compass Response.....	60
Training.....	60
Testing.....	60
Results.....	61
Discussion.....	62
Acknowledgments.....	69
Tables.....	70
Figures.....	74
Supplemental Materials.....	79
Literature Cited.....	81
Chapter III. Use of bio-loggers to characterize red fox behavior with implications for studies of magnetic alignment responses in free-roaming animals.....	84
Abstract.....	84
Background.....	85
Methods.....	90
Bio-logging Recording Specifications.....	91
Behavioral Recording Sessions.....	91
Statistical Analysis.....	94
Accelerometer Data Analysis.....	94
Accelerometer Feature Extraction.....	95
Behavioral Classification.....	95
Magnetometer Data Analysis.....	96

Magnetometer Classifier Training.....	99
Results.....	100
Behavioral Classification.....	100
Generalizability of the Classifier to New Foxes.....	101
Magnetometer Data.....	102
Classification Results.....	102
Discussion.....	103
Conclusions.....	114
Acknowledgments.....	116
Tables.....	117
Figures.....	119
Supplemental Materials.....	124
Literature Cited.....	125
 Chaper IV. Evidence for Plasticity in Nest Building Responses Mediated by Magnetic Cues in Epigeic Mice.....	 129
Abstract.....	130
Introduction.....	130
Methods.....	132
Training.....	132
Testing.....	134
Series 1.....	136
Series 2.....	137
Series 3.....	138

Series 4.....	139
Results.....	139
Series 1.....	139
Series 2.....	140
Series 3.....	140
Series 4.....	141
Discussion.....	141
Tables.....	147
Figures.....	148
Literature Cited.....	150
Chapter V. Conclusions.....	152
Literature Cited.....	160

List of Figures

Chapter I.

Figure 1: Schematic of magnetic vectors generated by Earth's geomagnetic field.....	28
Figure 2: Illustration of magnetite-based transduction mechanism.....	29
Figure 3: Anisotropic magnetic field effects on radical pair system.....	30
Figure 4: Schematic of vertical and horizontal components of Earth's magnetic field vectors.....	31
Figure 5: Magnetic orientation of a) mole rats and b) European robins.....	32
Figure 6: Effect of pulse re-magnetization on magnetic orientation in mole rats.....	33
Figure 7: Quadramodal magnetic orientation in insects.....	33
Figure 8: Plasticity of avian magnetic compass responses to magnetic field strength in European robins.....	34
Figure 9: Wavelength dependent shift in learned magnetic compass responses of adult <i>Drosophila</i>	35
Figure 10: Interconversion of the light-dependent redox states within the flavin chromophore of Cryptochrome	36
Figure 11: Evidence for antagonistic light-dependent magnetic compass mechanism in Eastern red-spotted newts.....	37
Figure 12: Absorption changes in (a <i>Drosophila</i> (DmCry1) and zebrafish (b (ZfCRY-DASH) cryptochromes produced by blue light exposure.....	37
Figure 13: Proposed 3-D patterns of response created by a light-dependent radical pair mechanism: a) simplified model based on reduced number of hyperfine interactions, b) tryptophan-flavin radical pair model.....	39
Figure 14: Learned shoreward magnetic compass orientation in red-spotted newts when tested under a, b) full- and short-wavelength light and c) long-wavelength light.....	40

Chapter II.

Figure 1: Spontaneous orientation of 2 nd instar <i>Drosophila melanogaster</i> larvae.....	74
--------------------------------------------------------------------------------------------------------	----

Figure 2: Pooled distribution of directional responses from all three strains of <i>Drosophila melanogaster</i> larvae.....	75
Figure 3: Distributions of directional responses from 2 nd instar Canton-S <i>Drosophila melanogaster</i> larvae tested with the ambient horizontal component in (A all four magnetic field alignments and (B with the horizontal components cancelled.....	76
Figure 4: Magnetic compass response of adult <i>Drosophila melanogaster</i> depends on whether flies were trained along the magnetic north-south (A) or east-west (B) axis.....	77
Figure 5: Learned magnetic compass response of adult male C57BL/6 mice trained along the A) ~north-south or B) ~east-west magnetic axis.....	78
 Chapter III.	
Figure 1: Photos of the two adult red foxes (A, B) used to develop magnetic ethograms equipped with tri-axial accelerometer and magnetometer bio-logging devices.....	119
Figure 2: Types of obstacles used to collect accelerometer (behavioral) and magnetometer (compass) data. A) Square, B) vertical wall, and C) four-corridor obstacles used to collect accelerometer (behavioral) and magnetometer (compass) data. D) Schematic of four-corridor obstacle.....	120
Figure 3: Acceleration signatures on each of the three axes (x, y, and z) for stereotypical leaping (A), foraging (B), and trotting (C) behaviors in Fox1.....	121
Figure 4: A) Scatter-plot of data collected from Fox1 in the three-dimensional space given by the first three principal component projections. B-D) Two-dimensional projections onto all possible pairs of the first three principle components.....	122
Figure 5: Radial circular plots showing magnetic classifier prediction relative to ground-truth classification made by a human observer A) when treating each <i>sample</i> as an independent data point and B) when treating each <i>event</i> as an independent data point.....	123
 Chapter IV.	
Figure 1: Series 1 distribution of A) topographic, B) magnetic, and C) relative to trained bearings from C57BL/6 mice.....	148
Figure 2: Series 2 distribution of A) topographic, B) magnetic, and C) relative to trained bearings from C57BL/6 mice.....	148

Figure 3: Series 3 distribution of A) topographic, B) magnetic, and C) relative to trained bearings from C57BL/6 mice.....149

Figure 4: Series 4 distribution of A) topographic, B) magnetic, and C) relative to trained bearings from C57BL/6 mice.....149

List of Tables and Supplemental Material

Chapter II.

Table 1: Spontaneous alignment responses of Berlin, Canton-S, and Oregon-R X Canton-S strains of *Drosophila melanogaster* 2nd instar larvae.....70

Table 2: Table 2. Spontaneous alignment responses of 2nd instar *Drosophila melanogaster* tested in an earth-strength magnetic field, or with the magnetic field cancelled.....72

Figure S1: Spontaneous orientation of 2nd instar *Drosophila melanogaster* larvae relative to the alignment of magnetic north.....79

Figure S2: Pooled distributions of bearings from three stains of 2nd instar *Drosophila melanogaster* larvae plotted relative to A) topographic and B) magnetic north.....80

Chapter III.

Table 1: Confusion matrix showing 10-fold cross-validation performance of the 5-nearest neighbor classification algorithm run on Fox1117

Table 2: Confusion matrix showing performance of the 5-nearest neighbor classification algorithm trained on data from Fox1 and tested on data from Fox2.....117

Table 3: Summary of the data set used to train the random forest classifier.....117

Table 4: Confusion matrix for the random forest classifier treating each *sample* as an observation.....118

Table 5: Confusion matrix for the random forest classifier treating each *event* as an observation.....118

Supplemental Table 1: Number of trotting, foraging, and mousing-like leaps recorded from three different device orientations on Fox1.....124

Supplemental File 1: Example of Fox2 exhibiting a ‘mousing-like’ leap out of the 10x10x1m arena.....124

Supplemental File 2: Example of Fox2 exhibiting a ‘mousing-like’ leap out of the 10x10x1m arena.....124

Supplemental File 3: Example of Fox1 trained to jump over a barrier and immediately come to a stop preventing a collision with a second, smaller barrier.....	124
Supplemental File 4: Example of Fox1 trained to approach a ~1m tall barrier by walking down one of four corridors.....	124
Supplemental File 5: Example of Fox1 exhibiting ‘mousing-like’ behavior using the 4-corridor arena.....	124
Supplemental File 6: Example of Fox1 exhibiting behavior defined as ‘trotting’ for the behavioral analysis.....	124
Supplemental File 7: Example of Fox1 exhibiting behaviors defined as ‘foraging’ for the behavioral analysis.....	124
Chapter IV.	
Table 1: Nest building orientation in male C57BL6J male mice.....	147
Table 2: Summary of training and testing conditions.....	147

Attribution

David H. Dommer, Assistant Vice President, Academic Affairs, University of Mount Olive, Mount Olive, North Carolina. David was a collaborator on Chapter II and is a co-author on the manuscript resulting from this research.

William W. Altizer, Undergraduate Research Student, Biological Sciences, Virginia Tech, Blacksburg, VA. Will participated in data collection for Chapter II and is a co-author on the manuscript resulting from this research.

Rachel Muheim, Associate Professor, Faculty of Science, Lund University, Lund, Sweden. Rachel was a collaborator on Chapters II and IV and is a co-author on the manuscripts resulting from this research.

John B. Phillips, Professor, Biological Sciences, Virginia Tech, Blacksburg, VA. John served as my Committee Chair and was a collaborator on all chapters of my dissertation, and therefore, is a co-author on all resulting manuscripts.

Justin A. Blanco, Assistant Professor, Department of Electrical and Computer Engineering, United States Naval Academy, Annapolis, Maryland, United States of America. Justin was a collaborator on Chapter III and was responsible for statistical analysis of accelerometer and magnetometer data. Therefore, Justin is a joint first author on the resulting manuscript.

Pascal Malkemper, Researcher, Department of General Zoology, Faculty of Biology, University of Duisburg-Essen, 45117 Essen, Germany, Pascal assisted in the conceptual framework and experimental design for Chapter III and the conceptual framework for Chapter IV. Therefore, Pascal is a co-author on resulting manuscript from Chapter III and will be a co-author of any published work from Chapter IV.

Chris R. Anderson, Associate Professor, Department of Electrical and Computer Engineering, United States Naval Academy, Annapolis, Maryland, United States of America. Chris served as a Committee Member and assisted was responsible for the development of the radio-frequency collar discussed in Chapter III and the conceptual framework for this research. Chris is a co-author on the manuscript resulting from Chapter III.

Daniel C. Sweeney, PhD Candidate, Department of Biomedical Engineering and Mechanics, Virginia Tech, Blacksburg, Virginia, United States of America. Daniel assisted with the statistical analysis and conceptual framework for Chapter III and is a co-author of the manuscript resulting from this research.

Charles W. Hewgley, Assistant Professor, PMP, Department of Electrical and Computer Engineering, United States Naval Academy, Annapolis, Maryland, United States of America. Charles assisted with the experimental design and statistical analysis for Chapter III and is a co-author on the manuscript published from this research.

Jaroslav Červený, Professor, Department of Game Management and Wildlife Biology, Faculty of Forestry and Wood Sciences, Czech University of Life Sciences, 16521 Praha 6, Czech Republic. Jaroslav assisted with the conceptual framework and experimental design in Chapter III and is a co-author on the manuscript published from this research.

Vlastimil Hart, Professor and Department Head, Department of Game Management and Wildlife Biology, Faculty of Forestry and Wood Sciences, Czech University of Life Sciences, 16521 Praha 6, Czech Republic. Vlasta assisted with the conceptual framework and experimental design in Chapter III and is a co-author on the manuscript published from this research.

Václav Topinka, Researcher, Department of Game Management and Wildlife Biology, Faculty of Forestry and Wood Sciences, Czech University of Life Sciences, 16521 Praha 6, Czech Republic. Václav assisted with the conceptual framework and experimental design in Chapter III and is a co-author on the manuscript published from this research.

Elisa Belotti, PhD Candidate, Department of Game Management and Wildlife Biology, Faculty of Forestry and Wood Sciences, Czech University of Life Sciences, 16521 Praha 6, Czech Republic. Elsia assisted with the conceptual framework and experimental design in Chapter III and is a co-author on the manuscript published from this research.

Hynek Burda, Professor, Department of Game Management and Wildlife Biology, Faculty of Forestry and Wood Sciences, Czech University of Life Sciences, 16521 Praha 6, Czech Republic. Hynek assisted with the conceptual framework and experimental design in Chapter III and is a co-author on the manuscript published from this research.

Madison Davis, Undergraduate Research Student, School of Education, Virginia Tech, Blacksburg, Virginia, Unites States of America. Madison assisted with data collection, analysis and experimental design for Chapter IV and will be co-author on any publications resulting from this research.

Shruthi Ganesh, Undergraduate Research Student, Virginia-Maryland College of Veterinary Medicine, Blacksburg, Virginia, Unites States of America. Shruthi assisted with data collection, analysis and experimental design for Chapter IV and will be co-author on any publications resulting from this research.

Ella Rak, Undergraduate Research Student, Department of Dairy Sciences, Virginia Tech, Blacksburg, Virginia, United States of America. Ella assisted with data collection, analysis and experimental design for Chapter IV and will be co-author on any publications resulting from this research.

Kelsie Brumet, Undergraduate Research Student, Department of Biological Sciences, Virginia Tech, Blacksburg, Virginia, United States of America. Kelsie assisted with data collection, analysis and experimental design for Chapter IV and will be co-author on any publications resulting from this research.

Hunter Bayne, Undergraduate Research Student, Department of Biological Sciences, Virginia Tech, Blacksburg, Virginia, United States of America. Hunter assisted with data collection, analysis and experimental design for Chapter IV and will be co-author on any publications resulting from this research.

Chapter I. Introduction to Magnetoreception

The use of geomagnetic field cues to help guide spatial behavior has been demonstrated in all major classes of vertebrates (fish, amphibians, reptiles, birds and mammals) [1-9], and several classes of invertebrates (insects, crustaceans, and mollusks) [10-18]. To date, behavioral studies provide evidence for the involvement of magnetic cues in spatial tasks that include magnetic compass orientation, spontaneous magnetic alignment (SMA), and deriving geographic position, i.e., a ‘magnetic map’ [4, 9, 19-24]. Although magnetic orientation has been demonstrated across a diverse range of taxonomic groups, the physiological and biophysical basis of this behavior is not fully understood. Findings from neurophysiological and behavioral studies designed to further characterize the functional properties of the magnetic sense have been the impetus for several theoretical models attempting to explain the mechanism(s) mediating magnetoreception in terrestrial animals. After providing a brief description of the general properties of the geomagnetic field, the mechanism(s) thought to underlie spatial responses influenced by magnetic field cues in terrestrial vertebrates are reviewed below.

The Earth produces a dipole magnetic field, whose poles are located close to its rotational poles; the angle between these points is referred to as magnetic declination. Magnetic field intensity varies in a more or less predictable fashion from approximately 60,000 nT at the magnetic poles to 26,000 nT at the magnetic equator [25]. Similar to intensity, the inclination or ‘dip-angle’ is maximum at the poles (inclination = 90° , i.e. perpendicular to the horizontal plain), and decreases as it approaches the equator where the inclination reaches 0° (Figure 1). Spatial anomalies caused by iron-containing mineral deposits in the Earth’s crust as well as temporal anomalies caused by showers of charged particles emitted by sun flares, commonly known as “magnetic storms”, produce additional

variation in both the intensity and direction (i.e., declination and/or inclination) of the geomagnetic field [4].

Despite spatial and temporal anomalies which typically vary less than 1% in intensity and less than 1% in both inclination and declination, the magnetic field provides an omnipresent and reliable source of spatial information that can be used for orientation and navigational tasks regardless of the time of day, season of the year, or weather conditions. For example, magnetic compass orientation in migratory birds is unaffected by small changes (e.g. < 20%) in magnetic intensity and the magnetic compass would be expected to operate over the entire migratory range where the variation in magnetic inclination and intensity is greater than the typical variation of spatial and temporal magnetic anomalies [26]. Research involving organisms from a range of disparate taxa have provided evidence for two different magnetoreception in terrestrial animals; a magnetite-based mechanism (MBM) [5, 27-29], and a light-dependent mechanism (LDM) [15, 16, 26, 30-32]. These two magnetoreception mechanisms differ in their biophysical and physiological properties, and are not necessarily mutually exclusive. Indeed, evidence consistent with the involvement of two types of mechanisms possessing different biophysical characteristics (i.e., dual mechanisms) has been reported in the same species [33, 34]. However, it is unlikely that natural selection would have maintained two separate biophysical sensory mechanisms only to provide redundant spatial information (i.e., magnetic compass information), but rather that species possessing dual mechanisms take advantage of the different biophysical properties of each mechanism to extract different types of spatial information from the magnetic field. For example, in amphibians and birds a LDM appears to be used to provide directional ('compass') information, while a MBM appears to be used to detect spatial variation in the magnetic field (e.g., magnetic intensity and/or inclination) to provide magnetic 'map' information used during navigation [35, 36].

Magnetite-based magnetic mechanism

The MBM is thought to involve magnetically sensitive crystals that, within a certain size range, exhibit a stable magnetic moment analogous to the needle of a navigator's compass that aligns with respect to the geomagnetic field and can be used to distinguish magnetic North from South. Two compounds synthesized in biological systems have been proposed to provide the biological substrate (i.e. the 'compass needle') underlying the MBM, biogenic magnetite (Fe_3O_4) and greigite (Fe_3S_4), both of which form stable magnetic moments (i.e., would experience torque when exposed to an external applied magnetic field) [37]. Furthermore, these crystals may exist in one of two size classes, single domain or superparamagnetic. Single-domain (SD) particles are large enough to retain an intrinsic magnetic moment that is fixed with respect to the crystalline structure, analogous to a compass needle fixed inside a sensory cell. In the case of SD particles, the geomagnetic field will exert a torque on the crystalline structure itself, or on the entire structure (e.g. sensory hair) housing these particles, causing a physical re-alignment relative to the external field. This torque induced stress could then be coupled to a transduction pathway that opens or closes membrane channels altering the electrical potential of the cell (Figure 2). Superparamagnetic particles (SPM) are smaller in size, and unlike SD particles, lack a permanent magnetic moment. And therefore, SPM particles do not rotate to align with respect to an external magnetic field. Instead, the particle's magnetic moment tracks an external magnetic field. A different type of transduction mechanism must be coupled to superparamagnetic particles, as individual SPM crystals cannot exert mechanical forces within in the cell causing membrane depolarization like their SD counterparts. Regardless of the crystalline structure involved, a consistent property of all MBM-based responses characterized to date is that they make use of the polarity of the magnetic field, and therefore discriminate magnetic North from magnetic South [27, 38] analogous to a

human navigator's compass. Although theoretical modeling and behavioral evidence from some animals are consistent with a MBM providing only polarity- based compass information, a MBM may also play a role in detecting slight variation in magnetic intensity and/or inclination used to derive one coordinate of a magnetic map for long- distance navigation and homing [5, 19, 21, 27]. This will be discussed in more detail below. Both behavioral evidence and physiological recordings suggest that magnetite-based receptors are most likely associated with the trigeminal nerve in vertebrates [39-44].

Light-dependent magnetic compass

The light-dependent magnetic compass (LDMC) is based on a light-dependent biochemical reaction that forms long-lived ($> 1 \mu s$) radical pair intermediates and is sensitive to the Earth strength geomagnetic field. The "radical pair mechanism" (RPM), first proposed by Ritz et al., 2000, is thought to require an ordered array of photoreceptors containing a structured alignment of radical pair forming products providing the basis for directional sensitivity to the magnetic field. This biochemical reaction begins when a flavin chromophore molecule absorbs a photon of light, raising an electron to a higher energy state. The excited state leads to an electron transfer from a donor protein to the nearby flavin, resulting in the formation of a radical pair and the redistribution of charge across the molecule. The radical pair can exist in an overall singlet state, in which each radical contains an unpaired electron with anti-parallel spins, or a triplet-state in which the unpaired electrons have parallel spins. An important requirement of the RPM is that the radical pair state in which the spin coherence of the two unpaired electrons persist is long lived ($> 1 \mu s$), providing an opportunity for the magnetic field to influence the spin state of unpaired electrons (see below) [45]. Initially upon radical pair formation, both electrons maintain the same spin behavior (i.e., spin coherence) and over time (e.g. $> 1 \mu s$) spin relaxation causes the spins to dephase, oscillating from

the singlet state to the triplet state at frequencies that abolish the initial spin coherence present at radical pair formation [46-48]. Upon initial radical pair formation, the radical system is in the singlet-state and the electron readily back transfers to the energetically favored fully oxidized form (i.e. ground state), therefore abolishing the radical pair. However, some radical pairs proceed to the triplet-state (i.e. radical pairs whose electrons possess parallel spins), where electron back transfer is a forbidden transition, therefore increasing the lifetime of the radical pair and increasing the likelihood that the change in charge distribution within the molecule could cause a conformational change in the protein that converts into the signaling state, or a precursor to the signaling state [46, 49]. As is discussed below, the magnetic field is thought to increase the proportion of triplet-state radical pair product in radicals in certain alignments relative to the magnetic field, increasing the likelihood of a conformational change in the protein, providing the basis for a quantum mechanical compass sensor.

Indeed, a variety of studies have demonstrated magnetic field effects on the radical pair intersystem mixing (i.e., singlet-triplet interconversion) [50, 51], and recently, effects of Earth- strength magnetic fields (e.g., 50 μ T) on radical pair behavior have been reported in vitro [52]. Importantly however, in order to provide directional information and function as a chemical compass (i.e., provide magnetic compass information as shown in several vertebrate and invertebrate animals), there must be an anisotropic magnetic field effect where modulation of the electron spin dynamics only occurs in radical pairs positioned in specific alignments relative to the magnetic field vector. If, for example, the magnetic field were to have similar quantum effects on radical pair reactions regardless of their alignment relative to the magnetic field lines, directional sensitivity would not be possible, even if the radical pair molecules contained some degree of ordered structure. In vitro experiments using photochemically generated radical pairs have demonstrated the anisotropic

nature of the magnetic field's influence on the singlet-triple intersystem mixing, consistent with a radical pair mediated compass mechanism (Figure 3) [46, 52, 53].

Theoretical proposals that the functional properties of a magnetic inclination compass could be mediated by a quantum mechanical mechanism involving photoexcitation [54], coupled with behavioral evidence from a variety of vertebrates and invertebrates exhibiting light-dependent magnetic orientation [10, 15, 18, 26, 32, 44, 55-66], gave way to the proposal that the biological substrate mediating magnetic orientation resides in the visual system. Indeed, a specialized class of photopigments, cryptochrome (Cry), is the only animal photopigment that forms radical pair intermediates upon photoexcitation and fulfills a number of the other requirements for magnetic sensing (see below). Until recently, it was thought that a magnetoreception mechanism relying on cryptochrome photopigments required the molecules to be in an ordered array. Findings from avian photoreceptors found ordered bands of Cry photopigments housed in the outer segments of cones, suggesting some degree of Cry photopigment organization in the visual system, and given its location in the outer segment of the ultra-violet cones, could be bound to membranes in the photoreceptor further stabilizing the molecule [67]. However, more recent theoretical models suggest other possibilities including the proposal that some degree of rotational flexibility (e.g. the molecule could be restrained only on one axis) of magnetically sensitive photopigments could be tolerated [68-70], or that 'order' can be created within a completely disordered population of photopigments if polarized light is absorbed by only those photopigments aligned orthogonal to the plane of light propagation, e.g., in the vertebrate eye by means of photoselection effects resulting from polarized light entering the pupil and reaching the retina resulting in preferential excitation of photopigment molecules aligned in the plane orthogonal to the direction of light propagation [71]. A recent behavioral study of LDMC orientation in zebra finches

(*Taeniopygia guttata*) suggests magnetic responses are dependent on the alignment of polarization relative to the applied magnetic field [72]. Although these findings do not provide evidence for, or against, photoselection at the receptor level underlying magnetic compass orientation, they do suggest that birds are indeed sensitive to polarized light in spatial tasks mediated by a LDMC.

Further support of the involvement of a radical pair process underlying magnetic sensitivity comes from models of radical pair dynamics in the presence of applied magnetic fields [47, 48], and evidence for magnetic field effects on radical pair recombination kinematics in vitro [50, 51, 73, 74]. These findings provide a biophysical basis for radical pair mediated magnetoreception. If located within specialized photoreceptors, cryptochromes residing in specific alignments with respect to the axis of an external magnetic field should experience an increased yield of triplet-state radical, relative to singlet-state product, providing a basis for a biochemical LDMC [53].

As discussed above, the alignment of the magnetic field relative to the radical pair is thought to prolong the lifetime of the radical state increasing the likelihood that the protein undergoes a conformational change leading to the signaling state [46, 49]. If the signaling state alters the efficiency of phototransduction, then photoreceptors in specific alignments with respect to the magnetic field would show an increased (or decreased) response to light, and provide the basis for a light-dependent magnetic sensory system [46]. Therefore, it has been proposed that the LDM is perceived as a pattern of brighter and darker components superimposed on an animal's visual surroundings and fixed in alignment to magnetic north [53] (see below for additional details). In the so-called "radical pair mechanism", the effect of the magnetic field on the radical pair is independent of polarity (i.e. North from South), and therefore is consistent with evidence found in birds, amphibians, and some insects that use the inclination of the magnetic field (dip angle) to distinguish "poleward" from "equatorward" directions, rather than North from South [2, 30, 75-78].

As briefly mentioned above, theoretical and empirical evidence suggests that Cry, ultra- violet/blue light sensitive photopigments found in a wide variety of plants and animals, may be involved in a magnetically sensitive radical pair mechanism. Crys share similar structural properties to a class of DNA repair proteins, the photolyases, that catalyze the repair of UV light- induced DNA damage in virtually all prokaryotes and most eukaryotes [79]. Although both families are structurally similar and undergo light-dependent electron transfer reactions through similar pathways, the key differences between Cry and photolyases is that Crys lack DNA repair activity and contain a carboxyl terminus extension or ‘tail’ made of a poorly conserved amino acid sequence, which is not present in the photolyases [52, 70, 79-84]. The c-terminal tail appears to be important for Cry’s functional role and the specific amino acid sequence may determine its specific activity which has been shown to mediate a diverse suite of biological processes [85]. For example, Crys are best known for their regulation of biological rhythms, including both light-dependent and light-independent signaling functions [86]. In some animals, Crys play an essential role in the photoentrainment of circadian clocks and are involved in non- visual light responses [86-94]. In mammals, photoentrainment of the circadian clock is mediated by Crys localized in the retina [93, 95-98]. Crys have been shown to function in the photoentrainment pathway of *Drosophila*’s endogenous circadian clock [99-103], and in the response to changes in day length that trigger the mass spawning patterns in hundreds of species of reef-building corals each year [104].

The biophysical properties unique to both the MBM and LDM, and the types of magnetic information that can be extracted from each mechanism, provides a way to determine which mechanism underlies magnetically sensitive spatial behaviors by performing a series of diagnostic tests. However, these mechanisms need not be mutually exclusive and evidence from amphibians [33] and birds [34] is consistent with the involvement of both a MBM and LDMC. From a functional

perspective, it's likely that dual mechanisms operating in tandem provide different types of magnetic information which could be used to perform more complex navigational tasks, rather than selection maintaining two mechanisms that provide redundant information used for performing the same spatial task. The diagnostic tests used to characterize the functional and biophysical properties of the MBM and LDM are listed below:

(1) As stated above, the MBM is likely to provide polar compass information (distinguishes magnetic North from South), while the LDM is proposed to be sensitive to the axis of the magnetic field and distinguishes between the two ends of the magnetic axis by the inclination angle, and therefore, the LDM is often referred to as an inclination compass. Organisms using a magnetite-based compass are not expected to show a reversal in orientation headings when the vertical component of the magnetic vector is inverted (i.e. reversing inclination, while leaving the horizontal component unchanged; Figure 4), consistent with the response seen by functionally blind subterranean mole-rats (Figure 5a.). Specifically, several families of subterranean mole-rats have been show to exhibit spontaneous nest building behavior in which individuals or pairs of mole-rats construct nests at the edge of circular arenas. Mole rats have shown a consistent preference to build nests towards magnetic south-east (Figure 5a, left distribution). When the horizontal component of the magnetic field is experimentally rotated by 180° (i.e. mN = geographic South) mole-rats again tend to position nests in the magnetic south- east direction of the arena, but in a different topographic or 'absolute' position, providing strong support for the involvement of magnetic cues underlying spontaneous magnetic nest building orientation in mole-rats (Figure 5a, middle distribution). In experiments in which the vertical component of the magnetic field is inverted, nest building orientation is unaffected and mole-rats continue to position nests in a south-east magnetic direction (Figure 5a, right distribution). These experiments suggest that the magnetic compass response in

subterranean mole-rats is mediated by a compass mechanism that is sensitive to the horizontal polarity of the magnetic field, consistent with a MBM mechanism.

In contrast, compass orientation in animals using an inclination-sensitive LDM respond to inversion of the vertical component of the magnetic field (i.e. reversing the inclination), by changing their direction of orientation by 180° , even though the polarity of the horizontal component of the magnetic field remains unchanged. An inclination-sensitive compass response was first demonstrated by Wolfgang and Roswitha Wiltschko in European Robins (Figure 5b). During spring and fall migrations robins exhibit robust magnetic compass orientation in the appropriate migratory direction (Figure 5b, left distribution). Similar to the mole-rat experiments discussed above, a rotation of the magnetic field results in a rotation of the birds' compass response and provides evidence for the involvement of a magnetic compass underlying migratory responses in songbirds (Figure 5b, left and middle distributions). Experiments where the vertical component of the magnetic field was inverted, but the horizontal component remained unchanged resulted in a $\sim 180^\circ$ reversal of orientation, suggesting that the compass response is sensitive to the inclination of the magnetic field, not the polarity (Figure 5b, right distribution).

Therefore, it appears that the birds are able to detect the slope of the magnetic field lines indicating poleward from equatorward directions. Further evidence for the use of an inclination-sensitive magnetic compass comes from experiments in which birds were tested in a horizontal magnetic field (i.e. inclination angle = 0°). As predicted, birds tested under these conditions were unable to distinguish between the two ends of the magnetic axis, and exhibited random magnetic compass orientation. These results are consistent with the involvement of an inclination-sensitive, polarity independent mechanism, like the one proposed to mediate the LDM involving radical-pair

intermediates. Similar inclination sensitive magnetic compasses have been demonstrated in newts and sea turtles [33, 105].

(2) Pulse remagnetization experiments can also help to distinguish between the two proposed compass mechanisms. Particles of magnetite thought to be the biological substrate mediating a MBM can be remagnetized by exposure to a rapid (< 5 msec), high intensity ($\sim 500\mu\text{T}$), magnetic pulse applied in a non-parallel alignment relative to the magnetic moment of the biogenic crystals. Specifically, if the pulse is applied such that the magnetized particle does not have time to rotate into alignment with respect to the magnetic direction of the pulse, then the magnetic moment of the particle itself will be remagnetized along the axis of the applied pulse. Exposure of the animal to a biasing field 5-10 times the intensity of the geomagnetic field can be used to align the particles *in situ* prior to application of the magnetic pulse. Reversing the direction of the biasing field so that it is aligned parallel, or anti-parallel to the pulse remagnetization field, exposes the animal to the same electrical artifacts from the high intensity and rapidly changing pulse field while the SD particles exhibit the same (i.e. unchanged) or reversed magnetization, respectively. Treatment of such applied pulses in, for example, an anti-parallel direction would be expected to alter the directional response of an organism that relies on a MBM. For example, when mole-rats were exposed to remagnetization pulses aligned antiparallel to the biasing field, nest building orientation shifted approximately 90° compared to controls (Figure 6). Furthermore, the effect of pulse remagnetization in mole-rats lasted at least three months [106], which is expected since there is no intrinsic mechanism for the animal to ‘correct’ the remagnetization of single-domain particles once they are fully formed. However, evidence suggests that some animals may rely less on input from a MBM after pulse remagnetization treatments, and therefore overcome the effects more quickly [107]. In contrast, a radical pair- based LDM will be unaffected by a strong electromagnetic pulse,

and similar pulse remagnetization treatments done with young migratory birds thought to rely on a LDM, had no effect on magnetic compass headings [35].

(3) The intensity of the ambient magnetic field is also thought to differentially affect a MBM and LDM. A MBM is predicted to show a positive correlation between magnetic field strength and accuracy of orientation. A higher intensity field should decrease the variance in particle alignment caused by thermal agitation and, therefore, provide more accurate directional magnetic information, just as you would expect from increasing magnetic field intensity when using a human navigator's compass. Indeed, quadramodal magnetic compass orientation seen in dancing honeybees when the comb is rotated from the vertical to the horizontal plane (so the gravity vector no longer provides a reference to align the dance) results in a progressive increase in the strength of response when the ambient field strength increases from 5 μ T to 50 μ T to 500 μ T (Figure 7a) [108]. In contrast, behavioral evidence from European robins suggests that the LDM has a narrowly tuned functional window in which the compass can appropriately operate. An increase or decrease in total intensity of roughly 30% from the ambient field has been shown to disrupt seasonally appropriate migratory headings leading to disorientation (Figure 8) [109, 110]. However, the functional window does not appear to be fixed, but is dependent on the bird's prior experience. Birds exposed to magnetic field intensities outside the range they had previously experienced exhibited appropriate migratory headings when they were given prior exposure (3 to 4 days) to the increased or decreased intensity. Interestingly, after pre-exposure to field strengths well beyond those found on Earth, robins were able to orient in both the high intensity field and the natural strength field, but not at intermediate intensities for which they had no prior exposure. Importantly, these findings suggest that prior exposure at extreme magnetic values does not simply stretch the functional range under which the magnetic compass can operate, but rather suggests that birds need experience at each novel intensity

value (+/- 30%) to 'calibrate' the compass. As will be discussed below, this is consistent with the hypothesis that the magnetic field strength alters the pattern of magnetic input, with which the birds can adapt to and use as a compass reference after some period of experience, in addition to other patterns experienced at other magnetic intensities. It is noteworthy, that in contrast to the effects of low intensity magnetic fields on a MBM, a recent study has shown that the avian magnetic compass can adapt to field strengths less than 10% of the local field strength (i.e. $4\mu\text{ T}$) after 24hrs of exposure, demonstrating the plasticity of the LDM, and its ability to function over the range of magnetic field intensities that an individual may encounter during its migratory journey, and those that ancestors of modern birds have been exposed to over the past ~ 1 million years [111].

(4) In contrast to a MBM, a LDM based on a radical pair mechanism is predicted to be sensitive to low-level radio-frequency (RF) fields when the frequencies which match the energy-level splitting between radical pair spin states modulating the singlet-triplet interconversion. Indeed, extremely weak AC fields (equal to or less than 0.1% of the static geomagnetic field) in the low MHz range (i.e., 1-100 MHz) have been shown to alter radical pair interconversion in vitro [112]. Furthermore, radical pair species where one electron is magnetically isolated (i.e. no hyperfine interactions) would be expected to have a peak RF sensitivity at the Larmor frequency, defined as the precession frequency of an electron around the ambient magnetic field. This was demonstrated in experiments with European robins (*Erithacus rubecula*) that were disoriented when exposed to both broadband, which included the Larmor frequency (0.1-10 MHz), and the discrete Larmor frequency (1.3MHz) fields applied on a non-parallel axis with respect to the geomagnetic field [113]. Importantly, the Larmor frequency is not fixed, but rather a function of the ambient magnetic field strength. Consistent with the effect of low-level radio frequency fields being due to direct interaction with the quantum spin state of a radical pair system, when the local magnetic field

intensity was doubled, exposure to a 1.3MHz field no longer resulted in disorientation (i.e., robins exhibited seasonally appropriate magnetic compass orientation). In contrast, when the intensity of the RF field was doubled, corresponding to the Larmor Frequency in a static field intensity twice that of the ambient field, the migratory orientation of robins tested in the ambient field was unaffected, while birds tested in the 2x magnetic field intensity were disoriented [114]. The effects of low-level radio frequency fields, and the interaction of frequency and static field intensity are consistent with the involvement of a radical pair mechanism where one partner of the radical pair is devoid of hyperfine interactions [114]. Similar radio frequency effects ‘tuned’ to the Larmor frequency have been shown in non-migratory chickens, zebra finches, and cockroaches [34, 72, 115, 116], and see discussion of effect of LF radio frequency fields on yearling snapping turtles below [117]. Importantly, radio frequency effects on orientation were only observed when the angle between the applied RF fields and the magnetic field were applied in non-parallel orientations. In contrast, when the two stimuli were presented in parallel alignments, the seasonally appropriate magnetic compass orientation of robins was unaffected, suggesting that the effect of RF fields is directly coupled to magnetic input, rather than the result of a non-specific effect on the bird’s behavior (e.g., a change in motivation). Consistent with this conclusion, experiments with Eastern red-spotted newts (*Notophthalmus viridescens*) have shown that exposure to low level RF noise (0.5-10 MHz) disrupted magnetic compass orientation, but not celestial compass orientation, suggesting a direct effect of RF exposure on the magnetic compass response, rather than a non-specific effect on behavior and/or motivation (unpublished data, personal comm. JBP).

Although RF exposure has been shown to disrupt magnetic compass orientation in animals using a LDM, AC field intensities many orders of magnitude higher would be required to disrupt a MBM, which would be caused by increased thermal agitation [118]; but see [119]. Therefore, effects of

low-level RF provide another diagnostic test to distinguish between the two compass mechanisms. In experiments with subterranean mole-rats thought to use a MBM (see earlier discussion), RF exposure had no effect on spontaneous magnetic nest building behavior at an intensity $\sim 1000\times$ higher than that shown to affect migratory birds, suggesting that the presence of RF does not necessarily abolish magnetic responses, but only those mediated by a hypersensitive biophysical process involving quantum spin states similar to the proposed radical pair models [120].

(5) Finally, a radical pair based biochemical reaction underlying the LDMC should be sensitive to the characteristics of light input, whereas the MBM should function independently of light. A wealth of evidence from a variety of taxa suggests that magnetic compass orientation in animals such as amphibians and birds is sensitive to both the wavelength and intensity of light [for reviews see 44, 53, 57, 58, 121]. For example, behavioral evidence from Eastern red spotted newts trained to orient relative to the magnetic field under full spectrum (white) light, exhibited appropriate compass orientation when tested under wavelengths ≤ 450 nm, were disoriented at wavelengths around 475 nm, and exhibited a 90° counterclockwise rotated orientation at wavelengths ≥ 500 nm (light intensities $12.3\text{-}12.6 \log \text{ quanta/cm}^2/\text{s}$) [31]. The magnetic compass mechanism of European robins also appears to be dependent on the wavelength of light, as low-to-moderate intensities of blue and green light yield appropriate migratory headings, but wavelengths beyond approximately 570 nm cause disorientation [for review see 57]. In more recent studies, similar wavelength-dependent effects of light have been found on the magnetic compass orientation Australian silvereyes, garden warblers, carrier pigeons, and domestic chickens tested under monochromatic light ranging from 370nm to 670nm [57]. Light-dependent shifts in the direction of magnetic compass orientation have also been demonstrated in both adult (Figure 9) and larval fruit flies (*Drosophila melanogaster*), and in adult mealworm beetles (*Tenebrio molitor*) [10, 32, 122].

Over the past two decades, support for Cry's role in light-dependent magnetic orientation involving radical-pair reactions has gained traction. Both theoretical models and in vitro experiments indicate that Earth-strength magnetic fields can influence the spin chemistry (specifically the ratio of singlet to triplet product yield) of a radical pair process, and Cry seems to be a well-suited candidate to mediate this reaction [51, 52, 74, 118, 123]. In both plants and animals, Cry has been shown to undergo photo-induced radical-pair reactions resulting in the formation of long-lived ($> 1 \mu s$), spin-correlated radical intermediates involving the light absorbing flavin (FAD) cofactor [48]. Cry's protein structure is also well-suited to function as a biological magnetoreceptor, and the spacing of the highly conserved trio of tryptophan amino acids and flavin provide an electron transfer pathway for the formation of the radical pair during photoreduction, allowing the electron to 'jump' across the amino acids resulting in the appropriate spacing between the two unpaired electrons for a magnetic field effect [124]. In photolyases, thought to be a homologue of Cry, photoreduction takes place via electron transfer between a triad of tryptophan residues and the FAD cofactor [125]. The same tryptophan triad is conserved in avian Cry, likely providing a similar electron transport pathway for photo-induced radical pair formation [126, but see 127].

One suggestion for Cry's molecular role in magnetoreception is that the magnetic field has antagonistic effects on both the photo-reduction of the fully oxidized form to the radical semiquinone form of the flavin chromophore ($FAD_{ox} \rightarrow FAD\bullet^-$ or $FADH\bullet$) and the photo-reoxidation of the radical form back to the fully oxidized form ($FAD\bullet^-$ or $FADH\bullet \rightarrow FAD_{ox}$). Under this reaction scheme, blue light (short wavelength) converts the fully oxidized form of the flavin chromophore into the semi-reduced, flavosemiquinone form, increasing the proportion of radical pair intermediates that could then proceed to the signaling state (Figure 10, top reaction), while

green light (long wavelength) catalyzes the oxidation of the flavin back to the fully oxidized form, shifting the relative radical pair products back to a non-signaling state (Figure 10, bottom reaction) [128]. Although this reaction scheme is consistent with antagonistic behavioral effects on magnetic compass orientation shown in adult *Drosophila* and newts [10, 66], birds continue to exhibit appropriate magnetic compass orientation under green light (e.g., 565nm) and are disoriented under yellow (e.g., 590nm) light [26]. Currently, the exact spectral reaction scheme is unknown, and may not be consistent across unrelated species.

In addition to theoretical support, behavioral studies have provided evidence for a direct link between Cry and magnetoreception. In conditioning experiments to magnetic stimuli (i.e. 10x increase in magnetic field intensity), Cry deficient adult *Drosophila*, were unable to respond to an external magnetic stimulus, yet arrhythmic wild-type flies responded to magnetic stimuli similar to that of controls, suggesting that a fully functioning circadian clock is not required for magnetic conditioning [15]. This study also found that magnetosensory behavior was lost when flies were exposed to wavelengths greater than 420nm, consistent with the absorption spectrum of cryptochrome, although the interpretations of these results remain unclear. However, a more recent study using transgenic *Drosophila* containing point mutations which disrupted the FAD-tryptophan amino acid electron transport pathway, suggests that the biophysical mechanisms allowing for radical pair formation originally proposed may be more complex than previously realized [16]. Further support for photosensitive, Cry-dependent magneto-sensitivity comes from research investigating photo-induced effects on the locomotory rhythm in adult *Drosophila* and indicate an effect of the magnetic field on a Cry-dependent, blue light-induced changes in the free running rhythm [129].

Furthermore, evidence for light-dependent magnetic compass mechanisms with antagonistic short- and long-wavelength inputs like those found in amphibians, birds, and insects are consistent with a cryptochrome-based mechanism. As briefly discussed above, Eastern red-spotted newts exhibited a 90° difference in the axis of magnetic compass orientation relative to the trained magnetic direction when tested under short- versus long-wavelength light (< 450 nm and >500 nm) (Figure 11). Additionally, orientation was abolished when newts were tested at intermediate wavelengths (475 nm), a point at which both pathways could be activated equally causing the antagonistic inputs to cancel (Figure 11). Additional evidence from both adult and larval [122] *Drosophila* support the antagonistic LDMC theory; shifts in orientation consistent with antagonistic patterns of magnetic input were observed when flies were tested under short- (365 nm) and long-wavelength (500 nm) inputs (adult data, Figure 9).

A light-dependent magnetic compass that receives antagonistic short- and long-wavelength input is consistent with the absorption changes in *Drosophila* cryptochrome when exposed to varying wavelengths of light (Figure 12a). At intermediate wavelengths (420 nm – 500 nm) the fully oxidized form of the radical is preferentially excited, whereas, at short- (<400 nm) and long-wavelength (> 500 nm) wavelengths the radical flavosemiquinone form is preferentially excited. Interestingly, amphibian cryptochrome (eg. Cry-DASH from *Xenopus laevis*), similar to that of zebrafish cryptochrome (ZfCRY-DASH) (Figure 12b) exhibits a spectral transition at approximately 475nm consistent with the behavioral evidence from newts (Figure 11). The correspondence between the absorption properties of Cry and the spectral dependence of magnetic compass orientation seen in newts and *Drosophila*, provides further evidence that cryptochrome mediates the molecular and biophysical pathways of the LDM.

One model, proposed by Ritz et. al., 2000 [46], suggests that the LDM produces a complex 3-dimensional pattern with axial (i.e. bimodal) or bi-axial (i.e. quadramodal) components (Figure 13a), however, more complex, and likely more realistic models involving additional hyperfine interactions within the radical pair system are becoming available (Figure 13b) [47, 53]. More specifically, if the reaction products (i.e. ratio between signaling vs. non- signaling forms of the protein) resulting from a light-dependent, radical pair based magnetic compass mechanism are coupled to the visual system, a visual pattern fixed with respect to the magnetic input (i.e. magnetic north) may be produced providing a visual reference with which to guide spatial behaviors [53]. In animals with simple photoreception organs and/or those in which extraocular photoreceptors mediate the LDMC, such a pattern may be perceived by means of a separate sensory pathway.

Although the proposed patterns are likely oversimplifications, particularly that shown in Figure 13a, they do contain certain properties such as an axially symmetrical pattern and quadramodal components that are likely to be consistent with the actual pattern(s) produced by the magnetic field. Indeed, evidence that photoreceptors specialized for detection of the Earth's magnetic field may be located in the retina of birds and mammals [113, 130], as well as the compound eye of some insects [32, 58] led to suggestions that the pattern produced by a radical pair mechanism may be perceived as a 3-dimensional pattern of light intensities and/or color superimposed on the animal's visual surroundings and that this pattern may serve as a directional (i.e. compass) reference and possibly a spherical grid or coordinate system aiding in spatial perception and/or navigation [53]. The intersection of the 3-dimensional pattern derived from radical-pair systems like those modelled by Cintolesi et al. [47] and Rodgers and Hore [81] where the horizontal plane may form a quadramodal pattern when reduce to two dimensions, and is consistent with quadramodal magnetic responses seen in a variety of organisms, particularly insects. For example, resting positions of blowflies

exhibit quadramodal patterns of response (Figure 7b) [131], as well as American cockroaches (*Periplaneta Americana*) that show quadramodal alignment preferences along the cardinal compass directions [132]. Furthermore, the axial symmetry, a consistent feature of most models derived from radical pair reactions, is consistent with the reliance on an inclination-sensitive magnetic compass, and may help to explain the ~North-South spontaneous bimodal alignment (SMA) reported to occur in most vertebrates [9, 133] (and see below).

Although spontaneous bimodal and quadramodal orientation has been observed in a variety of organisms, the adaptive and functional relevance of this behavior remains unclear. Characterizing the spectral dependence of these magnetic responses, as well as determining if they are sensitive to low-level RF fields, e.g. as suggested by studies of spontaneous nest building orientation in wood mice (*Apodemus sylvaticus*) [8], should help to elucidate the biophysical mechanisms mediating SMA and would provide an assay that could be used to determine the functional significance of SMA in vertebrate and invertebrate taxa.

Behavioral Responses Mediated by Magnetic Cues

As discussed above, a variety of spatial responses have been shown to be mediated by Earth-strength magnetic fields, and evidence linking a MBM or LDM to specific behavioral responses has emerged over the past several decades. This section provides a brief overview of the spatial responses that have been shown to involve magnetic input and, where appropriate, includes behavioral evidence to help determine the mechanism underlying each response. Magnetic field effects on non-spatial responses (e.g. geotaxis in *Drosophila*, nociception in mice, hypocotyl elongation in plants), have also been reported in previous studies, but will not be discussed here. For more information on these responses see [18, 134, 135], respectively.

Innate Magnetic Compass Orientation

More than 70 years of research on migratory birds has shown that magnetic cues play a fundamental role in seasonal migration. Behavioral evidence from juvenile birds captured during their first migratory journey and tested individually show well-oriented magnetic compass responses which suggest that the magnetic compass preference is innate or ‘genetically preprogrammed’, rather than learned through experience or from simply following the flight paths of more experienced conspecifics. For example, offspring from two populations of blackcaps (*Sylvia atricapilla*) raised in isolation show seasonally appropriate migratory compass responses corresponding to magnetic south-east and south-west, suggesting an innate migratory preference unique to each population. However, cross-breeding experiments between the two populations where the F1 generation was raised in captivity resulted in mean magnetic compass preferences that were intermediate between the two parent populations (i.e. magnetic south). This effect was not sex specific and the variance in the F1 generation was similar to that of the parent populations, supporting the hypothesis for the genetic inheritance of magnetic compass responses in migratory birds [136]. These findings were replicated in additional populations of blackcaps with different migratory routes [137]. Separate experiments with juvenile Tasmanian silvereyes (*Zosterops lateralis*) also provide evidence that seasonal migration was based in part on innate magnetic directional preferences. Juveniles caught on their native range just after fledging, with no prior migratory experience, exhibited seasonally appropriate magnetic compass orientation when tested under full spectrum and green (571nm) light. However, when tested under long-wavelength light (633nm) the young birds were disoriented [138]. Furthermore, pulse re-magnetization treatments had no effect on magnetic compass orientation in juvenile silvereyes [138] and is *inconsistent* with the involvement of a MBM. In addition, a wealth of evidence from European robins show low-level RF field effects on migratory magnetic compass

orientation, providing strong evidence for the involvement of a radical-paired based mechanism underlying the LDMC responses in birds [139].

Furthermore, transoceanic migrations by loggerhead sea turtles (*Caretta caretta*) that hatch from beaches along the Florida coast also appear to be guided by an innate magnetic program that helps maintain their multi-year migratory route in the Atlantic Gyre circling around the Sargasso Sea [140]. When hatchling turtles were exposed to eight different magnetic field values that match specific points along the gyre, they exhibited magnetic orientation responses that keep them from straying outside the gyre currents [141]. However, unlike migratory birds, magnetic compass orientation of sea turtles exhibits properties of both a MBM and a LDM, and therefore, the mechanism(s) mediating magnetic orientation in sea turtles remains unclear [for details see 105, 142, 143, 144].

Learned Magnetic Compass Orientation

The Phillips Lab has pioneered development of behavioral assays that take advantage of the ability of a variety of vertebrates and invertebrates to learn spatial tasks using the directional information provided by magnetic cues. Training paradigms typically require the animal to learn the direction of, e.g. a food reward or nesting refuge relative to the ambient magnetic field. The advantages of training assays include 1) the ability to elicit behavioral responses in multiple magnetic directions, rather than animals being restricted to fixed (e.g. migratory compass) compass headings, 2) study learned compass responses outside of seasonal migratory periods, and 3) expose animals to controlled manipulations in training and/or testing conditions to better characterize the effects of experimental treatments (e.g. exposure to low-level RF fields, exposure to monochromatic wavelengths of light), on the mechanisms mediating magnetic orientation, and how these behaviors are integrated into other forms of spatial cognition.

A detailed characterization of learned shoreward magnetic compass responses in Eastern red-spotted newts has provided direct evidence for the involvement of a light-dependent magnetic compass mechanism mediated by extra-ocular photoreceptors. Groups of newts trained in outdoor tanks to a particular shore direction under natural, i.e. full spectrum light exhibited shoreward magnetic compass orientation when tested under full spectrum or short-wavelength (400nm, 450nm) light consistent with a learned magnetic compass response (Figure 14A). However, when tested under long-wavelength light of equal intensity, newts exhibited a 90° *counterclockwise* rotation of magnetic compass response (Figure 14B). Newts trained under long-wavelength (>500nm) light exhibited appropriate shoreward compass orientation when tested under similar long-wavelength light (Figure 14C, right distribution), however, exhibited a 90° *clockwise* rotation in magnetic compass orientation when tested under full spectrum light (Figure 14C, left distribution). These findings rule out an indirect effect of light. For example, if newts were no longer motivated to orient under long-wavelength light, or if long-wavelength light ‘shut off’ the compass response altogether, then newts would not be predicted to exhibit magnetic orientation under any testing condition when exposed to long-wavelength light. However, as see in Figure 14B, C, right distributions, magnetic compass responses, although rotated, are well-oriented when tested under long-wavelength light. Rather, the pattern of magnetic input appears to be affected (e.g. rotated) by the wavelength of light. Newts trained under full spectrum light and tested under long-wavelength light showed a 90° CCW rotation of response (Figure 14B, right distribution), as if the pattern of magnetic input had been rotated 90° CCW. If true, newts trained under long-wavelength would perceive a pattern of magnetic input which was also rotated 90°CCW. Tested under the same long-wavelength spectrum would produce the same shift in the perceived pattern and newts should be able to orient in the shoreward magnetic compass direction, as was shown (Figure 14C, right

distribution). However, when trained under a 90° CCW rotated pattern (i.e. long-wavelength), and tested under full- spectrum, where the perceived pattern is not rotated, would be expected to produce a 90° CW shift in magnetic compass orientation. Indeed, newts trained and tested under this condition exhibited a CW rotation in response, consistent with the involvement of a light-dependent magnetic compass mechanism that receives antagonistic short- and long-wavelength input (Figure 14C, left distribution).

In additional experiments, light-filtering caps covering extra-ocular photoreceptors in the pineal complex were used to 1) bolster the hypothesis that the wavelength effects on newt magnetic compass orientation discussed above are mediated by a light-dependent, photoreceptor based mechanism, and 2) establish that the photoreceptors involved in this process are located in the pineal complex, an extra-ocular cluster of photoreceptors positioned on the dorsal surface of the head [145].

Several other assays provide evidence for learned magnetic compass responses in vertebrates, including trained nest building orientation in inbred laboratory mice [6], rapid learning of magnetic compass orientation in a watermaze assay involving laboratory mice [7], and conditioned magnetic compass responses in young domesticated chickens, which was shown to be light-dependent and sensitive to RF exposure in the low-MHz range, properties consistent with a light-dependent radical-pair based mechanism [110, 146]. Recently, non-migratory Zebra finches have been shown to exhibit trained magnetic compass orientation that is sensitive to both low- levels of RF exposure and the axis of polarized green light [72].

Spontaneous Magnetic Alignment

A wealth of recent studies provide support of spontaneous magnetic alignment (SMA) behavior, a type of non-goal oriented spatial behavior during which an animal aligns their head direction, or body axis relative to the magnetic field lines [for reviews see 9, 12, 133]. Vertebrates exhibiting SMA typically align the long axis of their body (e.g. the axis of the spine in quadruped mammals) along the magnetic North-South axis, whereas invertebrates show quadramodal preferences aligning along the cardinal (i.e. N, S, E, W) or anti-cardinal (i.e. NE, SE, SW, NW) compass axes [12, 132]. In both cases, the adaptive significance underlying SMA remains unclear, however, some functional roles for SMA have been put forward in recent years. For example, SMA may provide a strategy to help structure an animal's spatial surroundings in familiar and novel landscapes by consistently aligning the head direction such that familiar habitats can be more easily recognized and novel environments can be learned using a systematic alignment 'rule'. Many insects use a retinotopic matching strategy where a pattern of landmark arrays imaged on the retina can be matched to a stored pattern learned in previous visits to the same site [147]. Experimental evidence has shown that when learning a new environment, or searching for a goal across a familiar landscape, honeybees will orient in a consistent magnetic direction thought to reflect a systematic strategy when attempting to establish a retinotopic match. Rotation of the Earth's magnetic field corresponded to a rotated alignment of the bee's orientation during goal searching behavior and suggests that an Earth-based magnetic coordinate frame helps to organize spatial behavior and memory in hymenopterans [148]. Additional explanations for the functional significance underlying SMA in insects is discussed in Chapter II.

An intriguing case of SMA comes from predatory red foxes (*Vulpes vulpes*) that show a 4-fold increase in hunting success when 'mousing' attacks are aligned along the north-northeast magnetic axis [149]. It was proposed that the magnetic field may server as a range-finder or targeting system

used to coordinate the distance and/or trajectory of the mousing attack. Mousing red foxes provide the only example with a clear fitness advantage for SMA and future studies on this system will likely help to characterize SMA behaviors in a variety of vertebrates. This is discussed in detail in Chapter III.

Magnetic Map

In the behaviors discussed above (i.e. magnetic compass orientation and SMA) information derived from the magnetic field can be used to provide directional information in order to, e.g. align in a consistent or preferred heading, or help to guide animals in the seasonally appropriate compass direction during migration. However, without some form of a global positioning or ‘map’ sense, the use of only a compass (magnetic or otherwise) is not suitable for long-distance navigation like those found in many animals. The ‘gradient-like’ features of the magnetic field make it well-suited to provide the basis of a magnetic map used for a global positioning sense. As discussed above, the inclination and magnetic intensity form approximately parallel gradients, both increasing toward each magnetic pole. Furthermore, each component varies relatively predictably, providing the basis for a global-scale gradient that can be used to extract at least one coordinate (i.e. latitudinal position derived from inclination and/or intensity) of a multi- coordinate map. If these gradients are learned during local navigation within the home range, then extrapolating the magnetic values to unfamiliar areas provides a strategy for determining global position. In terms of migratory and/or homing navigation, comparing magnetic values between the animal’s position and the home value would help to derive the relative position along the route.

However, there are several challenges that must be met in order to derive positional information from the properties of the geomagnetic field. First, the spatial variation, although predictable, is very subtle, varying 5-10nT/km in intensity and 0.01° in inclination/km [25]. Therefore, a map

reading error equivalent to ~1% of the average magnetic field intensity could result in an error of up to ~5,000km when based on intensity measurements, or a 5° error in the inclination reading could result in an error equivalent to 500km. Since the spatial variation in the geomagnetic field is extremely weak, the sensory system must be extremely sensitive and precise to have any functional value as a positioning system, especially during short-distance navigation. Next, both spatial and temporal magnetic anomalies can produce relatively large changes in the magnetic field, making a magnetic map unreliable and/or unusable at specific locations and/or during specific times (e.g., during solar storms). However, large and/or rapid fluctuations in map measurements could be an indicator that the map readings are unreliable, preventing an individual from using magnetic map information during these periods [150]. Furthermore, secular variation (i.e. variation occurring from year to year) would cause the home and goal magnetic values to drift over an individual's lifetime. This could be overcome by continuously updating the learned values, or taking measurements immediately before leaving the site. Lastly, solar winds cause a daily variation of 30-100nT and ~0.3° fluctuation in inclination [4] and could result in large errors in map readings if sampling is not done systematically. However, averaging multiple measurements taken throughout the day could help to reduce the noise in the daily variation, or measurements could be taken during sunrise and sunset when temporal variation is minimal and relatively consistent from day to day [151].

Figures:

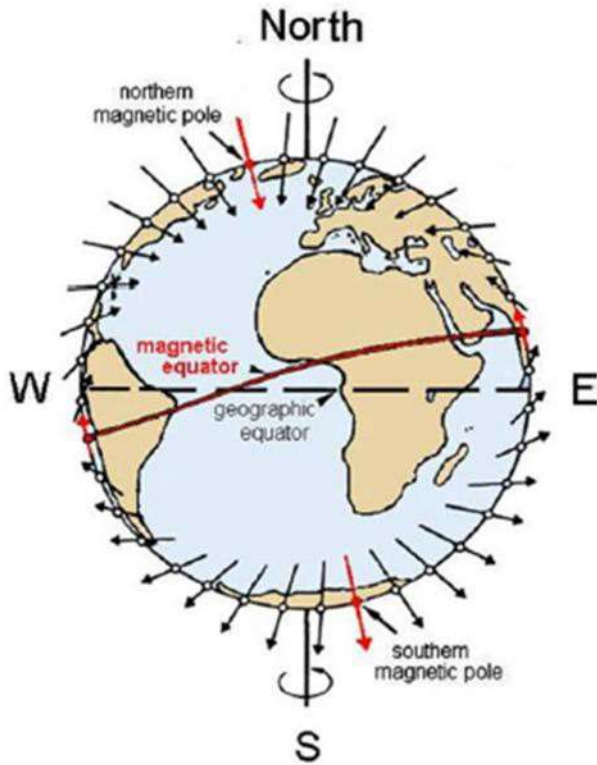


Figure 1. A schematic of magnetic vectors generated by Earth's geomagnetic field. Arrows indicate local vector angle; arrow length is proportional to magnetic intensity. Displacement of the magnetic pole from the geographic (i.e. rotational) pole is also shown, as well as the magnetic equator (red vectors) [figure from 4].

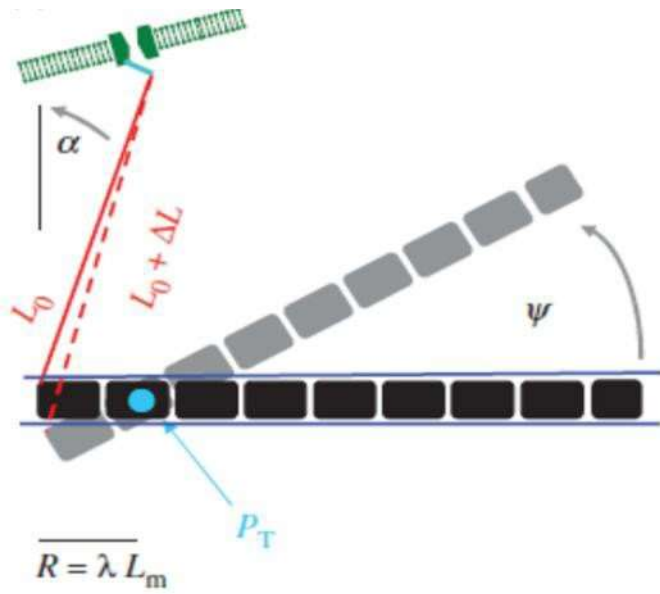


Figure 2. Illustration of magnetite-based transduction pathway fixed to a pivot point (P_T) within a specialized sensory cell. The illustration show a single-domain (SD) magnetite particle attached to a force-gated transmembrane ion channel, where the magnetic torque generated by an external magnetic force is transmitted to the gated channel (figure from [152]).

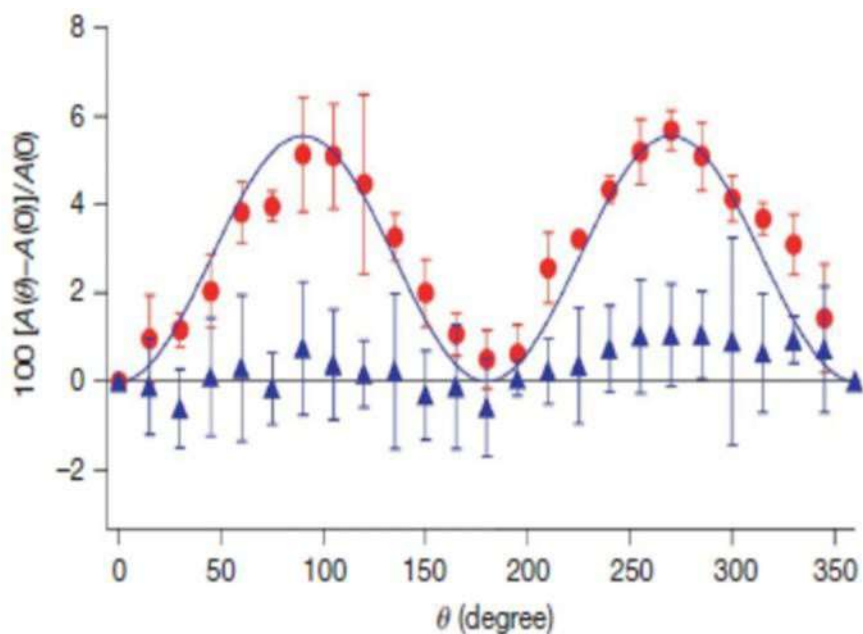


Figure 3. Anisotropic magnetic field effect on photochemically formed radical pairs. Red circles show anisotropic photoabsorption measurements (y-axis) of a radical pair in relative alignments to an applied magnetic field (3mT). Blue triangles are data from experiments when the polarization axis of the probe light was vertically aligned, and no directionally-dependent effect was expected [Data from 52].

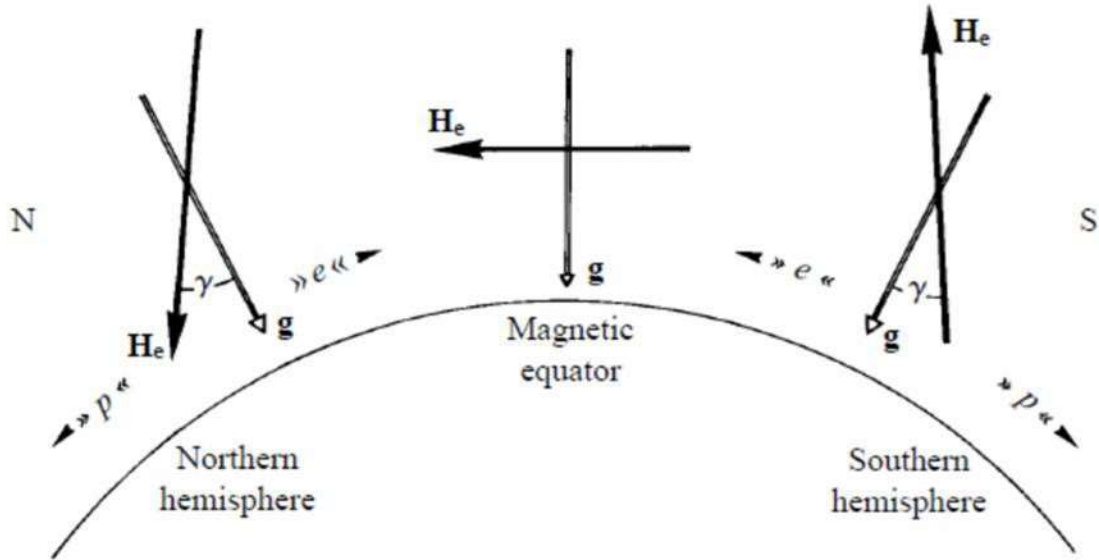


Figure 4. Schematic showing the horizontal and vertical components of the geomagnetic field. In the northern hemisphere, the vertical component of the magnetic field points downward towards the center of the earth, while in the southern hemisphere the vertical component points upward away from the center of the Earth. In both the northern and southern hemispheres, inclination angle decreases as it approaches the equator, where it has an inclination of zero degrees, i.e. magnetic field aligned horizontally. In both the northern and southern hemispheres the inclination angle increases towards the poles, where the inclination is -90 degrees at the south magnetic pole and $+90$ degrees at the north magnetic pole [Figure from 153].

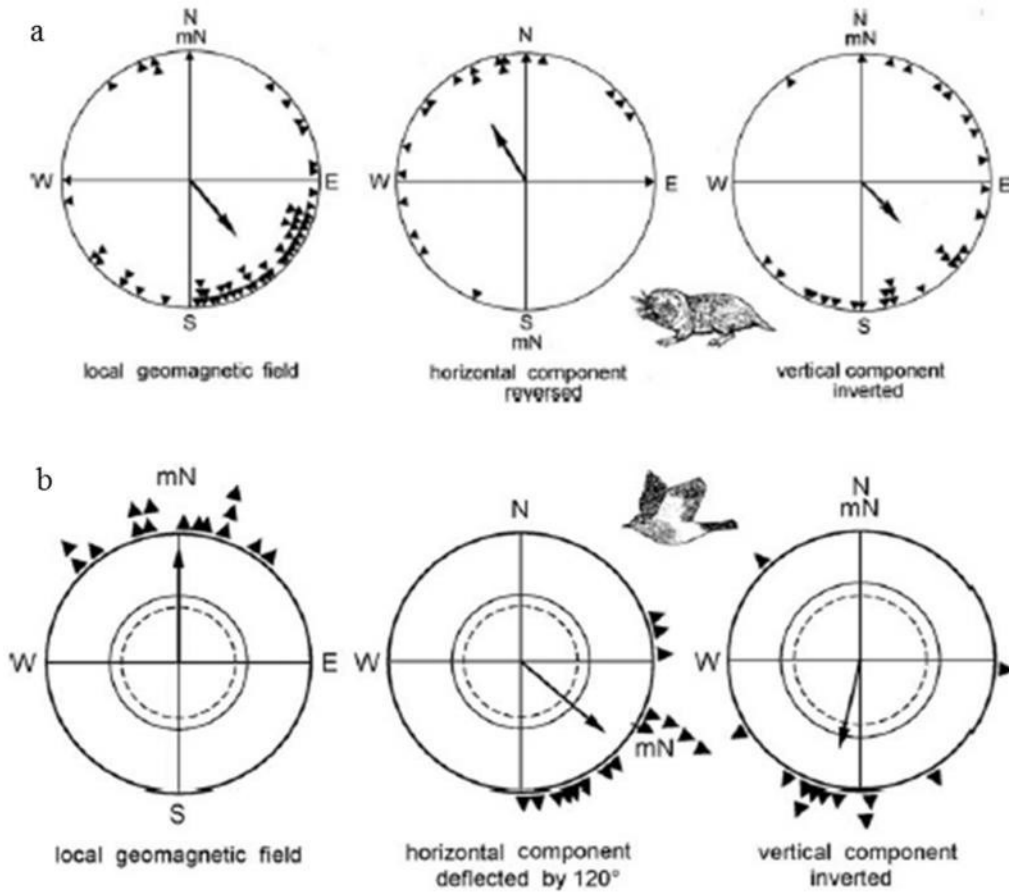


Figure 5. a) Orientation of mole rats *Cryptomys* Sp. providing evidence for the use of a polarity compass [27]. b) Orientation of migratory European robins exhibiting an inclination sensitive compass [26]. “N” indicates geographic north, whereas “mN” indicates the position of magnetic north. Triangles at the periphery of each circle represent the orientation from a single individual and the vector stemming from the center of each distribution represents the mean direction of the distribution with its length indicating the strength of response. The inner dashed and solid circles in b) represent the 90% and 95% confidence intervals for those distributions.

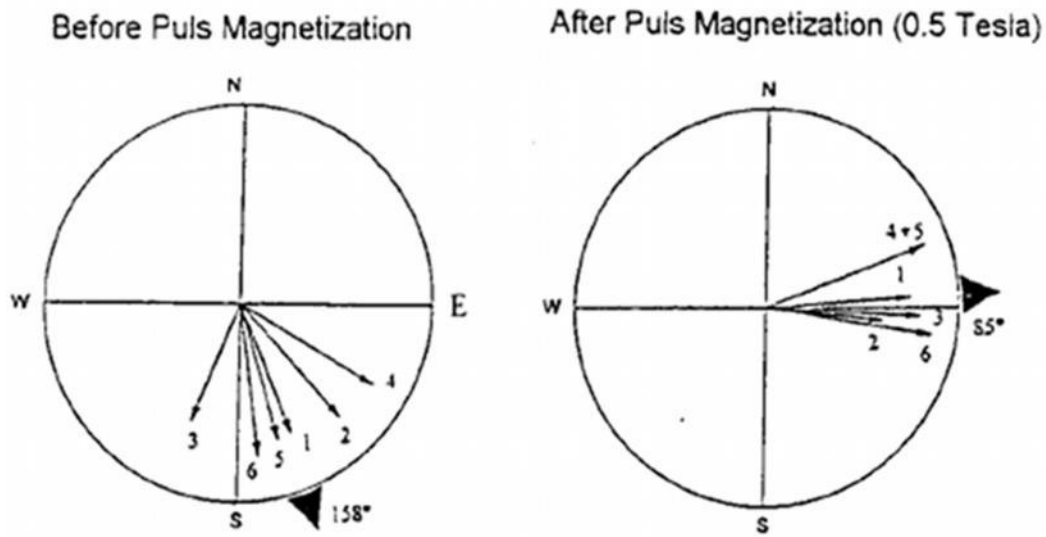


Figure 6. Effect of pulse remagnetization on spontaneous nest building orientation in subterranean mole rats (*Cryptomys*). Six different family groups were tested as described above. The distribution on the left shows orientation prior to the pulse remagnetization treatment, whereas the distribution on the right shows orientation of the same groups of individuals after one exposure to a pulse remagnetization treatment. Each arrow numbered 1-6 represents the mean vector bearing of one family of mole-rats with the arrow length representing the strength of the mean response. The black arrow on the periphery of each distribution represents the mean bearing of the distribution. Figure from [106].

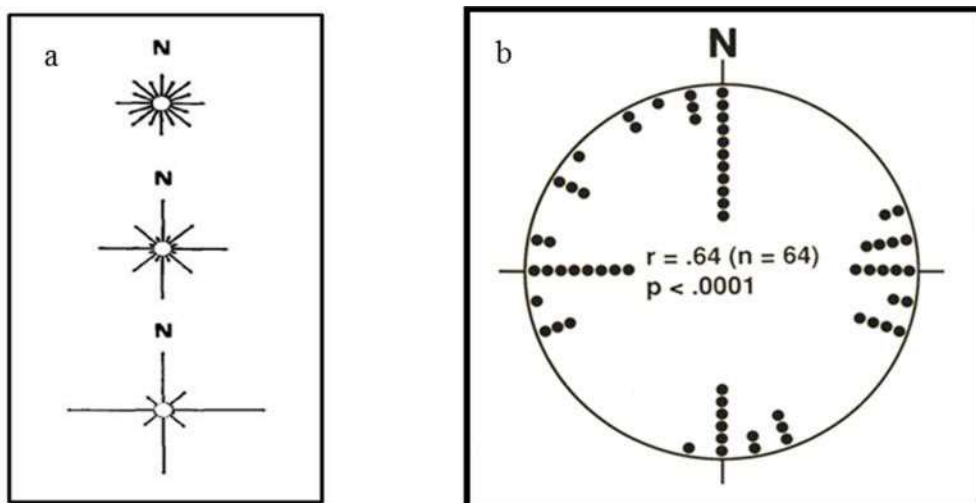


Figure 7. Quadramodal magnetic compass orientation in insects. (a) Quadramodal honeybee dance on a horizontal comb; magnetic field intensity = 5 μT (top), 50 μT (middle), 500 μT (bottom) [data from 108]. (b) Resting positions of blowflies on a horizontal surface [data from 131].

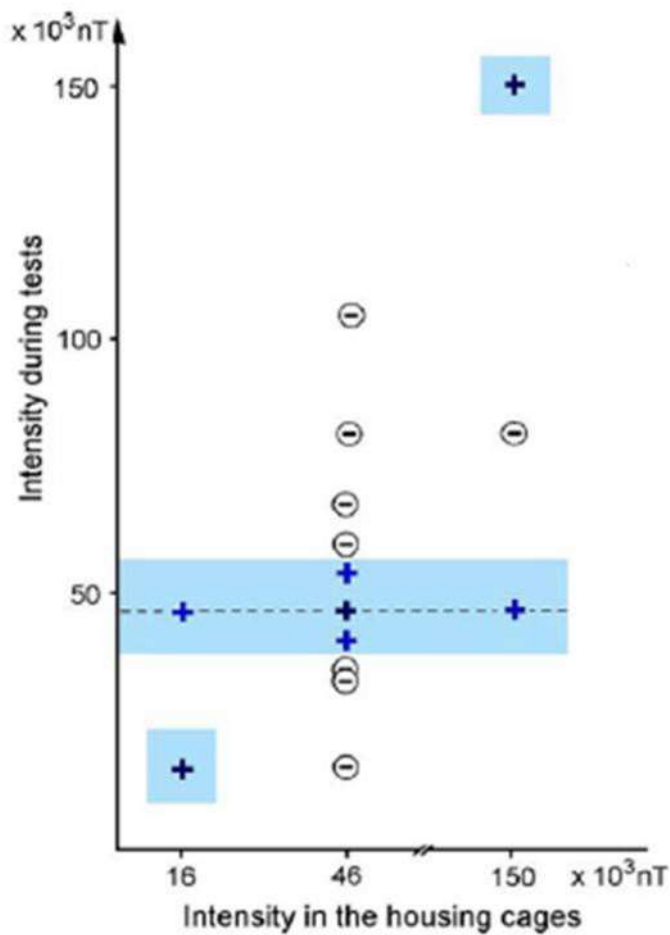


Figure 8. Plasticity of avian magnetic compass responses to various magnetic field strengths with and without prior exposure. The x and y axes indicate the field strength of the housing cages (i.e. prior exposure) and testing field strength in nT, respectively. The “+” sign indicates seasonally appropriate magnetic compass orientation whereas the “-“ sign represents loss of magnetic orientation. Blue shaded regions represent a combination of holding and testing conditions in which the discrepancy in magnetic field strength is less than ~30%. These data provide evidence for the plasticity of the avian magnetic compass and a functional window of magnetic responses that can be ‘tuned’ by previous experience to intensities well outside the range of the natural magnetic field intensity, consistent with the involvement of a LDMC [Data from 109].

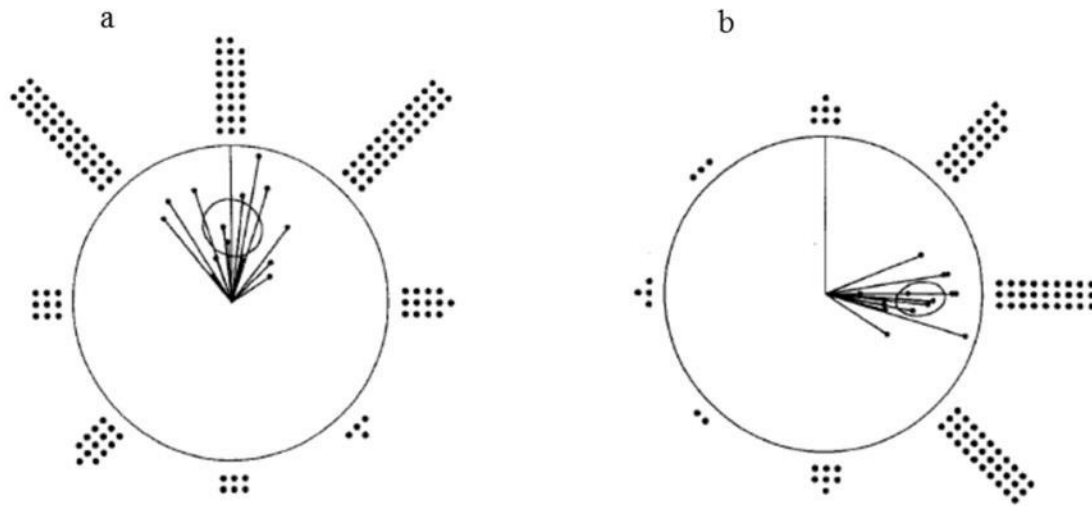


Figure 9. Wavelength dependent shifts in magnetic compass orientation of male *Drosophila melanogaster* under a) 365 nm and b) 500 nm light ($10.1 \log \text{ quanta/cm}^2/\text{sec}$). Data points on the edge of each distribution represent individual bearings, while vectors inside each distribution represent the mean response for each test. Each distribution includes data from tests carried out under 16 conditions (4 trained directions x 4 magnetic field alignments in testing) [data from 10].

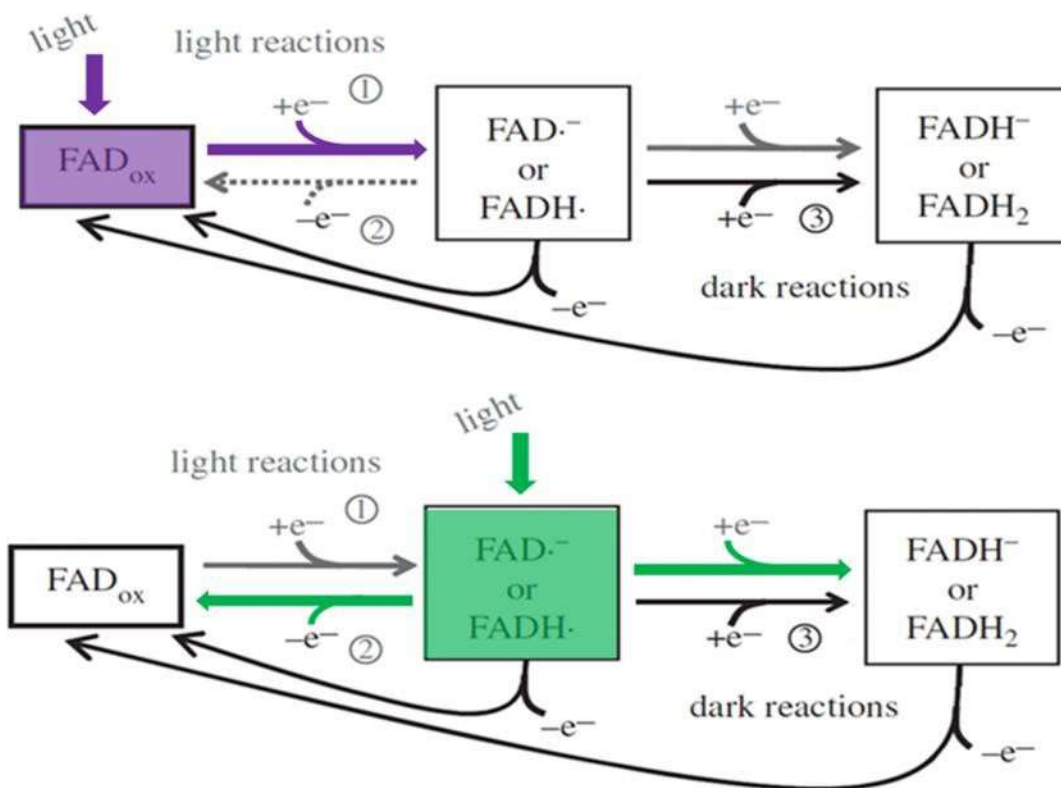


Figure 10. Interconversion of the light-dependent redox states within the flavin chromophore of Cryptochrome. Numbers show various points in the flavin reduction reaction where magnetic field effects could take place resulting in an increased ratio of singlet-to-triplet yield of radical product. Top reaction highlighted in purple shows the effect of short wavelength light on the fully oxidized form of the FAD cofactor, driving the reaction to the semi-reduced, or flavosemiquinone form. Long-wavelength light has been shown to have antagonistic effects on magnetic compass orientation, and a possible reaction scheme is shown in green (bottom reaction). Long-wavelength light could drive the reaction either back to the fully oxidized ground state or towards the fully reduced form. In either case, the magnetic field could have an effect on the product yield, resulting in an antagonistic effect on the pattern of response [from 128].

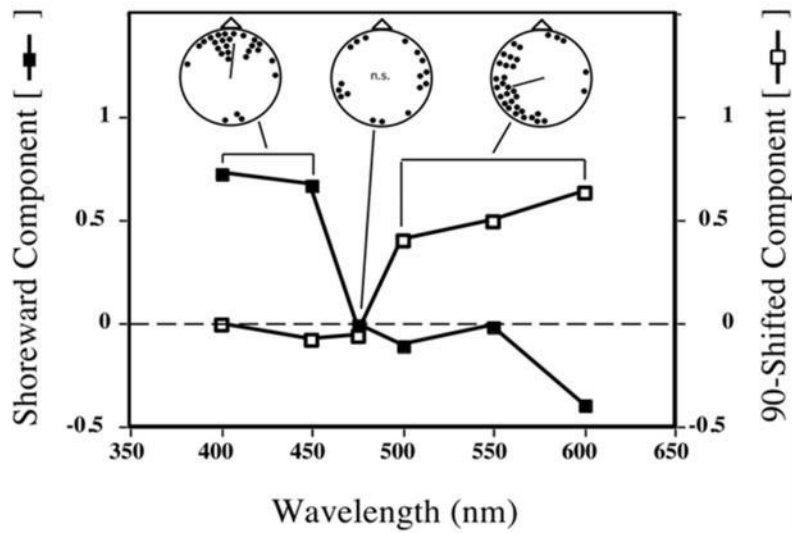


Figure 11. Evidence for an antagonistic light-dependent magnetic compass in Eastern red-spotted newts. Open triangles indicate trained shoreward direction [31].

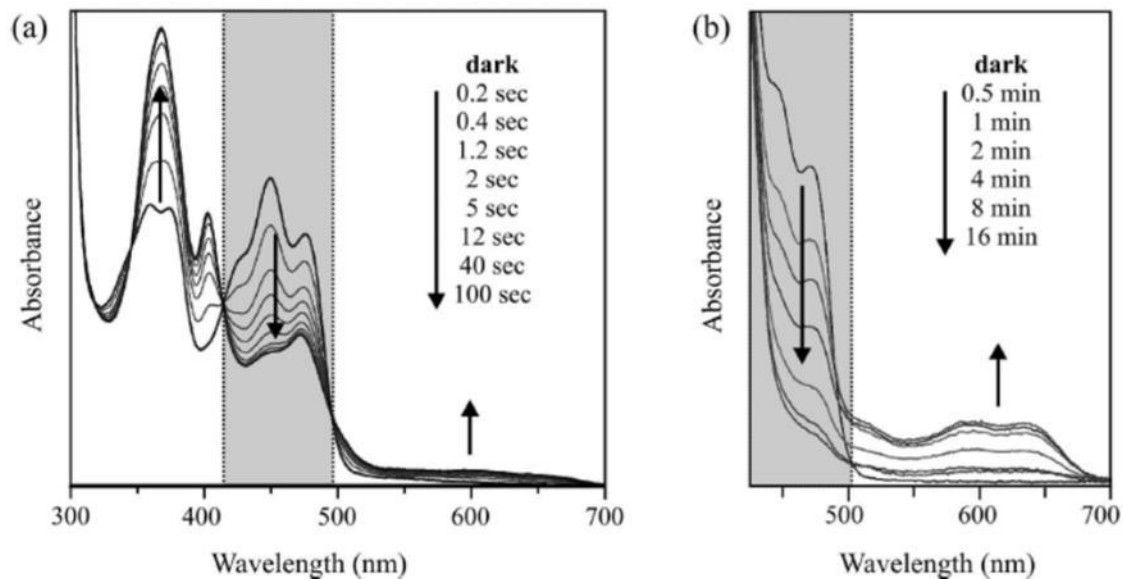


Figure 12. Absorption changes in (a) *Drosophila* (DmCry1) and zebrafish (b) (ZfCRY-DASH) cryptochromes produced by blue light exposure. Lines indicate relative absorbance during varying periods of blue light exposure resulting from the conversion of the fully oxidized form of the flavin chromophore (FAD_{ox}), to the partially reduced radical form ($FAD\cdot^-$ or $FADH\cdot$); gray shaded areas show the region of the spectrum where the fully oxidized form is preferentially excited [adapted from 154].

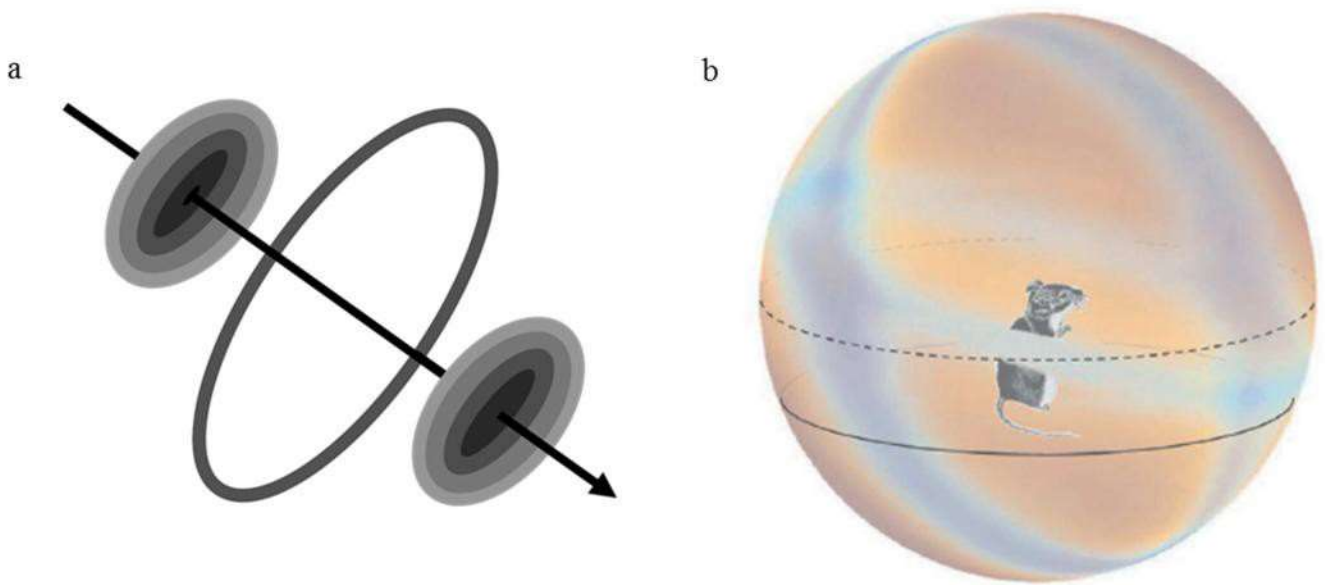


Figure 13. Proposed 3-D patterns of response created by a light-dependent radical pair mechanism. a) Simplified model based on a reduced number of hyperfine interactions within a radical pair system. Black arrow indicates magnetic direction (northern hemisphere) and inversion of the slope of the pattern would be expected in the southern hemisphere, providing the basis for an inclination-based magnetic compass [adapted from 46]. b) Theoretical visual pattern generated by a model tryptophan-flavin radical pair reacting in an Earth-strength magnetic field where the magnetic nuclei are aligned along non-parallel axes. The different color components of the spherical pattern, as indicated by the mouse located inside the sphere, represent the increased and decreased response of photoreceptors which are superimposed on the animal's visual surroundings and could be used to guide magnetic-dependent spatial behaviors [from 53].

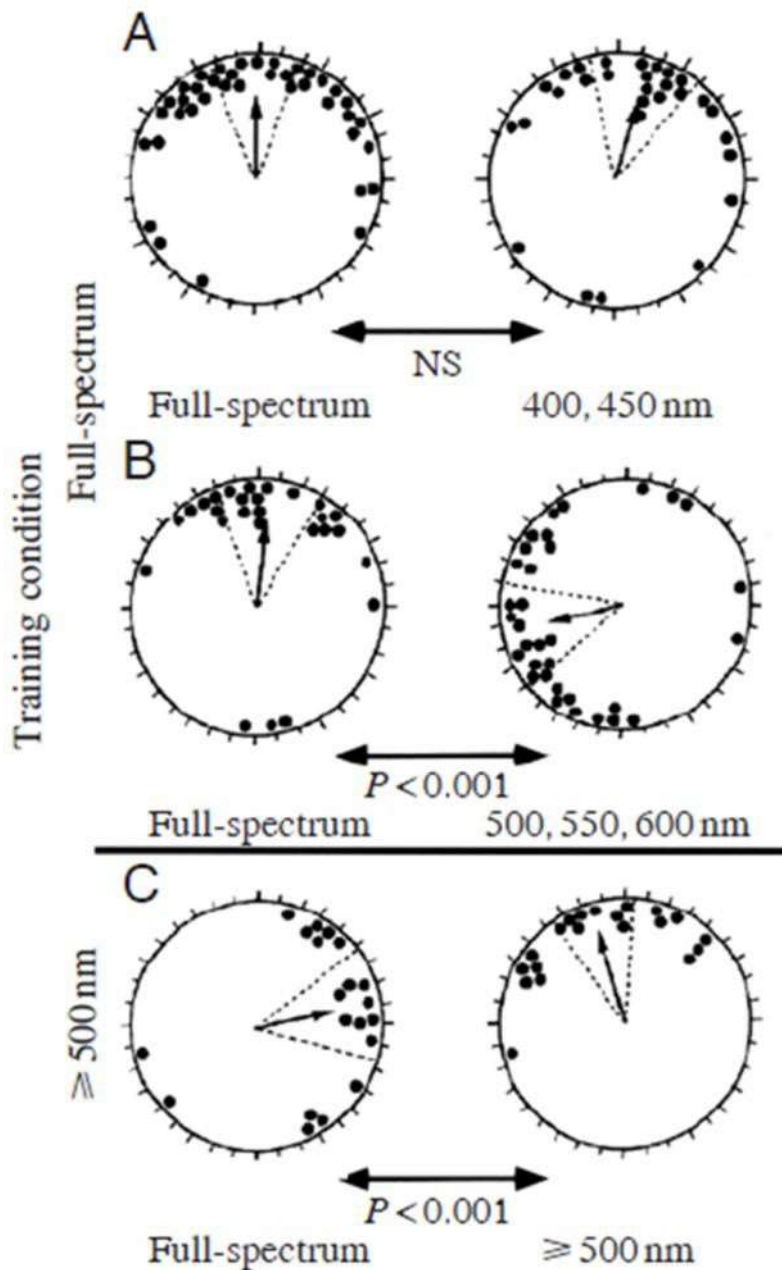


Figure 14. Learned shoreward magnetic compass orientation in red-spotted newts is mediated by a light-dependent magnetic compass. Groups of newts were trained in outdoor tanks under full-spectrum light in different shoreward magnetic directions. When tested individually in visually symmetrical circular arenas, newts exhibited learned magnetic compass orientation, consistent with the shoreward direction under (A, B – left distribution) full-spectrum and short-wavelength (400nm and 450nm) light. B – right distribution) When tested under long wavelength light ($\geq 500\text{nm}$) of equal quantal flux, newts exhibited a 90° *CCW* compass response. Alternatively, when newts were trained and tested under long-wavelength light, shoreward magnetic compass

orientation was restored, similar to response exhibited in (A and (B – left distribution. However, when tested under full-spectrum light, newts exhibited a 90° *CW* shift, providing evidence for a direct effect of light on newt magnetic compass orientation (see text for additional information). All distributions are pooled such that the shoreward direction is at the top of each circle. Each black circle indicates the response from an individual newt from one trial. Black arrows in each distribution represent the mean and the length of the arrow is a measure of the strength of the response. Dotted lines on either side of the mean represent the 95% CI intervals. P-values listed between each distribution come from a Watson U^2 test comparing the degree of clustering, magnitude of scatter, and mean between two distributions. $P < 0.05$ is used to determine if there is a significant difference between the pair of distributions.

Literature Cited

1. Diebel, C.E., et al., *Magnetite defines a vertebrate magnetoreceptor*. *Nature*, 2000. **406**(6793): p. 299-302.
2. Phillips, J.B., *Magnetic compass orientation in the Eastern red-spotted newt (*Notophthalmus viridescens*)*. *Journal of Comparative Physiology A Sensory Neural and Behavioral Physiology*, 1986. **158**(1): p. 103-9.
3. Lohmann, K.J., et al., *Regional magnetic fields as navigational markers for sea turtles*. *Science*, 2001. **294**(5541): p. 364-366.
4. Wiltschko, R. and W. Wiltschko, *Magnetic orientation in animals*. 1995: Springer Berlin.
5. Burda, H., et al., *Magnetic compass orientation in the subterranean rodent *Cryptomys hottentotus* (*Bathyergidae*)*. *Cellular and Molecular Life Sciences*, 1990. **46**(5): p. 528-530.
6. Muheim, R., et al., *Magnetic compass orientation in C57BL/6J mice*. *Learning & Behavior*, 2006. **34**(4): p. 366-373.
7. Phillips, J.B., et al., *Rapid Learning of Magnetic Compass Direction by C57BL/6 Mice in a 4-Armed 'Plus' Water Maze*. *PLOS ONE*, 2013. **8**(8): p. e73112.
8. Malkemper, E.P., et al., *Magnetoreception in the wood mouse (*Apodemus sylvaticus*): influence of weak frequency-modulated radio frequency fields*. *Sci. Rep.*, 2015. **4**.
9. Malkemper, E.P., M.S. Painter, and L. Landler, *Shifted magnetic alignment in vertebrates: Evidence for neural lateralization?* *Journal of Theoretical Biology*, 2016. **399**: p. 141-147.
10. Phillips, J.B. and O. Sayeed, *Wavelength-dependent effects of light on magnetic compass orientation in *Drosophila melanogaster**. *Journal of Comparative Physiology A Sensory Neural and Behavioral Physiology*, 1993. **172**(3): p. 303-8.
11. Dommer, D.H., et al., *Magnetic compass orientation by larval *Drosophila melanogaster**. *Journal of Insect Physiology*, 2008. **54**(4): p. 719-26.
12. Painter, M.S., et al., *Spontaneous magnetic orientation in larval *Drosophila* shares properties with learned magnetic compass responses in adult flies and mice*. *Journal of Experimental Biology*, 2013. **216**: p. 1307-1316.
13. Lohmann, K.J., et al., *Magnetic orientation of spiny lobsters in the ocean: experiments with undersea coil systems*. *Journal of Experimental Biology*, 1995. **198**(Pt 10): p. 2041-2048.
14. Arendse, M. and C. Kruyswijk, *Orientation of *Talitrus saltator* to magnetic fields*. *Netherlands Journal of Sea Research*, 1981. **15**(1): p. 23-32.
15. Gegebar, R.J., et al., *Cryptochrome mediates light-dependent magnetosensitivity in *Drosophila**. *Nature*, 2008. **454**(7207): p. 1014-8.
16. Gegebar, R.J., et al., *Animal cryptochromes mediate magnetoreception by an unconventional photochemical mechanism*. *Nature*, 2010. **463**(7282): p. 804-807.
17. Guerra, P.A., R.J. Gegebar, and S.M. Reppert, *A magnetic compass aids monarch butterfly migration*. *Nature Communications*, 2014. **5**.
18. Fedele, G., et al., *An electromagnetic field disrupts negative geotaxis in *Drosophila* via a CRY-dependent pathway*. *Nat Commun*, 2014. **5**.
19. Phillips, J.B., et al., *Behavioral titration of a magnetic map coordinate*. *Journal of Comparative Physiology A: Neuroethology, Sensory, Neural, and Behavioral Physiology*, 2002. **188**(2): p. 157-160.
20. Fischer, J.H., et al., *Evidence for the use of magnetic map information by an amphibian*. *Animal*

- behaviour, 2001. **62**(1): p. 1-10.
21. Boles, L.C. and K.J. Lohmann, *True navigation and magnetic maps in spiny lobsters*. *Nature*, 2003. **421**(6918): p. 60-63.
 22. Freake, M.J., R. Muheim, and J.B. Phillips, *Magnetic maps in animals: a theory comes of age?* *Quarterly Review of Biology*, 2006. **81**(4): p. 327-347.
 23. Lohmann, K.J. and C.M.F. Lohmann, *Sea turtles, lobsters, and oceanic magnetic maps*. *Marine and Freshwater Behaviour and Physiology*, 2006. **39**(1): p. 49-64.
 24. Lohmann, K.J., C.M.F. Lohmann, and N.F. Putman, *Magnetic maps in animals: nature's GPS*. *Journal of Experimental Biology*, 2007. **210**(21): p. 3697-3705.
 25. Skiles, D.D., *The geomagnetic field its nature, history, and biological relevance*, in *Magnetite Biomineralization and Magnetoreception in Organisms*. 1985, Springer. p. 43-102.
 26. Wiltschko, W. and R. Wiltschko, *Magnetic orientation and magnetoreception in birds and other animals*. *Journal of Comparative Physiology A: Neuroethology, Sensory, Neural, and Behavioral Physiology*, 2005. **191**(8): p. 675-93.
 27. Marhold, S., W. Wiltschko, and H. Burda, *A magnetic polarity compass for direction finding in a subterranean mammal*. *Naturwissenschaften*, 1997. **84**(9): p. 421-423.
 28. Arendse, M., *Magnetic field detection is distinct from light detection in the invertebrates *Tenebrio* and *Talitrus**. 1978.
 29. Wiltschko, R. and W. Wiltschko, *The magnetite-based receptors in the beak of birds and their role in avian navigation*. *Journal of Comparative Physiology A*, 2013. **199**(2): p. 89-98.
 30. Wiltschko, W. and R. Wiltschko, *Magnetic compass of European robins*. *Science*, 1972. **176**(4030): p. 62-64.
 31. Phillips, J.B. and S.C. Borland, *Behavioural evidence for use of a light-dependent magnetoreception mechanism by a vertebrate*. *Nature*, 1992. **359**: p. 142-144.
 32. Vácha, M., T. Puzova, and D. Drstková, *Effect of light wavelength spectrum on magnetic compass orientation in *Tenebrio molitor**. *Journal of Comparative Physiology A: Neuroethology, Sensory, Neural, and Behavioral Physiology*, 2008. **194**(10): p. 853-9.
 33. Phillips, J.B., *Two magnetoreception pathways in a migratory salamander*. *Science*, 1986. **233**(4765): p. 765-767.
 34. Wiltschko, R., et al., *Magnetoreception in birds: different physical processes for two types of directional responses*. *Human Frontier Science Program Journal*, 2007. **1**(1): p. 41-48.
 35. Munro, U., et al., *Evidence for a magnetite-based navigational 'map' in birds*. *Naturwissenschaften*, 1997. **84**(1): p. 26-28.
 36. Phillips, J.B., et al., *'Fixed-axis' magnetic orientation by an amphibian: non-shoreward-directed compass orientation, misdirected homing or positioning a magnetite-based map detector in a consistent alignment relative to the magnetic field?* *Journal of Experimental Biology*, 2002. **205**: p. 3903-3914.
 37. Winklhofer, M., *Magnetoreception*. *Journal of the Royal Society Interface*, 2010. **7**(Suppl 2): p. S131-S134.
 38. Wang, Y., et al., *Bats respond to polarity of a magnetic field*. *Proceedings of the Royal Society B: Biological Sciences*, 2007. **274**(1627): p. 2901-2905.
 39. Kirschvink, J.L., M.M. Walker, and C.E. Diebel, *Magnetite-based magnetoreception*. *Current opinion in neurobiology*, 2001. **11**(4): p. 462-467.
 40. Mora, C.V., et al., *Magnetoreception and its trigeminal mediation in the homing pigeon*. *Nature*, 2004. **432**(7016): p. 508-511.
 41. Zapka, M., et al., *Visual but not trigeminal mediation of magnetic compass information in a*

- migratory bird*. Nature, 2009. **461**: p. 1274 - 1277.
42. Heyers, D., et al., *Magnetic field changes activate the trigeminal brainstem complex in a migratory bird*. Proc Natl Acad Sci USA, 2010. **107**: p. 9394 - 9399.
 43. Wu, L.-Q. and J.D. Dickman, *Magnetoreception in an Avian Brain in Part Mediated by Inner Ear Lagena*. Current Biology, 2011. **21**(5): p. 418-423.
 44. Mouritsen, H. and P.J. Hore, *The magnetic retina: light-dependent and trigeminal magnetoreception in migratory birds*. Current Opinion in Neurobiology, 2012. **22**(2): p. 343-352.
 45. Hiscock, H.G., et al., *The quantum needle of the avian magnetic compass*. Proceedings of the National Academy of Sciences, 2016. **113**(17): p. 4634-4639.
 46. Ritz, T., S. Adem, and K. Schulten, *A model for photoreceptor-based magnetoreception in birds*. Biophysical Journal, 2000. **78**(2): p. 707-718.
 47. Cintolesi, F., et al., *Anisotropic recombination of an immobilized photoinduced radical pair in a 50- μ T magnetic field: a model avian photomagnetoreceptor*. Chemical Physics, 2003. **294**(3): p. 385-399.
 48. Solov'yov, I.A., D.E. Chandler, and K. Schulten, *Magnetic field effects in Arabidopsis thaliana cryptochrome-1*. Biophysical Journal, 2007. **92**(8): p. 2711-2726.
 49. Evans, E.W., et al., *Magnetic field effects in flavoproteins and related systems*. Interface focus, 2013. **3**(5): p. 20130037.
 50. Timmel, C., et al., *Effects of weak magnetic fields on free radical recombination reactions*. Molecular Physics, 1998. **95**(1): p. 71-89.
 51. Brocklehurst, B., *Magnetic fields and radical reactions: recent developments and their role in nature*. Chemical Society Reviews, 2002. **31**(5): p. 301-311.
 52. Maeda, K., et al., *Chemical compass model of avian magnetoreception*. Nature, 2008. **453**(7193): p. 387-390.
 53. Phillips, J.B., R. Muheim, and P.E. Jorge, *A behavioral perspective on the biophysics of the light-dependent magnetic compass: a link between directional and spatial perception?* Journal of Experimental Biology, 2010. **213**(19): p. 3247-3255.
 54. Schulten, K., C.E. Swenberg, and A. Weller, *A biomagnetic sensory mechanism based on magnetic field modulated coherent electron spin motion*. Zeitschrift für Physikalische Chemie, 1978. **111**: p. 1-5.
 55. Diego-Rasilla, F.J., R.M. Luengo, and J.B. Phillips, *Use of a light-dependent magnetic compass for y-axis orientation in European common frog (Rana temporaria) tadpoles*. Journal of Comparative Physiology A: Neuroethology, Sensory, Neural, and Behavioral Physiology, 2013. **199**: p. 1-10.
 56. Foley, L.E., R.J. Gegear, and S.M. Reppert, *Human cryptochrome exhibits light-dependent magnetosensitivity*. Nat Commun, 2011. **2**: p. 356.
 57. Wiltschko, W., R. Wiltschko, and T. Ritz, *The mechanism of the avian magnetic compass*. Procedia Chemistry, 2011. **3**(1): p. 276-284.
 58. Phillips, J.B., P.E. Jorge, and R. Muheim, *Light-dependent magnetic compass orientation in amphibians and insects: candidate receptors and candidate molecular mechanisms*. Journal of The Royal Society Interface, 2010. **7 Suppl 2**: p. S241-56.
 59. Diego-Rasilla, F.J., R.M. Luengo, and J.B. Phillips, *Light-dependent magnetic compass in Iberian green frog tadpoles*. Naturwissenschaften, 2010. **97**(12): p. 1077-1088.
 60. Wiltschko, R., et al., *Light-dependent magnetoreception: orientation behaviour of migratory*

- birds under dim red light*. J Exp Biol, 2008. **211**(Pt 20): p. 3344-50.
61. Freake, M.J. and J.B. Phillips, *Light-dependent shift in bullfrog tadpole magnetic compass orientation: evidence for a common magnetoreception mechanism in anuran and urodele amphibians*. Ethology, 2005. **111**(3): p. 241-254.
 62. Vácha, M. and H. Soukopova, *Magnetic orientation in the mealworm beetle Tenebrio and the effect of light*. J Exp Biol, 2004. **207**(Pt 7): p. 1241-8.
 63. Muheim, R., J. Backman, and S. Akesson, *Magnetic compass orientation in European robins is dependent on both wavelength and intensity of light*. Journal of Experimental Biology, 2002. **205**(Pt 24): p. 3845-3856.
 64. Deutschlander, M.E., J.B. Phillips, and S.C. Borland, *The case for light-dependent magnetic orientation in animals*. Journal of Experimental Biology, 1999. **202** (Pt 8): p. 891-908.
 65. Ritz, T., D.H. Dommer, and J.B. Phillips, *Shedding light on vertebrate magnetoreception*. Neuron, 2002. **34**(4): p. 503-506.
 66. Phillips, J.B. and S.C. Borland, *Wavelength specific effects of light on magnetic compass orientation of the eastern red-spotted newt Notophthalmus viridescens*. Ethology Ecology & Evolution, 1992. **4**(1): p. 33-42.
 67. Nießner, C., et al., *Avian Ultraviolet/Violet cones identified as probable magnetoreceptors*. PLoS ONE, 2011. **6**(5): p. e20091.
 68. Solov'yov, I.A., H. Mouritsen, and K. Schulten, *Acuity of a cryptochrome and vision-based magnetoreception system in birds*. Biophysical Journal, 2010. **99**(1): p. 40-49.
 69. Hill, E. and T. Ritz, *Can disordered radical pair systems provide a basis for a magnetic compass in animals?* Journal of The Royal Society Interface, 2010. **7**(Suppl 2): p. S265-S271.
 70. Lau, J.C., et al., *Effects of disorder and motion in a radical pair magnetoreceptor*. Journal of The Royal Society Interface, 2009: p. rsif20090399.
 71. Lau, J.C.S., C.T. Rodgers, and P.J. Hore, *Compass magnetoreception in birds arising from photo-induced radical pairs in rotationally disordered cryptochromes*. Journal of the Royal Society Interface, 2012. **9**: p. 3329–3337.
 72. Muheim, R., S. Sjöberg, and A. Pinzon-Rodriguez, *Polarized light modulates light-dependent magnetic compass orientation in birds*. Proceedings of the National Academy of Sciences, 2016. **113**(6): p. 1654-1659.
 73. Schulten, K., et al., *Magnetic field dependence of the geminate recombination of radical ion pairs in polar solvents*. Zeitschrift für Physikalische Chemie, 1976. **101**(1-6): p. 371-390.
 74. Timmel, C.R. and K.B. Henbest, *A study of spin chemistry in weak magnetic fields*. Philosophical Transactions of the Royal Society of London A: Mathematical, Physical and Engineering Sciences, 2004. **362**(1825): p. 2573-2589.
 75. Vácha, M., D. Drštková, and T. Půžová, *Tenebrio beetles use magnetic inclination compass*. Naturwissenschaften, 2008. **95**(8): p. 761-765.
 76. Wiltschko, W. and R. Wiltschko, *Light-dependent magnetoreception in birds: the behaviour of European robins, Erithacus rubecula, under monochromatic light of various wavelengths and intensities*. J Exp Biol, 2001. **204**(Pt 19): p. 3295-302.
 77. Wiltschko, W. and R. Wiltschko, *Magnetoreception in birds: two receptors for two different tasks*. Journal of Ornithology, 2007. **148**(Suppl 1): p. S61 - S76.
 78. Walcott, C. and R.P. Green, *Orientation of homing pigeons altered by a change in the direction of an applied magnetic field*. Science, 1974. **184**(133): p. 180-2.
 79. Chaves, I., et al., *The cryptochromes: blue light photoreceptors in plants and animals*. Annual review of plant biology, 2011. **62**: p. 335-364.
 80. Maeda, K., et al., *Magnetically sensitive light-induced reactions in cryptochrome are consistent*

- with its proposed role as a magnetoreceptor*. Proceedings of the National Academy of Sciences, 2012. **109**(13): p. 4774-4779.
81. Rodgers, C.T. and P.J. Hore, *Chemical magnetoreception in birds: The radical pair mechanism*. Proceedings of the National Academy of Sciences, 2009. **106**(2): p. 353-360.
 82. Lau, J.C., C.T. Rodgers, and P. Hore, *Compass magnetoreception in birds arising from photo-induced radical pairs in rotationally disordered cryptochromes*. Journal of The Royal Society Interface, 2012. **9**(77): p. 3329-3337.
 83. Liedvogel, M., et al., *Chemical magnetoreception: bird cryptochrome 1a is excited by blue light and forms long-lived radical-pairs*. PLOS ONE, 2007. **2**(10): p. e1106.
 84. Biskup, T., et al., *Direct Observation of a Photoinduced Radical Pair in a Cryptochrome Blue-Light Photoreceptor*. Angewandte Chemie International Edition, 2009. **48**(2): p. 404-407.
 85. Yang, H.-Q., et al., *The C termini of Arabidopsis cryptochromes mediate a constitutive light response*. Cell, 2000. **103**(5): p. 815-827.
 86. Partch, C.L. and A. Sancar, *Cryptochromes and circadian photoreception in animals*. Methods in enzymology, 2005. **393**: p. 726-745.
 87. Helfrich-Förster, C., et al., *The circadian clock of fruit flies is blind after elimination of all known photoreceptors*. Neuron, 2001. **30**(1): p. 249-261.
 88. Rieger, D., R. Stanewsky, and C. Helfrich-Förster, *Cryptochrome, compound eyes, Hofbauer-Buchner eyelets, and ocelli play different roles in the entrainment and masking pathway of the locomotor activity rhythm in the fruit fly Drosophila melanogaster*. Journal of Biological Rhythms, 2003. **18**(5): p. 377-391.
 89. Helfrich-Förster, C., *Neurobiology of the fruit fly's circadian clock*. Genes, Brain and Behavior, 2005. **4**(2): p. 65-76.
 90. Dodson, C.A., P.J. Hore, and M.I. Wallace, *A radical sense of direction: signalling and mechanism in cryptochrome magnetoreception*. Trends in Biochemical Sciences, 2013. **38**(9): p. 435-446.
 91. Van Gelder, R.N., *Timeless genes and jetlag*. Proceedings of the National Academy of Sciences, 2006. **103**(47): p. 17583-17584.
 92. Partch, C.L. and A. Sancar, *Photochemistry and Photobiology of Cryptochrome Blue-light Photopigments: The Search for a Photocycle*. Photochemistry and Photobiology, 2005. **81**(6): p. 1291-1304.
 93. Sancar, A., *Regulation of the mammalian circadian clock by cryptochrome*. Journal of Biological Chemistry, 2004. **279**(33): p. 34079-34082.
 94. Sancar, A., *Photolyase and cryptochrome blue-light photoreceptors*. Adv Protein Chem, 2004. **69**: p. 73-100.
 95. Sancar, A., *Cryptochrome: the second photoactive pigment in the eye and its role in circadian photoreception*. Annual review of biochemistry, 2000. **69**(1): p. 31-67.
 96. Van der Horst, G.T.J., et al., *Mammalian Cry1 and Cry2 are essential for maintenance of circadian rhythms*. NATURE-LONDON-, 1999: p. 627-629.
 97. Thresher, R.J., et al., *Role of mouse cryptochrome blue-light photoreceptor in circadian photoresponses*. Science, 1998. **282**(5393): p. 1490-1494.
 98. Shearman, L.P., et al., *Interacting molecular loops in the mammalian circadian clock*. Science, 2000. **288**(5468): p. 1013-1019.
 99. Hall, J.C., *Cryptochromes: sensory reception, transduction, and clock functions subserving circadian systems*. Current opinion in neurobiology, 2000. **10**(4): p. 456-466.
 100. Emery, P., et al., *CRY, a Drosophila clock and light-regulated cryptochrome, is a major contributor to circadian rhythm resetting and photosensitivity*. Cell, 1998. **95**(5): p. 669-679.

101. Emery, P., et al., *Drosophila cryptochromes: A unique circadian-rhythm photoreceptor*. Nature, 2000. **404**: p. 456-457.
102. Emery, P., et al., *Drosophila CRY is a deep brain circadian photoreceptor*. Neuron, 2000. **26**(2): p. 493-504.
103. Stanewsky, R., et al., *The cryb mutation identifies cryptochrome as a circadian photoreceptor in Drosophila*. Cell, 1998. **95**(5): p. 681-692.
104. Levy, O., et al., *Light-responsive cryptochromes from a simple multicellular animal, the coral Acropora millepora*. Science, 2007. **318**(5849): p. 467-470.
105. Light, P., M. Salmon, and K. Lohmann, *Geomagnetic orientation of loggerhead sea turtles: evidence for an inclination compass*. Journal of Experimental Biology, 1993. **182**(1): p. 1-10.
106. Marhold, S., et al., *Magnetic orientation in common mole-rats from Zambia*. Orientation and navigation—birds, humans and other animals, 1997: p. 5-1.
107. Wiltschko, W., et al., *Magnetite-based magnetoreception: the effect of repeated pulsing on the orientation of migratory birds*. Journal of Comparative Physiology A Sensory Neural and Behavioral Physiology, 2007. **193**(5): p. 515-522.
108. Martin, H. and M. Lindauer, *The effect of the Earth's magnetic field on gravity orientation in the honey bee*. Apis mellifica, 1977: p. 145-187.
109. Wiltschko, W., *Further analysis of the magnetic compass of migratory birds*, in *Animal migration, navigation, and homing*. 1978, Springer. p. 302-310.
110. Wiltschko, W., et al., *The magnetic compass of domestic chickens, Gallus gallus*. Journal of Experimental Biology, 2007. **210**(Pt 13): p. 2300-10.
111. Winklhofer, M., et al., *Avian magnetic compass can be tuned to anomalously low magnetic intensities*. Proceedings of the Royal Society B: Biological Sciences, 2013. **280**(1763).
112. Rodgers, C.T., et al., *Low-field optically detected EPR spectroscopy of transient photoinduced radical pairs*. The Journal of Physical Chemistry A, 2005. **109**(23): p. 5035-5041.
113. Ritz, T., et al., *Resonance effects indicate a radical-pair mechanism for avian magnetic compass*. Nature, 2004. **429**(6988): p. 177-180.
114. Ritz, T., et al., *Magnetic compass of birds is based on a molecule with optimal directional sensitivity*. Biophysical Journal, 2009. **96**: p. 3451 - 3457.
115. Vácha, M., T. Puzova, and M. Kviclova, *Radio frequency magnetic fields disrupt magnetoreception in American cockroach*. Journal of Experimental Biology, 2009. **212**(21): p. 3473-3477.
116. Keary, N., et al., *Oscillating magnetic field disrupts magnetic orientation in Zebra finches, Taeniopygia guttata*. Front Zool, 2009. **6**: p. 25.
117. Landler, L., et al., *Spontaneous magnetic alignment by yearling snapping turtles: rapid association of radio frequency dependent pattern of magnetic input with novel surroundings*. PLOS ONE, 2015. **10**(5): p. e0124728.
118. Henbest, K.B., et al., *Radio frequency magnetic field effects on a radical recombination reaction: a diagnostic test for the radical pair mechanism*. Journal of the American Chemical Society, 2004. **126**(26): p. 8102-8103.
119. Kirschvink, J.L., et al., *Magnetite in human tissues: a mechanism for the biological effects of weak ELF magnetic fields*. Bioelectromagnetics, 1992. **13**(S1): p. 101-113.
120. Thalau, P., et al., *The magnetic compass mechanisms of birds and rodents are based on different physical principles*. Journal of The Royal Society Interface, 2006. **3**(9): p. 583-587.
121. Wiltschko, R. and W. Wiltschko, *Magnetoreception*. Bioessays, 2006. **28**(2): p. 157-168.
122. Dommer, D.H., *Behavioral Investigation of the Light-Dependent Magnetoreception Mechanism of Drosophila melanogaster*. Dissertation - Virginia Polytechnic Institute and State University, 2008.

123. Harkins, T.T. and C.B. Grissom, *Magnetic field effects on B12 ethanolamine ammonia lyase: evidence for a radical mechanism*. *Science*, 1994. **263**(5149): p. 958-960.
124. Hore, P. and H. Mouritsen, *The Radical-Pair Mechanism of Magnetoreception*. *Annual review of biophysics*, 2016(0).
125. Aubert, C., et al., *Intraprotein radical transfer during photoactivation of DNA photolyase*. *Nature*, 2000. **405**(6786): p. 586-590.
126. Liedvogel, M. and H. Mouritsen, *Cryptochromes—a potential magnetoreceptor: what do we know and what do we want to know?* *Journal of the Royal Society Interface*, 2010. **7**(Suppl 2): p. S147-S162.
127. Öztürk, N., et al., *Animal Type 1 Cryptochromes ANALYSIS OF THE REDOX STATE OF THE FLAVIN COFACTOR BY SITE-DIRECTED MUTAGENESIS*. *Journal of Biological Chemistry*, 2008. **283**(6): p. 3256-3263.
128. Solov'yov, I.A. and K. Schulten, *Magnetoreception through cryptochrome may involve superoxide*. *Biophysical Journal*, 2009. **96**(12): p. 4804-4813.
129. Yoshii, T., M. Ahmad, and C. Helfrich-Förster, *Cryptochrome mediates light-dependent magnetosensitivity of Drosophila's circadian clock*. *PLoS Biol*, 2009. **7**(4): p. e1000086.
130. Nießner, C., et al., *Cryptochrome 1 in retinal cone photoreceptors suggests a novel functional role in mammals*. *Scientific reports*, 2016. **6**.
131. Becker, G. and U. Speck, *Examinations on magnetic field orientation in Dipterans*. *Z Vergl Physiol*, 1964. **49**: p. 301-340.
132. Vácha, M., M. Kvalcova, and T. Puzova, *American cockroaches prefer four cardinal geomagnetic positions at rest*. *Behaviour*, 2010. **147**(4): p. 425-440.
133. Begall, S., et al., *Magnetic alignment in mammals and other animals*. *Mammalian Biology*, 2013. **78**: p. 10-20.
134. Prato, F.S., et al., *Light alters nociceptive effects of magnetic field shielding in mice: intensity and wavelength considerations*. *Journal of the Royal Society Interface*, 2009. **6**(30): p. 17-28.
135. Ahmad, M., et al., *Magnetic intensity affects cryptochrome-dependent responses in Arabidopsis thaliana*. *Planta*, 2007. **225**(3): p. 615-624.
136. Helbig, A.J., *Inheritance of migratory direction in a bird species: a cross-breeding experiment with SE-and SW-migrating blackcaps (Sylvia atricapilla)*. *Behavioral Ecology and Sociobiology*, 1991. **28**(1): p. 9-12.
137. Helbig, A., et al., *Inheritance of a novel migratory direction in central European blackcaps*. *Naturwissenschaften*, 1994. **81**(4): p. 184-186.
138. Munro, U., et al., *Effect of wavelength of light and pulse magnetisation on different magnetoreception systems in a migratory bird*. *Australian journal of Zoology*, 1997. **45**(2): p. 189-198.
139. Thalau, P., et al., *Magnetic compass orientation of migratory birds in the presence of a 1.315 MHz oscillating field*. *Naturwissenschaften*, 2005. **92**: p. 86 - 90.
140. Carr, A., *Rips, FADS, and little loggerheads*. *Bioscience*, 1986. **36**(2): p. 92-100.
141. Lohmann, K.J., N.F. Putman, and C.M.F. Lohmann, *The magnetic map of hatchling loggerhead sea turtles*. *Current Opinion in Neurobiology*, 2012. **22**(2): p. 336-42.
142. Lohmann, K.J. and C.M.F. Lohmann, *A light-independent magnetic compass in the leatherback sea turtle*. *Biological Bulletin*, 1993. **185**(1): p. 149-151.
143. Lohmann, K.J. and C.M.F. Lohmann, *Detection of magnetic inclination angle by sea turtles: a possible mechanism for determining latitude*. *Journal of Experimental Biology*, 1994. **194**(1): p. 23-32.
144. Irwin, W.P. and K.J. Lohmann, *Disruption of magnetic orientation in hatchling loggerhead sea turtles by pulsed magnetic fields*. *J Comp Physiol A Neuroethol Sens Neural Behav Physiol*,

2005. **191**(5): p. 475-80.
145. Deutschlander, M.E., S.C. Borland, and J.B. Phillips, *Extraocular magnetic compass in newts*. Nature, 1999. **400**(6742): p. 324-325.
 146. Freire, R., et al., *Chickens orient using a magnetic compass*. Current Biology, 2005. **15**(16): p. R620.
 147. Collett, T., *Landmark learning and guidance in insects*. Philosophical Transactions of the Royal Society of London B Biological Sciences, 1992: p. 295-303.
 148. Collett, T.S. and J. Baron, *Biological compasses and the coordinate frame of landmark memories in honeybees*. Nature, 1994. **368**(6467): p. 137-140.
 149. Červený, J., et al., *Directional preference may enhance hunting accuracy in foraging foxes*. Biology Letters, 2011. **7**(3): p. 355-357.
 150. Phillips, J.B., *Magnetic Navigation*. Journal of Theoretical Biology, 1996. **180**(4): p. 309-319.
 151. Willis, J., et al., *Spike dives of juvenile southern bluefin tuna (*Thunnus maccoyii*): a navigational role?* Behavioral Ecology and Sociobiology, 2009. **64**(1): p. 57-68.
 152. Winklhofer, M. and J.L. Kirschvink, *A quantitative assessment of torque-transducer models for magnetoreception*. Journal of the Royal Society Interface, 2010. **7**(Suppl 2): p. S273-S289.
 153. Wiltschko, W. and R. Wiltschko, *Magnetic orientation in birds*. Journal of Experimental Biology, 1996. **199**(Pt 1): p. 29-38.
 154. Zikihara, K., et al., *Involvement of Electron Transfer in the Photoreaction of Zebrafish Cryptochrome-DASH⁺*. Photochemistry and Photobiology, 2008. **84**(4): p. 1016-1023.

Chapter II. Spontaneous magnetic orientation in larval *Drosophila* shares properties with learned magnetic compass responses in adult flies and mice

Michael S. Painter¹, David H. Dommer², William W. Altizer¹, Rachel Muheim³, and John B. Phillips¹

¹Department of Biological Sciences, Virginia Tech, Blacksburg, Virginia, United States of America

²Department of Science and Mathematics, Mount Olive College, 652 R.B. Butler Drive Mount Olive, NC 28365, USA

³Department of Biology, Lund Vision Group, Lund University, Lund 223 62, Sweden

This manuscript has been published as: Painter, M.S., Dommer, D.H., Altizer, W.W., Muheim, R., and Phillips, J.B. (2013). Spontaneous magnetic orientation in larval *Drosophila* shares properties with learned magnetic compass responses in adult flies and mice. *Journal of Experimental Biology* (216),1307-1316.

Abstract

We provide evidence for spontaneous quadramodal magnetic orientation in a larval insect. Second instar Berlin, Canton-S, and Oregon-R X Canton-S strains of *Drosophila melanogaster* exhibited quadramodal orientation with clusters of bearings along the four anti-cardinal compass directions (i.e. 45°, 135°, 225°, 315°). In double-blind experiments, Canton-S *Drosophila* larvae exhibited quadramodal orientation in the presence of an earth-strength magnetic field, while this response was abolished when the horizontal component of the magnetic field was cancelled, indicating that the quadramodal behavior is dependent on magnetic cues, and may reflect properties of the underlying magnetoreception mechanism. A reanalysis of data from studies of learned magnetic compass orientation by adult *Drosophila melanogaster* and C57BL/6 mice suggest that the magnetoreception mechanism(s) mediating these responses exhibits a quadramodal pattern of response similar to that evident in the spontaneous orientation of larval flies. Therefore, characterizing the mechanism(s) of magnetoreception in flies may hold the key to understanding the magnetic sense in a wide array of terrestrial organisms.

Introduction

The role of geomagnetic field cues in behaviors such as navigation, migration, homing, and passive alignment have been documented in a diverse range of taxa [1-9]. While the adaptive significance of magnetoreception for large-scale spatial tasks such as migration and homing is intuitive, the

significance of magnetic alignment behavior, defined as non-goal-directed alignment of the body axis with respect to the magnetic field, remains unclear [10]. Furthermore, although theoretical and empirical evidence has provided insight into the molecular and biophysical mechanisms underlying magnetoreception, the specific mechanism(s) mediating magnetic alignment behavior have not been identified.

Adult insects have provided a number of examples of alignment behaviors, first reported in termites that exhibited a tendency to align their body axes quadramodally along the cardinal compass directions (i.e. N, S, E, or W) in their natural environment [11]. In laboratory studies, two species of termites (Termitidae) showed a quadramodal distribution of body axis alignments along the cardinal compass directions that shifted when the magnetic field was deflected by strong magnets, providing the first evidence that quadramodal alignment was mediated by information derived from the external magnetic field [reviewed by 1]. Additional evidence for quadramodal magnetic alignment in termites has come from studies of gallery building behavior [12].

Quadramodal magnetic alignment along the cardinal compass directions was subsequently documented in adults of several Dipteran species, i.e. blowflies (*Calliphora erythrocephala*), houseflies (*Musca domestica*), fruit flies (*Drosophila melanogaster*) [1, 13, 14], as well as in honeybees (*Apis mellifera*) [15]. A more recent study of resting American cockroaches (*Periplaneta americana*) also found a quadramodal magnetic preference coinciding with the cardinal compass axes [16].

Although a seemingly widespread behavior among insects, the adaptive significance of quadramodal magnetic alignment remains unclear. In some cases, like in eusocial termites, quadramodal gallery building may represent an efficient mechanism for organizing the activities

of a large and spatially distributed workforce in subterranean environments devoid of alternative cues. At the level of the individual, encoding changes in direction of movement with respect to a global reference system provided by the geomagnetic field could increase the accuracy of a path integration system [17, 18].

Alternatively (or in addition), the quadramodal response could reflect properties of the sensory mechanism(s) responsible for detecting the geomagnetic field. In terrestrial organisms there is evidence for two magnetoreception mechanisms sensitive to earth-strength magnetic fields [4, 19-21]. One mechanism relies on single domain or superparamagnetic crystals of biogenic magnetite [22-29]. A mechanical force resulting from the rotation or torque experienced by single domain magnetite particles in different relative alignments to the ambient magnetic field could directly or indirectly affect ion channel permeability. Alternatively, the local magnetic field generated by a magnetite particle that is free to rotate, tracking the alignment of the external field, could alter the rate of intracellular free-radical reactions that, in turn, affect the membrane potential [30, 31]. In the case of superparamagnetic magnetite that lack a stable magnetic moment, the magnetic field could interact with aggregations of crystals that produce attractive or repulsive forces resulting in mechanical stress on the surrounding cell membrane generating nerve impulses [32].

The second magnetoreception mechanism is based on a light-dependent process presumed to involve a specialized class of photopigments that form long-lived radical pair intermediates [19, 33-37]. In the light-dependent mechanism, the alignment of the magnetic field is proposed to affect the quantum spin dynamics of a photo-induced radical pair, altering the response of specialized photoreceptors to light. As a consequence, the magnetic field may be perceived as a 'visual' pattern of light intensity or color superimposed on the animal's surroundings that is fixed in alignment relative to the magnetic field [35, 38, 39].

Previous studies have led to conflicting conclusions about the mechanism of magnetoreception in insects. For example, Kirschvink (1981) showed that the effects of changes in magnetic field intensity on the strength of quadramodal orientation of honeybees obeys the Langevin function which relates the variability in the alignment of single domain particles relative to an external magnetic field to the opposing effects of thermal agitation [40]. These findings are consistent with a magnetite-based mechanism involving single domain crystals of magnetite; [but see 6].

In contrast, studies of the effects of light on learned magnetic compass orientation by adult male *Drosophila melanogaster* and mealworm beetles (*Tenebrio molitor*) have shown a wavelength-dependent 90° shift in orientation that is consistent with a light-dependent (presumably radical pair-based) magnetic compass Phillips [41, 42]. A similar light-dependent 90° shift in orientation in amphibians has been shown to result from a direct effect of light on the underlying magnetoreception mechanism, consistent with the involvement of a radical pair based mechanism. Interestingly, studies of adult *Drosophila* conditioned to a strong magnetic anomaly (10X the geomagnetic field strength) have also provided evidence for a light-dependent mechanism [43, 44; and see Discussion]. However, the possibility that light-dependent effects on compass orientation could result from an interaction between a non-light-dependent (e.g., magnetite-based) magnetic compass and non-magnetic, photoreceptor-based input cannot be excluded [31, 45, 46].

Here we report the first evidence for a quadramodal magnetic alignment response in a larval insect, second instar *Drosophila melanogaster*. Furthermore, we provide a reanalysis of data from an earlier study of adult *Drosophila melanogaster* [41] and male C57BL/6 mice [47] suggesting that a quadramodal pattern of response may be a property of the magnetoreception mechanism that underlies not only the spontaneous quadramodal orientation of larval flies, but also learned magnetic compass orientation by adult *Drosophila* and adult C57BL/6 mice.

Materials and Methods

Stocks

Berlin and Canton-S wild-type strains of *Drosophila melanogaster*, obtained from The Bloomington Stock Center, Indiana, and Oregon-R X Canton-S wild-type crosses were maintained at the testing facility. Strains were selected based on previous studies of adult *Drosophila* magnetic compass orientation [see 41] and magneto-sensitivity responses [see 43]. All adult strains were reared in 200 ml plastic bottles containing 50ml of Instant Carolina Drosophila Media (Formula 424 Blue) and 35ml distilled water. Dry active granulated yeast was added to the surface of the media and a partially submerged laboratory tissue was inserted in the bottom of each bottle to provide adults with a dry substrate. Every 7 days 100-150 adult flies were transferred to fresh bottles and once every four weeks adults were transferred to fresh bottles containing 1% Penicillin-Streptomycin solution to inhibit bacterial growth and maintain colony health. Flies were reared at 23 ± 2 °C, relative humidity of $35 \pm 10\%$, and maintained under a 12:12 hour light/dark cycle produced by two 100 W incandescent bulbs.

Rearing vials

Larvae were reared in vials made of Pyrex glass (Kimble Chase Opticlear: 25 cm diameter, 95 cm long) that transmits UV light down to ~ 320 nm. Fresh vials containing a media consisting of distilled water, degerminated yellow cornmeal, unsulphured molasses, and agar were prepared every 10 days and stored in a refrigerator. In preparation for use, vials were removed from the refrigerator, plugged with a cotton stopper and allowed to acclimate to room temperature (23 ± 2 °C) for a period of ~ 2 h, at which point the surface of the media was partially covered with dry granulated yeast and scored with a metal probe to facilitate egg deposition. Approximately 20-25

adult flies were passively transferred from a rearing bottle to each vial. The outside of each vial was cleaned with a laboratory tissue to remove fingerprints, and transferred into the rearing/testing enclosure.

Rearing and testing enclosure

Both rearing and testing took place in the same light-tight, environmentally controlled, radio-frequency shielded enclosure (Lindgren Enclosures, Inc. Model #12W-2/2-I). A “floating” floor supported at the edges of the experimental chamber helped to uncouple vibrations caused by the observer inside the chamber from the experimental apparatus. Environmental conditions were maintained at 20.5 ± 2.5 °C and a relative humidity of $30 \pm 25\%$ controlled by a portable air conditioner unit (MovinCool Office Pro 12) and dehumidifier (Ebac Industrial Products, Freestar model) located outside the shielded enclosure. Power was supplied by a custom-built six-channel power supply (Design Solutions LLC) located outside the enclosure. Wires entering the shielded enclosure passed through RF filters (ETS-Lindgren, model #EC-2005-1C) mounted on the outside of the enclosure shield (100 dB attenuation from 150 kHz to 10 GHz).

Rearing

Vials containing adult egg layers were transported into the experimental enclosure and placed vertically in the center of three horizontal Merritt coils, two aligned parallel and one perpendicular to geomagnetic north [North-South magnetic axis]. This coil design allows for the cancellation of the horizontal component of the geomagnetic field, achieved by one of the two coils aligned on the north-south axis, while leaving the vertical component unchanged. The two remaining coils are then used to produce a magnetic field aligned in one of four cardinal compass directions (i.e. magnetic north = N, S, E, W) with inclinations and total intensities similar to that of the ambient

magnetic field. In the current experiments, all rearing vials experienced the same alignment of magnetic north (mN = topographic N) prior to testing (total intensity $48,100 \pm 900$ nT, inclination $59.5 \pm 1^\circ$). Eggs laid in the vials were allowed to develop to the late second instar stage (130-160 total h).

Rearing vials were exposed to monochromatic UV light (365 nm, 12 nm bandwidth) produced by six Nichia UV light-emitting diodes (LEDs) (NSHU #550A) on a 24:0 hour light/dark cycle from a circular light source centered above the rearing apparatus. Three layers of UV-transmitting frosted mylar diffusers located between the light source and the tops of the coil elements ensured that the UV light reaching each vial was non-directional. Light intensity reaching the top of each vial was set to 10.1 ± 0.05 log quanta/cm²/s using a Keithly RFA 486 picoammeter with a calibrated United Detector Technology photodiode.

Testing

The spontaneous directional responses of individual second instar larvae were observed on 150 mm diameter plastic Petri plates filled with 60 ml of a distilled water, grape juice, agar, and sugar solution. Plates were covered and allowed to cool to room temperature prior to testing. The agar concentration prevented larvae from burrowing into the testing plate, restricting them to movement along the plate's surface. Using an incandescent headlamp equipped with a 630 nm long-pass filter, the observer entered the testing enclosure and removed the appropriate rearing vial from the rearing apparatus. A non-magnetic stainless steel probe was used to remove the media from the rearing vial which was then placed into a 40% sucrose solution that helped to separate larvae from the rearing media. Fine bristled paint brushes were used to collect second instar larvae floating on the top of the sucrose solution. The larvae were then cleaned of residual media and sucrose in a

distilled water bath and placed together in the center of an acclimation plate (identical to the testing plates). Once 12-15 larvae were collected, the acclimation plate was covered and placed inside of a light-tight black felt bag to minimize light exposure prior to testing trials. Larvae remained on the acclimation plate until tested; however, no larvae were tested that had remained on the plate for longer than 60 minutes.

Using a paintbrush moistened with distilled water, an individual larva was transferred from the acclimation plate to the center of the testing plate and immediately covered with an opaque 3 cm high x 1.5 cm diameter plastic cap that served as a release device. The testing plate was then lowered into a circular plate holder centered inside the testing coil elements and aligned with a reference mark at geomagnetic north. The testing plate was illuminated with diffuse monochromatic 365 nm light from an overhead circular light source identical to that in the rearing apparatus. The light intensity was adjusted to 10.1 ± 0.05 log quanta/cm²/s at the surface of the testing plate, equivalent to the intensities experienced during rearing. After 30 s, the release device was removed from the testing plate and the larva was allowed to move freely on the surface of the testing plate. In all trials, larvae were observed from a fixed position approximately 0.5 m from the center of the testing arena. Directional responses were recorded once the larvae crossed a 30 mm scoring radius, at which point the testing plate was immediately removed from the testing arena, and placed on a 360° circular template. The position of each larva was then transferred to the circular template to create a permanent record of the larvae's directional response. Tests were terminated and no directional responses were recorded if a larva failed to reach the 30 mm scoring boundary within 8 min, was found to have crawled inside the opaque release cap when it was removed, burrowed into the surface of the testing media, or if an auditory or vibratory disturbance (i.e. any noticeable disturbance from within or outside the testing enclosure) occurred during the

trial. The alignment of magnetic north was changed between trials (i.e. mN at geographic N, S, E, or W). Testing coil configurations and conditions were identical to those described for the rearing coil design. Overall, approximately equal numbers of larvae were tested in each of the four magnetic field alignments, with magnetic north at topographic North, East, South or West (each larva tested only once). Pooling bearings from larvae tested in the four magnetic field alignments was used to help to identify any effects of non-magnetic biases on the distribution of bearings.

A Rayleigh test was used to test for a non-random clustering of bearings. To test for quadramodal orientation, each bearing was doubled twice (modulo 360°) [48], and the resulting distribution of quadrupled bearings was analyzed using the Rayleigh test.

Double-Blind Horizontal Cancelled Field Experiment

Horizontal cancelled field experiments were carried out with Canton-S strain larvae to determine whether magnetic cues were mediating the quadramodal orientation. All protocols for rearing and testing remained identical to those described above. However, during this experiment, a second investigator located outside the testing enclosure controlled a switch that prevented power from reaching the stimulus coils. This eliminated the horizontal component of the magnetic field inside the testing apparatus to less than 1% of the natural geomagnetic field ($\sim 15 \text{ nT} \pm 6 \text{ nT}$), and prevented the animals to use any directional information provided by the magnetic field. Trials were conducted double-blind, with the observer unaware of the magnetic conditions (i.e. coils used to generate magnetic fields were powered or unpowered), while the second investigator was unaware of the directional responses of the larva. Communication between the observer and second investigator was restricted to indicating the beginning and end of each trial, so the magnetic field condition could be reset for the next trial. The presence or absence of the horizontal

component of the magnetic field was determined by the second investigator, while the alignment of the horizontal component (if present) was set by the observer using a switchbox located inside the testing enclosure.

Reanalysis of Adult *Drosophila* Data [see 41 for detailed methods].

Training

Groups of 4 to 8-day old adult Oregon-R *Drosophila melanogaster* were transferred into Pryex bottles and placed in a training enclosure equipped with a 365 nm overhead light source in a natural magnetic field. Bottles were placed such that light from above reflected off a central pyramid and into one of four arms corresponding with magnetic north, south, east and west. Each arm contained up to four bottles. The intensity of 365 nm (60 nm bandwidth) light reaching flies in the bottles was $10.0 \log$ quanta/cm²/s. Each group was trained for 6-10 days.

Testing

After training, groups of flies were tested in a radially symmetrical 8-arm maze made of opaque Plexiglas under diffuse 365 nm UV light at $11.3 \pm 0.1 \log$ quanta/cm²/s. A double-coil system was used to test flies in earth-strength fields aligned to magnetic north, south, east or west of equal intensity ($\pm 1\%$) and inclination ($\pm 0.5^\circ$). At the beginning of each test, flies were transferred to a release device centered underneath the 8-arm maze. After an acclimation period flies were released and allowed to move freely into the maze and given 30 min to exit the maze. Flies exiting the maze passed through a funnel trap into a test tube attached to each arm of the maze. In the original experiments [41], mean vectors were calculated by vector addition from the distribution of adult male bearings from each group of flies, and the distribution of mean vectors for the 16 conditions (4 trained directions X 4 magnetic field alignments in testing) plotted relative to the

trained magnetic direction was analyzed using the Hotelling's one-sample test. The reanalysis of the data from Phillips and Sayeed, 1993 was carried out to examine the fine structure of the distribution of adult male flies. We compared the distribution of individual flies in each of the four trained directions (each pooling data from four groups of flies tested in the four magnetic field alignments; see above).

Reanalysis of C57BL/6 Trained Magnetic Compass Response [see 47 for detailed methods].

Training

Male C57BL/6 mice, a common laboratory strain widely used as models of behavior and human disease, were trained in individual cages placed on a narrow wooden shelf with one end shaded (dark end) and the opposite end exposed to overhead light (light end). Four differently aligned shelves were used so that the dark end was aligned in one of four magnetic directions, i.e., 70°, 160°, 250° or 340° relative to geomagnetic north. A nestbox was located at the dark end of each cage where mice typically built a nest, and served to reinforce the training direction. Mice were held in training cages for a minimum of 5 days under a 15:9-h light/dark cycle illuminated by a diffuse overhead tungsten/halogen light source.

Testing

Directional responses were obtained from nest positions constructed overnight by mice tested individually in a radially symmetrical circular arena devoid of visual cues. Mice were tested in one of four magnetic field conditions corresponding to the cardinal compass axes (mN=360°, 90°, 180° or 270°). We compared the distribution of individual mice in each of the four trained directions (each pooling data from mice tested in the four magnetic field alignments; see above).

Results

Under 365 nm light, untrained second instar Berlin, Canton-S, and Oregon-R x Canton-S *Drosophila melanogaster* larvae exhibited a spontaneous preference for one of four absolute or “topographic” directions corresponding with magnetic NE, SE, SW, NW (“anti-cardinal”) compass directions (Fig. 1; and see Table 1). In each strain, the overall topographic and magnetic distributions of bearings were indistinguishable from random, indicating that there was no consistent unimodal topographic or magnetic clustering of bearings (Fig. 1; left and center diagrams; see also Fig. S1 and S2). When the directional responses of larvae from all three strains were combined, the distribution of topographic bearings showed a weak clustering at 126° relative to geomagnetic north ($n = 82$, $\alpha = 126^\circ$, $r = 0.2$, $p = 0.04$) (Fig. 2; left diagram), while the distribution of magnetic bearings (Fig. 2; center diagram) was indistinguishable from random ($p > 0.1$), indicating that the clustering of bearings was due to a weak topographic bias in the testing apparatus and not to a consistent unimodal direction of orientation relative to the magnetic field (Fig. S1 and S2).

The distributions of bearings were tested for quadramodality by quadrupling the bearings [48], which resulted in significant orientation in all strains of larvae tested (Fig. 1; right diagram). Because the alignments of the four magnetic fields differed by 90°, quadrupling the topographic bearings and quadrupling the magnetic bearings resulted in identical distributions. The pooled distribution of quadrupled bearings was strongly oriented ($n = 82$, $\alpha = 170^\circ$, $r = 0.42$, $p < 0.001$) (Fig 2; right diagram), corresponding to four clusters of bearings in the original distributions coinciding with the anti-cardinal axes (42°-132°-222°-312°) (Fig 2; left two diagrams). For all

strains, the latency to cross the 30 mm scoring radius ranged from 160 to 345 s, with a mean time to score of 218 s. Only one trial was discarded due to disturbances.

Canton-S larvae were tested in a double-blind series in which magnetic field conditions (i.e. horizontal component of the magnetic field present or absent) were intermixed in each test. Larvae exhibited anti-cardinal quadramodal orientation when magnetic compass cues were present (35° - 125° - 215° - 305° ; $n = 25$, $r = 0.39$, $p = 0.02$) (Fig. 3A; and see Table 2). There was a weak unimodal distribution of topographic bearings ($\alpha = 73^{\circ}$, $r = 0.35$, $p = 0.046$) (Fig. 3A; left diagram), although again the distribution of magnetic bearings was indistinguishable from random ($p > 0.1$; Fig. 3A; center diagram) indicating that the clustering of topographic bearings was due to a weak topographic bias in the testing apparatus and not to a consistent unimodal direction of orientation relative to the magnetic field. In contrast, when the horizontal component of the magnetic field was cancelled, both topographic ($n = 18$, $p > 0.1$) and magnetic ($p > 0.1$) distributions were indistinguishable from random, when analyzed either unimodally and with the bearings quadrupled (Fig. 3B; and see Table 2). During the double-blind series, the latency to cross the 30 mm scoring radius when the magnetic field was present ranged from 120 s to 300 s, with a mean time to score of 190 s. Latency times to score in trials when the magnetic field was cancelled ranged from 120 s to 360 s, and averaged 185 s. No trials were discarded due to disturbances.

Discussion

The findings in Figures 1 and 2 show quadramodal alignment responses in second instar *Drosophila* larvae. Although the larval response requires movement from the center of the testing plate, we refer to the behavior as an alignment response rather than compass orientation because it appears to be a spontaneous movement that is not goal oriented. A double-blind experiment in

which larvae were tested in the presence and absence of directional earth-strength magnetic cues confirmed that the quadramodal alignment is dependent on the magnetic field, and that no alternative, non-magnetic cue was present in the testing environment (Fig. 3).

Although quadramodal compass responses appear to be widespread in insects [1, 11, 12, 15, 16], the sensory mechanism(s) mediating this behavior have yet to be identified. As discussed earlier, there are two candidate mechanisms proposed to mediate magnetoreception in terrestrial organisms: (1) a magnetite-based mechanism (MBM) based on single domain or interacting superparamagnetic particles of magnetite believed to produce mechanical deformation of, or torque on, cell membrane structures that activate a coupled transduction mechanism [31] or, in the case of freely-rotating single domain particles to secondarily affect the rate of intracellular free-radical reactions that influence the opening or closing of membrane channels, and (2) a photoreceptor-based mechanism involving a specialized class of photopigments (cryptochromes) that form photo-excited radical pair intermediates sensitive to magnetic fields (radical pair mechanism or RPM) that in some animals may cause the magnetic field to be perceived as a pattern of light intensity superimposed on the animal's surroundings [35, 39].

In insects, evidence has been obtained for both MBM and RPM in different species. For example, honeybees dancing on a horizontal comb, which prevents the use of a gravity reference to align the waggle run, exhibit a strong quadramodal preference for the cardinal compass directions and a secondary preference for the anti-cardinal compass directions [15]. A reanalysis of these data by Kirschvink (1981) found that the relationship between the strength of quadramodal orientation and the intensity of the magnetic field plateaus at higher intensities, and conforms to the Langevin function that predicts the ratio of magnetic to thermal energies of single domain particles of magnetite [40]. These findings are consistent with a MBM that involves single domain particles

of magnetite in which variation in the alignment of the particles, and therefore, the scatter in the alignment of the waggle run, decreases with increasing magnetic field intensity. Unlike the MBM, the effect of the magnetic field on a RPM involves a resonance process that functions within a relatively narrow range of magnetic field intensities. Therefore, the strength of quadramodal orientation mediated by a RPM should peak at an intermediate intensity and decrease at both high and low magnetic field intensities [49] and is not consistent with the behavioral responses exhibited in honeybees.

In contrast to evidence for the involvement of a MBM in honeybees, learned magnetic compass responses in both adult fruit flies and adult mealworm beetles appear to be mediated by a light-dependent mechanism [reviewed by 19]. Adult male *Drosophila* exhibit robust unimodal magnetic orientation when trained and tested under short-wavelength (365 nm) light. However, when trained under short-wavelength (365 nm) light and tested under long-wavelength light (500 nm), males show a 90° clockwise shift in orientation relative to the trained magnetic direction, suggesting that the magnetic compass of adult *Drosophila* is affected by the wavelength of light [41]. Similar light-dependent responses were reported in mealworm beetles. When trained and tested under short-wavelength (390 nm) light, beetles oriented in the trained magnetic directions. When trained under the same short-wavelength light and tested under blue-green (500 nm) light, beetles shifted their orientation 90° clockwise relative to the trained magnetic direction [42]. While the wavelength-dependent effects of light on magnetic compass orientation in flies and beetles could result from a change in the behavioral response rather than a change in the directional input used to guide behavior, similar wavelength-dependent 90° shifts in magnetic compass orientation in both anuran and urodele amphibians have been shown to result from a direct effect of light on the underlying magnetoreception mechanism [50-52]. Furthermore, preliminary evidence for

photoreceptors sensitive to the alignment of an earth-strength magnetic field has been obtained in neurophysiological recordings from the frontal organ (an outgrowth of the pineal organ) of bullfrogs *Lithobates catesbeianus*, showing wavelength-dependent properties consistent with the behavioral effects observed in both amphibians and insects (Phillips and Borland, unpublished). These findings suggest that similar light-dependent magnetic compass mechanisms may be present in multiple orders of insects and amphibians. In addition to adult insects, learned compass orientation in second instar *Drosophila melanogaster* larvae trained and tested in four different magnetic directions under short wavelength (365 nm) light have also been reported [9]. However, these findings did not address the spectral dependence of the magnetic compass response.

Additional evidence for a light-dependent magnetoreception mechanism has come from experiments investigating naïve and conditioned responses of adult *Drosophila melanogaster* to a magnetic anomaly ten-times the intensity of the geomagnetic field presented in one arm of a T-maze [43, 44]. Under full spectrum light naïve flies avoided magnetic stimuli, while flies exhibited a conditioned response towards the magnetic stimulus when paired with a sucrose reward. In transgenic flies lacking a functional cryptochrome photopigment, as well as in wildtype flies tested under lighting conditions that excluded short-wavelength light (< 420 nm), both naïve and conditioned responses were abolished. Although Gegear et al.'s findings are consistent with a RPM-based magnetoreception mechanism in *Drosophila*, the relevance of these findings to quadramodal alignment and learned magnetic compass responses remains unclear as the strong magnetic stimuli used in these experiments could affect other physiological processes that are not directly involved in detection of earth-strength magnetic fields (e.g., cryptochrome-based photo-entrainment of circadian rhythms [53]).

A reanalysis of the earlier study of light-dependent magnetic compass orientation by adult *Drosophila* found evidence that adult flies trained and tested under UV light to magnetic north or south showed a unimodal distribution of bearings centered on the trained direction (Fig. 4A), while flies trained to magnetic east or west under the same lighting conditions exhibited a 90° (i.e. $\pm 45^\circ$) split around the trained direction (Fig. 4B; data from [41]). These responses suggest that when flies are orienting along the north-south axis the directional information obtained from the magnetic field is qualitatively different from that obtained when they are orienting along the east-west axis. This difference in behavior along the N-S and E-W axes is consistent with flies receiving magnetic input that exhibits a complex, axially symmetrical pattern of response (i.e. identical components 180° apart) [see discussion of mouse findings below].

The splitting on either side of the east-west trained axis (i.e. clusters of bearings at 45° and 135° for east trained flies, and at 225° and 315° for west trained flies) is consistent with the anti-cardinal quadramodal alignment response exhibited by larvae (Figs 1, 2). This suggests that the same magnetoreception mechanism is involved in the light-dependent magnetic compass orientation of adult *Drosophila* and the quadramodal magnetic alignment response of *Drosophila* larvae.

And although the pattern of response generated by a RPM-based magnetic compass is unknown, theoretical models of magnetically sensitive, radical pair systems are compatible with a complex, radially symmetrical pattern that intersects the horizontal plane in multiple (e.g., 2 or 4) directions and could produce quadramodal patterns of response [36, 54, 55]. Modeling of mechanisms involving single domain or super-paramagnetic magnetite indicates that in some configurations a MBM can also exhibit axial symmetry [31]. Given evidence that the intensity dependence of the quadramodal dance of honeybees fits the predictions of a MBM [40], but not a RPM [35], a magnetite-based receptor could be involved in the responses of both larval and adult flies.

However, it remains to be determined if a quadramodal pattern of response is likely to be generated by a MBM.

Surprisingly, dependence of the magnetic compass response on the axis of training similar to that observed in adult flies (Fig. 4) was also found in a reanalysis of data from an earlier study of magnetic compass orientation by male C57/BL6 mice. A $\sim 90^\circ$ split was observed in mice trained in directions close to magnetic east or west (70° and 250°) (Fig. 5B), but not to magnetic north or south (340° and 160°) (Fig. 5A) [data from 47]. It is noteworthy that the split in the response of east and west trained mice is centered on the cardinal compass directions (magnetic east and west), rather than the magnetic trained directions that were 20° CCW of the cardinal compass directions. Although nothing is known yet about spectral dependence of the mouse magnetic compass response, these findings suggest that both adult flies and mice are responding to different directional information along the north-south and east-west axes, i.e., that the magnetic compass produces a pattern of response with multiple components, rather than a simple reference direction. Both responses exhibit axial symmetry that is compatible with the involvement of either a RPM or a MBM.

While quadramodal magnetic responses have been demonstrated in adult insects belonging to a variety of taxonomic groups, it is interesting that *Drosophila* larvae aligned themselves along the 45° , or ‘anti-cardinal’ axes, in contrast to the cardinal compass alignments reported from previous studies of adult insects. This discrepancy does not appear to be species specific as previous studies have reported quadramodal alignment behaviors in adult *Drosophila melanogaster* along the cardinal compass axes [14] in contrast to the anti-cardinal orientation exhibited by second instar larvae. However, it should be noted that these alignment experiments were performed in complete darkness, suggesting these responses, like the quadramodal waggle run of honeybees, are mediated

by a MBM. This suggests that a MBM could mediate quadramodal magnetic orientation at least under certain conditions. Alternatively, if the quadramodal response exhibited by larval *Drosophila* is mediated by a light-dependent mechanism, the cardinal and anti-cardinal quadramodal responses could reflect more general differences in the response to light intensity by adult and larval flies. For example, wild-type adult *Drosophila* exhibit positive phototaxis, whereas second instar larvae exhibit negative phototaxis [56-58]. If flies using a RPM-based magnetic compass perceive the magnetic field as a symmetrical quadramodal pattern of increased light intensity, separated by contrasting regions of decreased light intensity [35, 39], the ‘complementary’ responses of larval and adult flies could reflect attraction towards, or away from, contrasting components of the pattern (i.e. perceived brightness) that parallels developmental changes in phototactic behavior.

If quadramodal magnetic orientation in both honeybees [40], and adult flies is mediated by a MBM, the light-dependence of these responses could result from a separate non-magnetic input. Jensen (2010) proposed that the properties of the light-dependent magnetic compass in birds and possibly other organisms can be explained by an interaction between a non-light-dependent magnetic compass (presumably magnetite-based) and a vision-based celestial compass (e.g., a spectral gradient or polarized light compass; [46]). It is noteworthy that Jensen’s model suggests that changes in the wavelength and intensity of light could alter the directional response of a hybrid magnetite-based magnetic and light-dependent polarized light (or spectral gradient) compass in a manner similar to that shown in amphibians [52].

In summary, our findings in Figures 1, 2 and 3 provide the first evidence for quadramodal magnetic alignment by a larval insect. Reanalysis of magnetic compass orientation by adult *Drosophila* and adult C57BL/6 mice suggests that a common underlying mechanism may mediate magnetic

dependent behaviors in larval and adult flies (Figs 2, 3, 4), and in some vertebrates (Fig 5; and see earlier discussion of similar light-dependent magnetic compass responses in flies and amphibians). Remarkably, magnetic responses in larval and adult flies exhibit properties that are consistent with the involvement of both MBM- and RPM-detectors. Therefore, the fly system is well suited to investigate whether these responses are mediated by a MBM, a RPM, or both, and whether the wavelength-dependent effects of light on magnetic compass orientation is due to the involvement of a light-dependent, RPM-based detector, or to secondary effects of light on a MBM-based detector [46]. Most importantly, evidence that magnetic responses in adult and larval flies share properties with those of honeybees, cockroaches, amphibians, and mice suggest that characterizing the mechanism of magnetoreception in flies will have broad implications for the magnetic sense in a wide variety of terrestrial organisms.

Acknowledgments

We would like to thank Lukas Landler and Paul W. Youmans for assistance with experiments and critical feedback during the preparation of this manuscript. We are also grateful to two anonymous reviewers for their insightful comments. This research was supported by grants from the National Science Foundation (IOS 06-47188 and IOS 07-48175), Virginia Tech Graduate Research Development Program, and Sigma-Xi.

Tables:

Table 1. Spontaneous alignment responses of Berlin, Canton-S, and Oregon-R X Canton-S strains of *Drosophila melanogaster* 2nd instar larvae.

Strain	Date of Test (Mo/Day/Yr)	Direction of magnetic north(°)	Topographic bearing(°)	Magnetic bearing(°)	Quadramodal bearing(°)
Berlin	1/28/2010	0	228	228	192
Berlin	2/4/2010	0	74	74	296
Berlin	2/11/2010	0	44	44	176
Berlin	2/18/2010	0	39	39	156
Berlin	2/18/2010	0	84	84	336
Berlin	1/28/2010	90	236	146	224
Berlin	1/28/2010	90	288	198	72
Berlin	2/4/2010	90	294	204	96
Berlin	2/4/2010	90	231	141	204
Berlin	2/11/2010	90	226	136	184
Berlin	2/18/2010	90	40	310	160
Berlin	2/18/2010	90	221	131	164
Berlin	2/18/2010	90	50	320	200
Berlin	1/28/2010	180	115	295	100
Berlin	2/4/2010	180	41	221	164
Berlin	2/4/2010	180	315	135	180
Berlin	2/11/2010	180	135	315	180
Berlin	2/18/2010	180	4	184	16
Berlin	2/18/2010	180	13	193	52
Berlin	1/28/2010	270	179	269	356
Berlin	2/4/2010	270	115	205	100
Berlin	2/11/2010	270	148	238	232
Berlin	2/18/2010	270	129	219	156
Berlin	2/18/2010	270	135	225	180
Canton-S	4/8/2010	0	147	147	228
Canton-S	4/9/2010	0	216	216	144
Canton-S	4/9/2010	0	148	148	232
Canton-S	4/15/2010	0	281	281	44
Canton-S	4/15/2010	0	120	120	120
Canton-S	4/15/2010	0	143	143	212
Canton-S	4/8/2010	90	235	145	220
Canton-S	4/9/2010	90	42	312	168
Canton-S	4/9/2010	90	27	297	108
Canton-S	4/15/2010	90	135	45	180

Canton-S	4/15/2010	90	48	318	192
Canton-S	4/15/2010	90	51	321	204
Canton-S	4/15/2010	90	120	30	120
Canton-S	4/9/2010	180	202	22	88
Canton-S	4/15/2010	180	151	331	244
Canton-S	4/15/2010	180	215	35	140
Canton-S	4/8/2010	270	142	232	208
Canton-S	4/9/2010	270	33	123	132
Canton-S	4/15/2010	270	45	135	180
Canton-S	4/15/2010	270	58	148	232
Oregon-R x Canton-S	2/4/2010	0	90	90	360
Oregon-R x Canton-S	2/4/2010	0	135	135	180
Oregon-R x Canton-S	2/12/2010	0	127	127	148
Oregon-R x Canton-S	2/19/2010	0	240	240	240
Oregon-R x Canton-S	2/19/2010	0	323	323	212
Oregon-R x Canton-S	2/26/2010	0	212	212	128
Oregon-R x Canton-S	2/26/2010	0	193	193	52
Oregon-R x Canton-S	3/26/2010	0	50	50	200
Oregon-R x Canton-S	3/26/2010	0	305	305	140
Oregon-R x Canton-S	3/26/2010	0	213	213	132
Oregon-R x Canton-S	2/4/2010	90	51	321	204
Oregon-R x Canton-S	2/4/2010	90	192	102	48
Oregon-R x Canton-S	2/12/2010	90	90	0	360
Oregon-R x Canton-S	2/12/2010	90	230	140	200
Oregon-R x Canton-S	2/19/2010	90	31	301	124
Oregon-R x Canton-S	2/19/2010	90	85	355	340
Oregon-R x Canton-S	2/26/2010	90	241	151	244
Oregon-R x Canton-S	2/26/2010	90	221	131	164
Oregon-R x Canton-S	2/26/2010	90	25	295	100
Oregon-R x Canton-S	2/26/2010	90	124	34	136
Oregon-R x Canton-S	3/26/2010	90	206	116	104
Oregon-R x Canton-S	3/26/2010	90	50	320	200
Oregon-R x Canton-S	3/26/2010	90	56	326	224
Oregon-R x Canton-S	3/26/2010	90	38	308	152
Oregon-R x Canton-S	2/4/2010	180	79	259	316
Oregon-R x Canton-S	2/12/2010	180	18	198	72
Oregon-R x Canton-S	2/26/2010	180	159	339	276
Oregon-R x Canton-S	2/26/2010	180	209	29	116
Oregon-R x Canton-S	3/26/2010	180	291	111	84
Oregon-R x Canton-S	3/26/2010	180	144	324	216
Oregon-R x Canton-S	2/4/2010	270	169	259	316
Oregon-R x Canton-S	2/12/2010	270	254	344	296
Oregon-R x Canton-S	2/19/2010	270	195	285	60

Oregon-R x Canton-S	2/19/2010	270	135	225	180
Oregon-R x Canton-S	2/26/2010	270	307	37	148
Oregon-R x Canton-S	2/26/2010	270	71	161	284
Oregon-R x Canton-S	3/26/2010	270	315	45	180
Oregon-R x Canton-S	3/26/2010	270	240	330	240

‘Topographic’, ‘magnetic’, and ‘quadamodal’ bearings obtained from Berlin, Canton-S, and Oregon-R X Canton-S wild-type 2nd instar *Drosophila melanogaster* larvae tested in one of four earth-strength magnetic field alignments; each larva tested only once.

Table 2. Spontaneous alignment responses of 2nd instar *Drosophila melanogaster* tested in an earth-strength magnetic field, or with the magnetic field cancelled.

Strain	Date of Test (Mo/Day/Yr)	Field	Direction of magnetic north(°)	Topographic bearing(°)	Magnetic bearing(°)	Quadramodal bearing(°)
Canton-S	4/23/2010	On	0	119	119	116
Canton-S	4/23/2010	On	0	305	305	140
Canton-S	4/29/2010	On	0	45	45	180
Canton-S	5/6/2010	On	0	124	124	136
Canton-S	5/11/2010	On	0	221	221	164
Canton-S	5/11/2010	On	0	135	135	180
Canton-S	5/12/2010	On	0	32	32	128
Canton-S	5/12/2010	On	0	31	31	124
Canton-S	4/23/2010	On	90	275	185	20
Canton-S	4/23/2010	On	90	58	328	232
Canton-S	4/29/2010	On	90	307	217	148
Canton-S	5/6/2010	On	90	310	220	160
Canton-S	5/11/2010	On	90	123	33	132
Canton-S	5/11/2010	On	90	161	71	284
Canton-S	5/12/2010	On	90	113	23	92
Canton-S	5/12/2010	On	90	148	58	232
Canton-S	4/23/2010	On	180	20	20	80
Canton-S	5/6/2010	On	180	109	289	76
Canton-S	5/11/2010	On	180	15	195	60
Canton-S	5/12/2010	On	180	57	237	228
Canton-S	4/23/2010	On	270	30	120	120

Canton-S	4/29/2010	On	270	329	59	236
Canton-S	5/11/2010	On	270	155	245	260
Canton-S	5/12/2010	On	270	102	192	48
Canton-S	5/12/2010	On	270	79	169	316
Canton-S	4/29/2010	Cancelled	n/a	34	n/a	136
Canton-S	4/29/2010	Cancelled	n/a	143	n/a	212
Canton-S	5/6/2010	Cancelled	n/a	335	n/a	260
Canton-S	5/6/2010	Cancelled	n/a	139	n/a	196
Canton-S	5/6/2010	Cancelled	n/a	71	n/a	284
Canton-S	5/6/2010	Cancelled	n/a	294	n/a	96
Canton-S	5/6/2010	Cancelled	n/a	323	n/a	212
Canton-S	5/6/2010	Cancelled	n/a	98	n/a	32
Canton-S	5/6/2010	Cancelled	n/a	303	n/a	132
Canton-S	5/11/2010	Cancelled	n/a	5	n/a	20
Canton-S	5/11/2010	Cancelled	n/a	111	n/a	84
Canton-S	5/11/2010	Cancelled	n/a	79	n/a	316
Canton-S	5/11/2010	Cancelled	n/a	345	n/a	300
Canton-S	5/11/2010	Cancelled	n/a	232	n/a	208
Canton-S	5/12/2010	Cancelled	n/a	63	n/a	252
Canton-S	5/12/2010	Cancelled	n/a	94	n/a	16
Canton-S	5/12/2010	Cancelled	n/a	284	n/a	56
Canton-S	5/12/2010	Cancelled	n/a	336	n/a	264

‘Topographic’, ‘magnetic’, and ‘quadramodal’ bearings of *Drosophila melanogaster* larvae tested in one of four alignments of an earth-strength magnetic field (= ‘On’), or tested when the horizontal component of the magnetic field was cancelled (= ‘Cancelled’).

Figures:

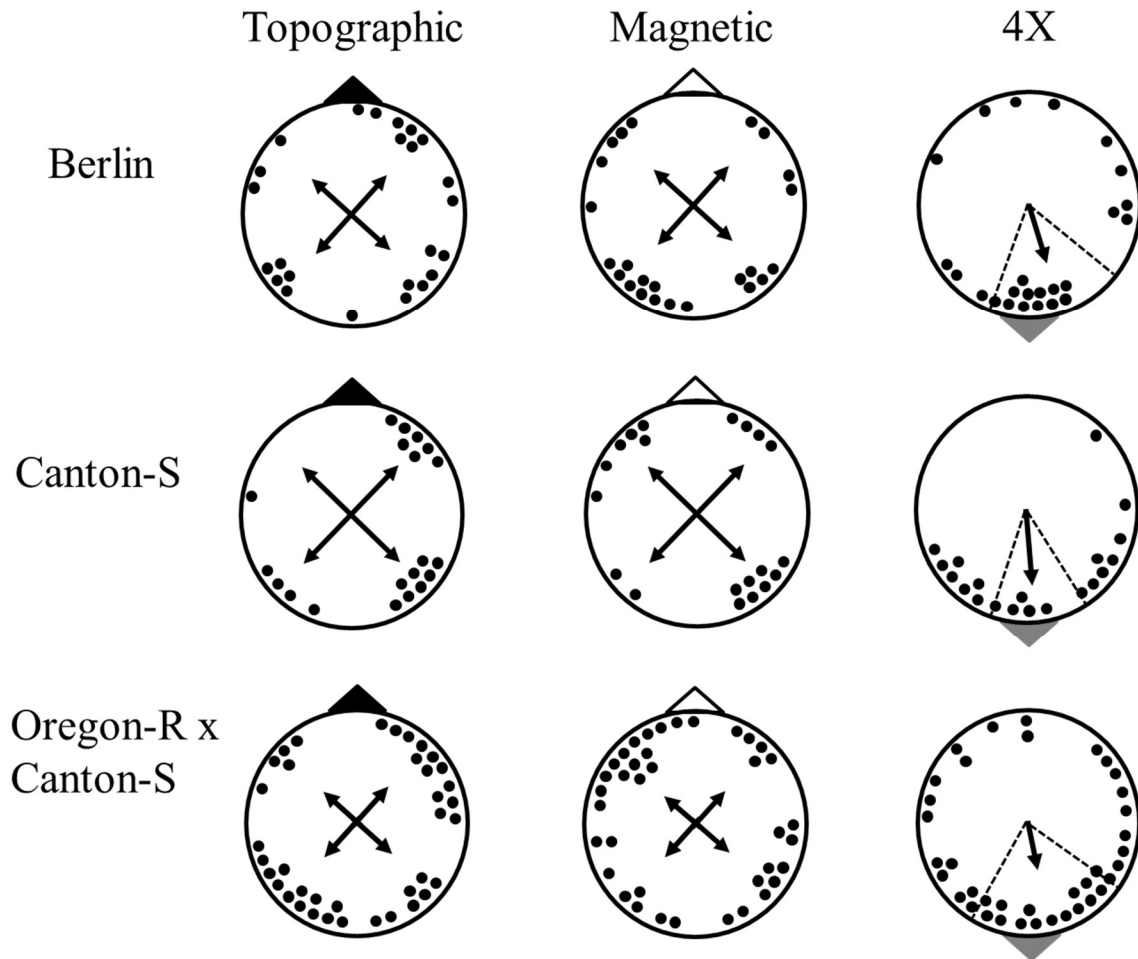


Figure 1. Spontaneous orientation of 2nd instar *Drosophila melanogaster* larvae. Distributions of bearings are shown for Berlin, Canton-S, and Oregon-R x Canton-S strains. The distributions are plotted as absolute or ‘topographic’ bearings (left diagrams), bearings relative to magnetic north (center diagrams), and quadrupled bearings (right diagrams). None of the distributions of topographic or magnetic bearings differed significantly from a random distribution ($p > 0.05$, Rayleigh test). The distribution of quadrupled bearings (“4X”; right diagrams) were significant for all strains, i.e., Berlin ($n = 24$, $\alpha = 164^\circ$, $r = 0.44$, $p < 0.009$), Canton-S ($n = 20$, $\alpha = 175^\circ$, $r = 0.63$, $p < 0.001$), and Oregon-R x Canton-S ($n = 38$, $\alpha = 168^\circ$, $r = 0.29$, $p < 0.05$). The mean quadramodal directions of orientation for Berlin larvae were 41° - 131° - 221° - 311° , for Canton-S larvae were 44° - 134° - 224° - 314° , and for Oregon-R x Canton-S larvae were 42° - 132° - 222° - 312° . Dashed lines show the 95% confidence interval. Black dots represent individual larval bearings tested in one of four magnetic field alignments. Black triangles indicate the direction of geographic north, open triangles indicate the direction of mN, and grey triangles indicate direction of quadrupled bearings corresponding to the anti-cardinal directions.

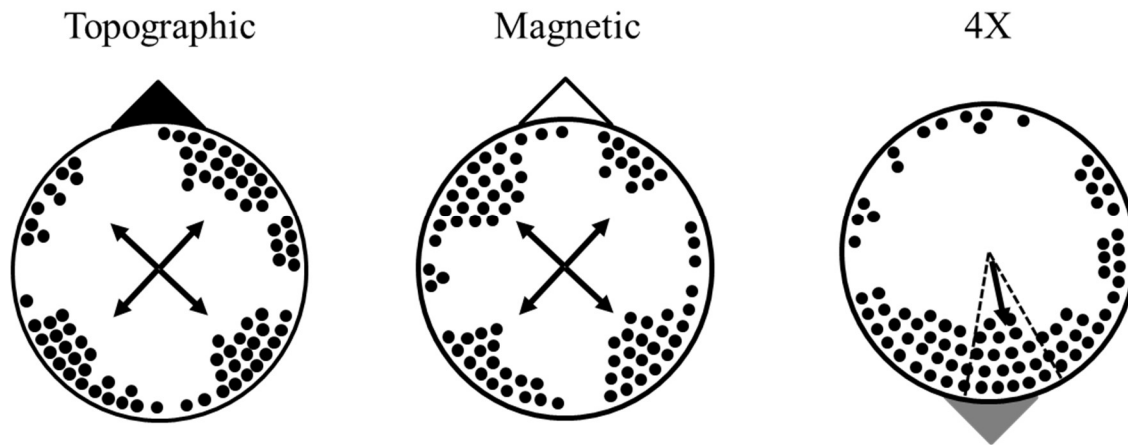


Figure 2. Pooled distribution of directional responses from all three strains of *Drosophila melanogaster* larvae. The combined distribution of quadrupled bearings (4X) was significantly oriented ($n = 82$, $\alpha = 170^\circ$, $r = 0.42$, $p < 0.001$; Rayleigh test). This indicates there was significant quadramodal clustering of bearings along the anti-cardinal axes at 42° - 132° - 222° - 312° . The topographic distribution also exhibited a weak unimodal clustering ($\alpha = 126^\circ$, $r = 0.198$, $p = 0.04$; mean vector not shown). Symbols are the same as in Fig. 1.

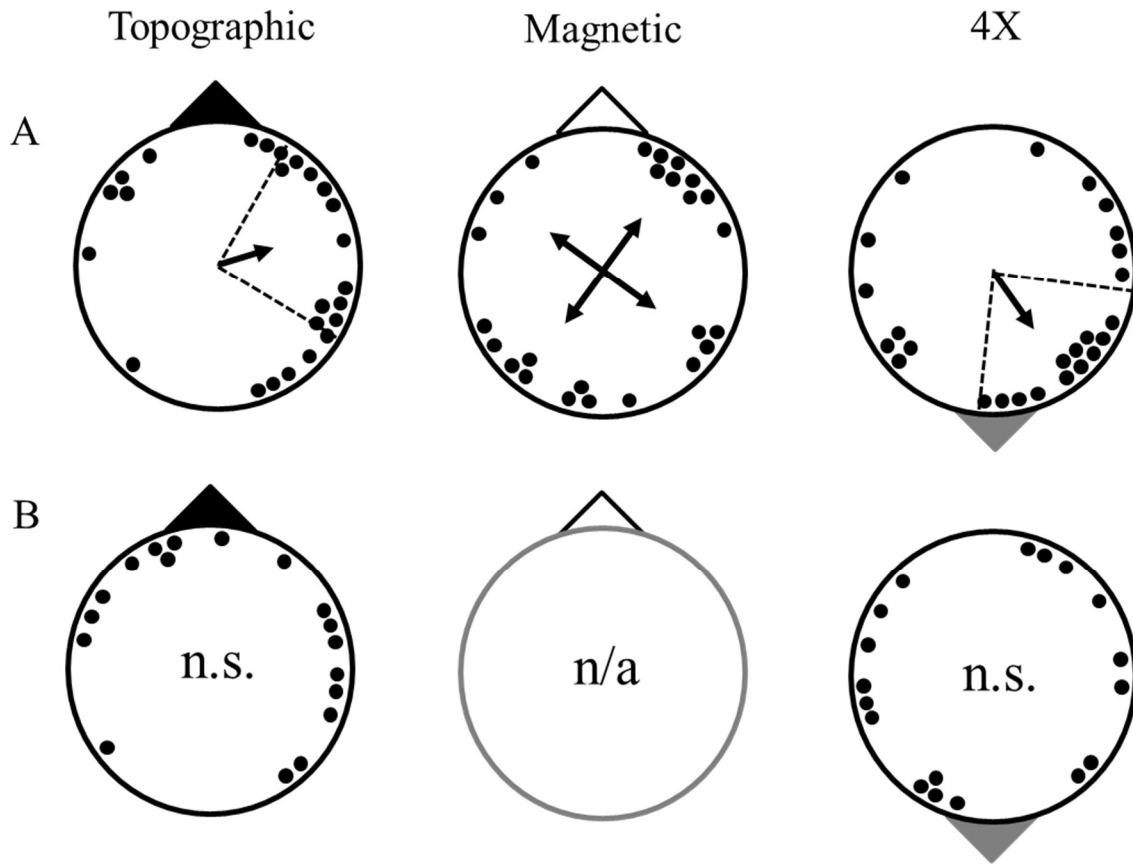


Figure 3. Distributions of directional responses from 2nd instar Canton-S *Drosophila melanogaster* larvae tested with the ambient horizontal component in all four magnetic field alignments (A) and with the horizontal components cancelled (B). (A) Larvae tested with magnetic cues present showed a non-random distribution of topographic bearings ($n = 25$, $\alpha = 73^\circ$, $r = 0.35$, $p = 0.05$; left diagram). However, the distribution of magnetic bearings (center diagram) was indistinguishable from random ($p > 0.1$; center diagram), indicating that the “topographic bias” in the left diagram was not a consistent unimodal response to the magnetic field. The distribution of quadrupled bearings (4X) was non-randomly distributed ($\alpha = 145^\circ$, $r = 0.40$, $p = 0.02$), indicating that the distributions of bearings were clustered quadrantly at 36° - 126° - 216° - 306° . (B) Larvae tested with the horizontal component of the magnetic field cancelled (no magnetic compass cues) were indistinguishable from random when analyzed as topographic bearings (left diagram) ($n = 18$, $p > 0.10$), or as quadrupled bearings (right diagram) ($p > 0.10$). Symbols are the same as Fig. 1.

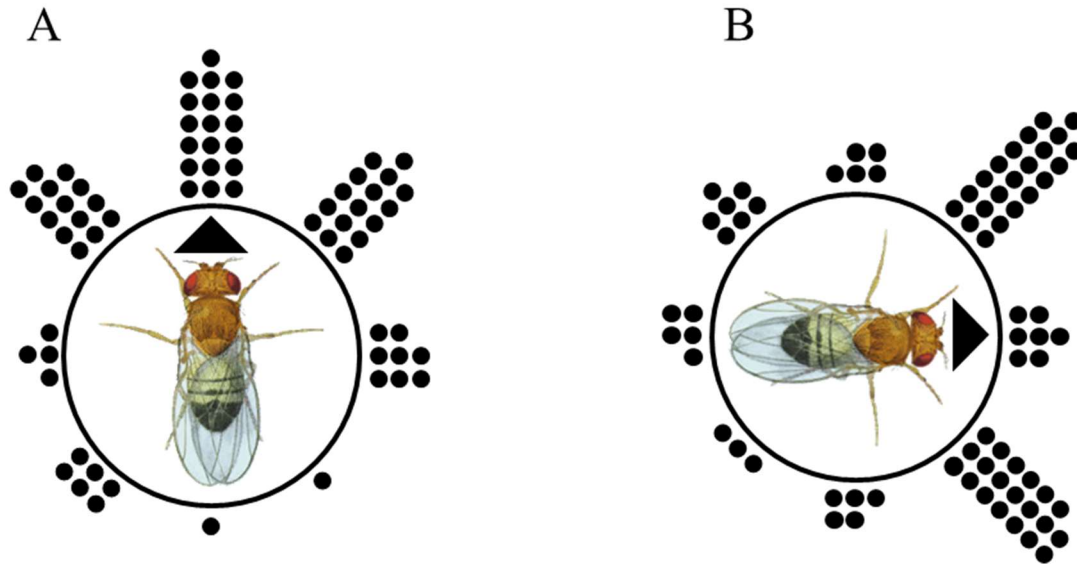


Figure 4. Magnetic compass response of adult *Drosophila melanogaster* depends on whether flies were trained along the magnetic north-south (A) or east-west (B) axis [data from 41]. A) Flies trained to the north or south (plotted relative to the trained magnetic direction at the top of the diagram) exhibited a unimodal distribution of bearings coinciding with the trained magnetic direction. B) Flies trained to the east or west (plotted relative to the trained magnetic direction at the right side of the diagram) exhibited a distribution of magnetic bearings that was split by $\pm 45^\circ$ on either side of the trained magnetic direction. Black symbols are the magnetic bearings of individual flies tested in groups in one of four magnetic field alignments (magnetic north at north, east, south or west). Each diagram includes directional bearings from flies tested in 8 different conditions (2 trained directions X 4 magnetic field alignments; [see 41 for details]). Black triangles indicate the trained magnetic direction.

A



B



Figure 5. Learned magnetic compass response of adult male C57BL/6 mice trained along the ~north-south (N-S) or ~east-west (E-W) magnetic axis [data from 47]. A) Mice trained in either direction along the N-S axis (340° and 160°) exhibited a robust unimodal response coinciding with the trained magnetic direction (responses of north and south trained mice combined and plotted relative to the expected magnetic direction--black triangle at the top of the circular distribution). In contrast, B) the magnetic bearings of mice trained along the E-W axis (70° and 250°) were split into two clusters $\pm 45^\circ$ on either side of the trained magnetic direction (responses of east and west trained mice combined and plotted relative to the expected magnetic direction--black triangle at the right side of the circular distribution). Black symbols represent individual nest positions; each mouse tested only once.

Supplemental Materials

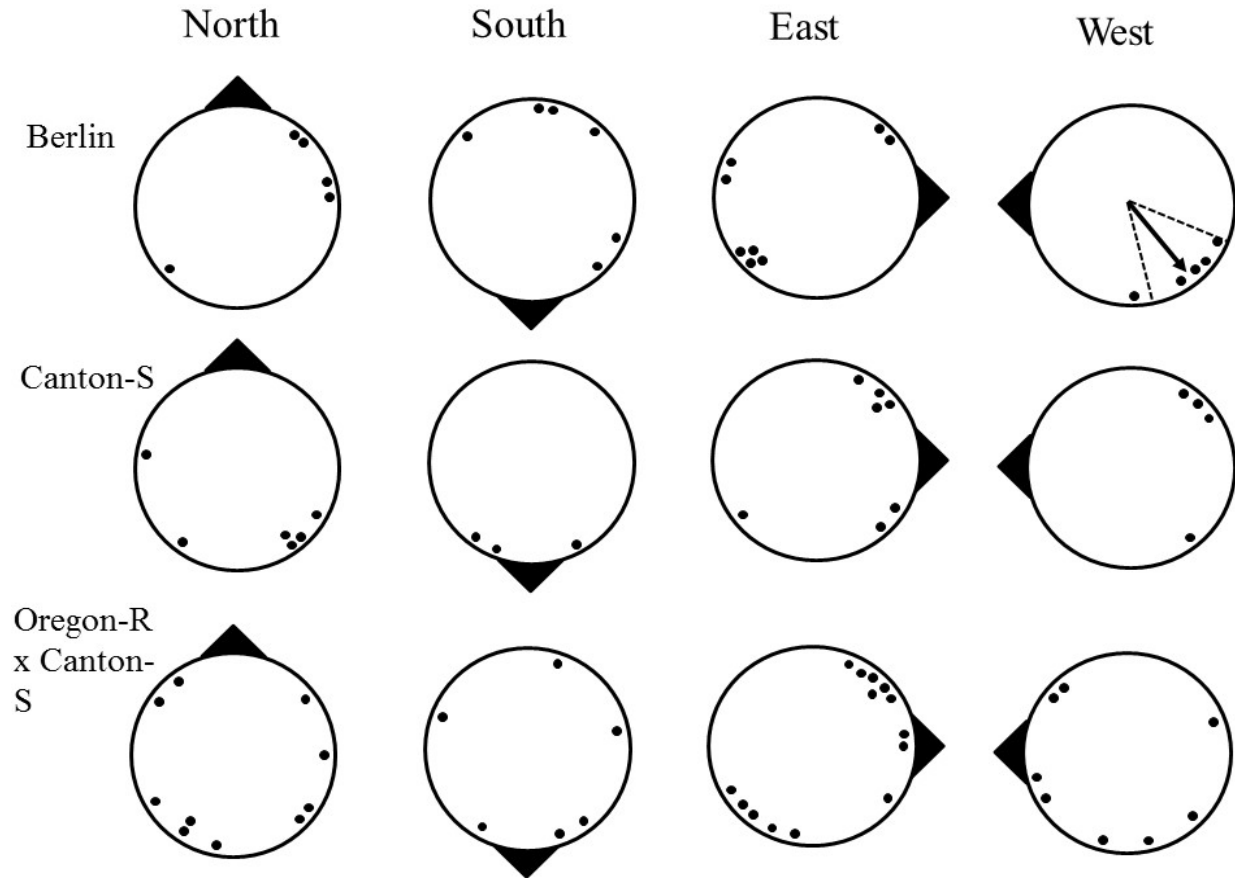


Figure S1. Spontaneous orientation of 2nd instar *Drosophila melanogaster* larvae relative to the alignment of magnetic north (black triangles). Distributions of bearings for Berlin, Canton-S, and Oregon-R x Canton-S larvae showing the absolute or topographic bearing of each larva in the four testing fields. In only one condition was there a non-uniform distribution (Berlin strain, West magnetic field alignment; 231°, $r = 0.93$, $p = 0.005$) indicating that the overall quadrangular distributions were not dependent on the alignment of magnetic north. Furthermore, there is no consistent unimodal bias in the distributions of topographic bearings (Fig 1, left diagrams) or magnetic bearings (Fig 1, center diagrams) for any of the strains, or in the pooled distributions of topographic bearings (Fig 2, left diagram) or magnetic bearings (Fig 2, center diagram), that could account for the significant clustering of quadrupled bearings (Fig 1 and 2, right diagrams). Black dots indicate individual larval bearings. For non-random distributions ($p < 0.05$, Rayleigh test), the black arrow represents the mean angle of the distribution with the length of the arrow indicating the mean vector length “ r ” (radius of each circle corresponds to $r = 1$). Dashed line indicates the 95% confidence interval for the mean vector bearing.

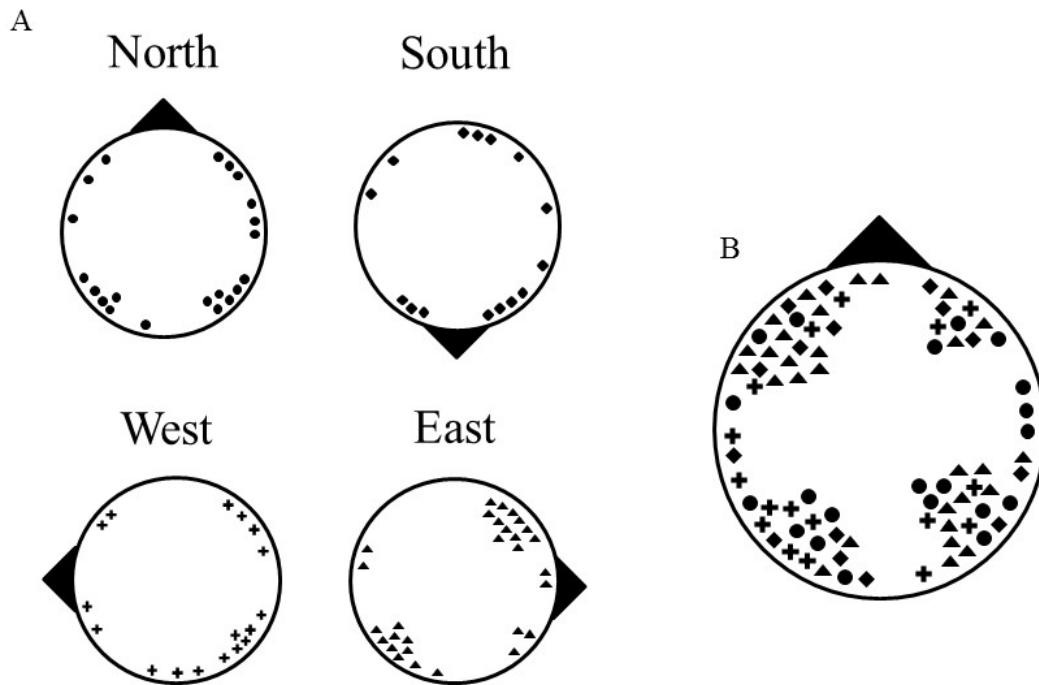


Figure S2. Pooled distributions of bearings from three stains of 2nd instar *Drosophila melanogaster* larvae. (A) Distributions of topographic bearings obtained in each of the four alignment of magnetic north (magnetic north aligned to North, South, West or East). (B) Pooled distribution of bearings from all four alignments of the magnetic field plotted relative to magnetic north. Symbols represent individual larval bearings and correspond to those shown in (A). Black triangles at the edge of each circle indicates the direction of magnetic north. The unimodal distributions of bearings pooled from all three strains were indistinguishable from random in all four alignments of magnetic north, as well as when the data were pooled with respect to magnetic north ($p > 0.10$, Rayleigh test) indicating that there was no consistent unimodal orientation relative to the magnetic field.

Literature Cited

1. Becker, G. and U. Speck, *Examinations on magnetic field orientation in Dipterans*. *Z Vergl Physiol*, 1964. **49**: p. 301-340.
2. Wiltschko, W. and R. Wiltschko, *Magnetic compass of European robins*. *Science*, 1972. **176**(4030): p. 62-64.
3. Stabrowski, A. and P.M. Nollen, *The responses of Philophthalmus gralli and P. megalurus miracidia to light, gravity and magnetic fields*. *International journal for parasitology*, 1985. **15**(5): p. 551-555.
4. Phillips, J.B., *Two magnetoreception pathways in a migratory salamander*. *Science*, 1986. **233**(4765): p. 765-767.
5. Chew, G. and G.E. Brown, *Orientation of rainbow trout (Salmo gairdneri) in normal and null magnetic fields*. *Canadian Journal of Zoology*, 1989. **67**(3): p. 641-643.
6. Wiltschko, R. and W. Wiltschko, *Magnetic orientation in animals*. 1995: Springer Berlin.
7. Wiltschko, W. and R. Wiltschko, *Magnetic orientation and magnetoreception in birds and other animals*. *Journal of Comparative Physiology A: Neuroethology, Sensory, Neural, and Behavioral Physiology*, 2005. **191**(8): p. 675-93.
8. Begall, S., et al., *Magnetic alignment in grazing and resting cattle and deer*. *Proceedings of the National Academy of Sciences*, 2008. **105**(36): p. 13451-13455.
9. Dommer, D.H., et al., *Magnetic compass orientation by larval Drosophila melanogaster*. *Journal of Insect Physiology*, 2008. **54**(4): p. 719-26.
10. Begall, S., et al., *Magnetic alignment in mammals and other animals*. *Mammalian Biology*, 2013. **78**: p. 10-20.
11. Roonwal, M.L., *Recent work on termite research in India (1947-57)*. 1958.
12. Becker, G., *Reaction of termites to weak alternating magnetic fields*. *Naturwissenschaften*, 1976. **63**(4): p. 201-202.
13. Becker, G., *Resting position according to magnetic direction, magnetic orientation in termites*. *Naturwissenschaften*, 1963. **50**: p. 455.
14. Wehner, R. and T.H. Labhart, *Perception of the geomagnetic field in the fly Drosophila melanogaster*. *Cellular and Molecular Life Sciences*, 1970. **26**(9): p. 967-968.
15. Martin, H. and M. Lindauer, *The effect of the Earth's magnetic field on gravity orientation in the honey bee*. *Apis mellifica*, 1977: p. 145-187.
16. Vácha, M., M. Kvalcova, and T. Puzova, *American cockroaches prefer four cardinal geomagnetic positions at rest*. *Behaviour*, 2010. **147**(4): p. 425-440.
17. Cheung, A., et al., *Animal navigation: general properties of directed walks*. *Biological Cybernetics*, 2008. **99**(3): p. 197-217.
18. Cheung, A., et al., *Animal navigation: the difficulty of moving in a straight line*. *Biological Cybernetics*, 2007. **97**(1): p. 47-61.
19. Phillips, J.B., P.E. Jorge, and R. Muheim, *Light-dependent magnetic compass orientation in amphibians and insects: candidate receptors and candidate molecular mechanisms*. *Journal of The Royal Society Interface*, 2010. **7 Suppl 2**: p. S241-56.
20. Lohmann, K.J. and S. Johnsen, *The neurobiology of magnetoreception in vertebrate animals*. *Trends Neurosci*, 2000. **23**(4): p. 153-9.
21. Mouritsen, H. and T. Ritz, *Magnetoreception and its use in bird navigation*. *Current Opinion in Neurobiology*, 2005. **15**(4): p. 406-414.
22. Marhold, S., W. Wiltschko, and H. Burda, *A magnetic polarity compass for direction finding in a subterranean mammal*. *Naturwissenschaften*, 1997. **84**(9): p. 421-423.

23. Marhold, S., et al., *Magnetic orientation in common mole-rats from Zambia*. Orientation and navigation—birds, humans and other animals, 1997: p. 5-1.
24. Munro, U., et al., *Evidence for a magnetite-based navigational 'map' in birds*. Naturwissenschaften, 1997. **84**(1): p. 26-28.
25. Burda, H., et al., *Magnetic compass orientation in the subterranean rodent *Cryptomys hottentotus* (Bathyergidae)*. Cellular and Molecular Life Sciences, 1990. **46**(5): p. 528-530.
26. Kobayashi, A. and J.L. Kirschvink, *Magnetoreception and EMF Effects: Sensory perception of the geomagnetic field in Animals and Humans*. 1995.
27. Van der Horst, G.T.J., et al., *Mammalian *Cry1* and *Cry2* are essential for maintenance of circadian rhythms*. NATURE-LONDON-, 1999: p. 627-629.
28. Wu, L.Q. and J.D. Dickman, *Neural correlates of a magnetic sense*. Science Signalling, 2012. **336**(6084): p. 1054.
29. Wu, L.-Q. and J.D. Dickman, *Magnetoreception in an Avian Brain in Part Mediated by Inner Ear Lagena*. Current Biology, 2011. **21**(5): p. 418-423.
30. Binhi, V., *Stochastic dynamics of magnetosomes and a mechanism of biological orientation in the geomagnetic field*. Bioelectromagnetics, 2006. **27**(1): p. 58-63.
31. Winklhofer, M. and J.L. Kirschvink, *A quantitative assessment of torque-transducer models for magnetoreception*. Journal of the Royal Society Interface, 2010. **7**(Suppl 2): p. S273-S289.
32. Davila, A., et al., *A new model for a magnetoreceptor in homing pigeons based on interacting clusters of superparamagnetic magnetite*. Physics and Chemistry of the Earth, Parts A/B/C, 2003. **28**(16): p. 647-652.
33. Ritz, T., et al., *Magnetic compass of birds is based on a molecule with optimal directional sensitivity*. Biophysical Journal, 2009. **96**: p. 3451 - 3457.
34. Ritz, T., et al., *Resonance effects indicate a radical-pair mechanism for avian magnetic compass*. Nature, 2004. **429**(6988): p. 177-180.
35. Ritz, T., S. Adem, and K. Schulten, *A model for photoreceptor-based magnetoreception in birds*. Biophysical Journal, 2000. **78**(2): p. 707-718.
36. Rodgers, C.T. and P.J. Hore, *Chemical magnetoreception in birds: The radical pair mechanism*. Proceedings of the National Academy of Sciences, 2009. **106**(2): p. 353-360.
37. Solov'yov, I., et al., *Chemical compass for bird navigation*, in *Quantum effects in biology*. 2014, Cambridge University Press.
38. Ritz, T., et al., *Photoreceptor-based magnetoreception: optimal design of receptor molecules, cells, and neuronal processing*. Journal of the Royal Society Interface, 2010. **7** Suppl 2: p. S135-S146.
39. Phillips, J.B., R. Muheim, and P.E. Jorge, *A behavioral perspective on the biophysics of the light-dependent magnetic compass: a link between directional and spatial perception?* Journal of Experimental Biology, 2010. **213**(19): p. 3247-3255.
40. Kirschvink, J.L., *The horizontal magnetic dance of the honeybee is compatible with a single-domain ferromagnetic magnetoreceptor*. Biosystems, 1981. **14**(2): p. 193-203.
41. Phillips, J.B. and O. Sayeed, *Wavelength-dependent effects of light on magnetic compass orientation in *Drosophila melanogaster**. Journal of Comparative Physiology A Sensory Neural and Behavioral Physiology, 1993. **172**(3): p. 303-8.
42. Vácha, M., T. Puzova, and D. Drstková, *Effect of light wavelength spectrum on magnetic compass orientation in *Tenebrio molitor**. Journal of Comparative Physiology A: Neuroethology, Sensory, Neural, and Behavioral Physiology, 2008. **194**(10): p. 853-9.
43. Gegear, R.J., et al., *Cryptochrome mediates light-dependent magnetosensitivity in *Drosophila**. Nature, 2008. **454**(7207): p. 1014-8.

44. Geegear, R.J., et al., *Animal cryptochromes mediate magnetoreception by an unconventional photochemical mechanism*. *Nature*, 2010. **463**(7282): p. 804-807.
45. Phillips, J.B., et al., *Behavioral titration of a magnetic map coordinate*. *Journal of Comparative Physiology A: Neuroethology, Sensory, Neural, and Behavioral Physiology*, 2002. **188**(2): p. 157-160.
46. Jensen, K.K., *Light-dependent orientation responses in animals can be explained by a model of compass cue integration*. *Journal of theoretical biology*, 2010. **262**(1): p. 129-141.
47. Muheim, R., et al., *Magnetic compass orientation in C57BL/6J mice*. *Learning & Behavior*, 2006. **34**(4): p. 366-373.
48. Batschelet, E., *Circular statistics in biology*. 1981, New York: Academic Press.
49. Timmel, C., et al., *Effects of weak magnetic fields on free radical recombination reactions*. *Molecular Physics*, 1998. **95**(1): p. 71-89.
50. Diego-Rasilla, F.J., R.M. Luengo, and J.B. Phillips, *Light-dependent magnetic compass in Iberian green frog tadpoles*. *Naturwissenschaften*, 2010. **97**(12): p. 1077-1088.
51. Freake, M.J. and J.B. Phillips, *Light-dependent shift in bullfrog tadpole magnetic compass orientation: evidence for a common magnetoreception mechanism in anuran and urodele amphibians*. *Ethology*, 2005. **111**(3): p. 241-254.
52. Phillips, J.B. and S.C. Borland, *Behavioural evidence for use of a light-dependent magnetoreception mechanism by a vertebrate*. *Nature*, 1992. **359**: p. 142-144.
53. Yoshii, T., M. Ahmad, and C. Helfrich-Förster, *Cryptochrome mediates light-dependent magnetosensitivity of Drosophila's circadian clock*. *PLoS Biol*, 2009. **7**(4): p. e1000086.
54. Cintolesi, F., et al., *Anisotropic recombination of an immobilized photoinduced radical pair in a 50- μ T magnetic field: a model avian photomagnetoceptor*. *Chemical Physics*, 2003. **294**(3): p. 385-399.
55. Lau, J.C.S., C.T. Rodgers, and P.J. Hore, *Compass magnetoreception in birds arising from photo-induced radical pairs in rotationally disordered cryptochromes*. *Journal of the Royal Society Interface*, 2012. **9**: p. 3329–3337.
56. Grossfield, J., *Non-sexual behavior of Drosophila*. *Genetics and biology of Drosophila*, 1978.
57. Sawin-McCormack, E.P., M.B. Sokolowski, and A.R. Campos, *Characterization and genetic analysis of Drosophila melanogaster photobehavior during larval development*. *Journal of neurogenetics*, 1995. **10**(2): p. 119-135.
58. Hassan, J., et al., *Behavioral characterization and genetic analysis of the Drosophila melanogaster larval response to light as revealed by a novel individual assay*. *Behavior genetics*, 2000. **30**(1): p. 59-69.

Chapter III. Use of bio-loggers to characterize red fox behavior with implications for studies of magnetic alignment responses in free-roaming animals.

Michael S. Painter^{1*}, Justin A. Blanco², E. Pascal Malkemper^{3,5}, Chris Anderson², Daniel C. Sweeney⁴, Charles W. Hewgley², Jaroslav Červený⁵, Vlastimil Hart⁵, Václav Topinka⁵, Elisa Belotti⁵, Hynek Burda^{3,5}, John B. Phillips¹

¹Department of Biological Sciences, Virginia Tech, Blacksburg, Virginia, United States of America

²Department of Electrical and Computer Engineering, United States Naval Academy, Annapolis, Maryland, United States of America

³Department of General Zoology, Faculty of Biology, University of Duisburg-Essen, 45117 Essen, Germany

⁴Department of Biomedical Engineering and Mechanics, Virginia Tech, Blacksburg, Virginia, United States of America

⁵Department of Game Management and Wildlife Biology, Faculty of Forestry and Wood Sciences, Czech University of Life Sciences, 16521 Praha 6, Czech Republic

*Corresponding author

We would like to declare that the first two authors listed (MSP and JAB) contributed equally to the manuscript and should be considered co-first authors.

This manuscript has been published as: Michael S. Painter, Justin A. Blanco, E. Pascal Malkemper, Chris Anderson, Daniel C. Sweeney, Charles W. Hewgley, Jaroslav Červený, Vlastimil Hart, Václav Topinka, Elisa Belotti, Hynek Burda, John B. Phillips (2016). Use of bio-loggers to characterize red fox behavior with implications for studies of magnetic alignment responses in free-roaming animals. *Animal Biotelemetry* 4:20

Abstract

Background: Spontaneous magnetic alignment (SMA), in which animals position their body axis in fixed alignments relative to magnetic field lines, have been shown in several classes of vertebrates and invertebrates. Although these responses appear to be widespread, the functional significance and sensory mechanism(s) underlying SMA remain unclear. An intriguing example comes from observations of wild red foxes (*Vulpes vulpes*) that show a ~four-fold increase in hunting success when predatory “mousing” attacks are directed towards magnetic north-northeast. This form of SMA is proposed to receive input from a photoreceptor-based magnetoreception mechanism perceived as a ‘visual pattern’ and used as a targeting system to increase the accuracy of mousing attempts targeting hidden prey. However, similar to previous observational studies of magnetic orientation in vertebrates, direct evidence for the use of magnetic cues, and field-based experiments designed to characterize the biophysical mechanisms of SMA are lacking. Here we

develop a new approach for studies of SMA using tri-axial accelerometer and magnetometer bio-loggers attached to semi-domesticated red foxes.

Results: Accelerometer data were recorded from 415 ground-truth events of three behaviors exhibited by an adult red fox. A 5-Nearest Neighbor classifier was developed for behavioral analysis and performed with an accuracy of 95.7% across all three behaviors. To evaluate the generalizability of the classifier, data from a second fox was tested yielding an accuracy of 66.7%, suggesting the classifier can extract behaviors across multiple foxes. A similar classification approach was used to identify the fox's magnetic alignment using two 8-way classifiers with differing underlying assumptions to distinguish magnetic headings in eight equally spaced 45° sectors. The magnetic heading classifiers performed with 90.0% and 74.2% accuracy, suggesting a realistic performance range for a classifier based on an independent set of training events equal in size to our sample.

Conclusions: We report the development of 'magnetic ethograms' in which the behavior and magnetic alignment of foxes can be accurately extracted from raw sensor data. These techniques provide the basis for future studies of SMA where direct observation is not necessary and may allow for more sophisticated experimental designs aimed to characterize the sensory mechanisms mediating SMA behavior.

Keywords: Accelerometer, Magnetometer, Magnetoreception, Spontaneous magnetic alignment, Light-dependent, Compass, Red fox, Radio-frequency, *Vulpes vulpes*

Background

Recent advances in bio-logging technology, and its increasing deployment in studies of animal behavior and physiology, are providing new approaches to investigate both large scale and fine scale properties of spatial behavior in domestic and free-roaming animals [1-3]. Among the many sensor options, tri-axial accelerometers can yield a wealth of valuable information about movements in 3-dimensional space, but need sophisticated analysis techniques to be properly interpreted [4]. There is no consensus on the statistical techniques to use in extracting behavioral data from accelerometer signatures; the available methods have been shown to have varying degrees of success in identifying differences in behavior and posture across a range of diverse kinematic patterns [5, 6]. In addition to accelerometers, bio-logging devices equipped with tri-axial magnetometers are now available, providing researchers with a continuous record of the

alignment of the sensor with respect to magnetic north. Therefore, if the alignment of the sensor is in a known and fixed alignment with respect to the animal, the magnetic heading of the individual can be identified. However, transforming raw magnetometer data into reliable directional headings of free-roaming subjects poses several challenges [4, and see Methods]. Yet despite the technical obstacles, developing behavioral classifiers that can reliably identify behaviors of interest from accelerometer signatures time-synched with magnetometer data has the potential to provide investigators with a record of spatio-temporal behavior in animals inhabiting diverse environments where direct observation may not be possible, or in animals where direct observation may influence behavior (i.e., observer bias).

In particular, ‘magnetic bio-loggers’ used in studies of animal navigation and orientation could provide important new evidence for behavioral responses dependent on the geomagnetic field [7-14]. For example, several studies have reported evidence of spontaneous magnetic alignment (SMA) behavior across a range of vertebrates that show a strong tendency to align the anteroposterior axis bimodally along the north-south magnetic axis [for reviews see 15, 16, and recently 17]. Although SMA appears to be widespread, exhibited by a wide range of taxa including both vertebrate [15, 16, 18, 19] and invertebrate groups [20-23], the functional significance and biophysical mechanism mediating this behavior remains poorly understood. Possibilities of the functional significance underlying SMA include that the magnetic field could provide a stable reference frame for coordinating movement in open landscapes [24], or help to coordinate group responses in social animals [25]. Furthermore, magnetic alignment has been proposed to be involved in retinotopic matching in honeybees, helping to recognize familiar environments [26], and may simplify encoding the spatial relationships between landmarks and/or help to place local maps of space into register [27]. Given the utility of magnetic cues underlying diverse spatial

behaviors, it's clear that the magnetic field is not used only as source of 'simple' directional information, but rather may play a more general role in organizing and structuring spatial behavior and cognition. Therefore, SMA may reflect a basic form of spatial positioning to optimize the use of magnetic input for more complex spatial behaviors. However, the majority of vertebrate SMA studies have relied on field observations, which are difficult to conduct following double-blind protocols, are subject to observer bias, and are not well-suited for experimental manipulations needed to confirm that alignment responses are directly mediated by magnetic cues. Furthermore, field studies have not implemented experimental designs aimed to characterize the sensory mechanisms underlying SMA that will be critical for helping to determine the functional significance of this widespread behavior.

An intriguing example providing the only clear evidence for a fitness advantage of SMA in mammals comes from predatory behavior in red foxes (*Vulpes vulpes*). Visual observations of 'mousing' red foxes, in which a fox is attracted to the sounds produced by small rodents, and then performs an arching leap ('mousing') to land on the prey from above, showed a strong tendency for mousing attacks to be directed towards magnetic north-northeast [28]. The north-northeast alignment of mousing behavior is consistent with SMA responses exhibited by a variety of terrestrial vertebrates [16]. Interestingly, when a direct view of the prey was obstructed by high vegetation or snow cover, foxes more accurately aligned their attacks to the north-northeast and were approximately three to four times more successful at capturing prey than when aligned in other magnetic directions [28]. The authors proposed that the alignment behavior observed in foxes could be mediated by a light-dependent magnetoreception mechanism, similar to that used by migratory birds, newts, and insects [7, 14, 29-34] where specialized photopigments undergo a photo-induced chemical reaction that is sensitive to the alignment of the magnetic field. In animals

where these photopigments are located in the retina, the magnetic field may be perceived as a 3-dimensional pattern of light intensity or color superimposed on the animal's visual surrounding and fixed in alignment with respect to magnetic north [27, 35]. Such a pattern could appear like a visual 'after image' that moves with the animal yet, remains fixed with respect to magnetic north [27]. Similar to the light-dependent magnetic compasses of migratory birds [36], newts [37], and sea turtles [38], that are sensitive to the inclination, not polarity, of the magnetic field lines, the inclination of the pattern of 'visual' input generated by a light-dependent magnetic mechanism could be used to estimate distance. Specifically, in the northern hemisphere, the magnetic field lines re-enter the Earth at increasing angles with increasing latitude, and therefore, some components of the 3-dimensional visual pattern would be superimposed on the substrate below the level of the retina [for additional details and proposed 3-dimensional patterns see 27, 35, 39, 40, 41]. The inclination of the magnetic field would not vary substantially (e.g., $\sim 0.1^\circ$) over a fox's home range [42], and therefore, the fox could approach the prey along a fixed compass heading until some component of the visual pattern generated by the light-dependent magnetic mechanism was superimposed on the sound source generated by a prey hidden beneath the substrate (analogous to centering the 'cross-hairs' of a gun sight), enabling the fox to initiate mousing attacks from a fixed distance. Given the indirect ('ballistic') trajectory of mousing attacks, the accuracy of such attacks may be greater if they are initiated from a fixed distance and performed using a stereotyped set of mousing mechanics. Interestingly, the small clustering of successful mousing attacks directed towards magnetic south [28] suggests that the opposite end of the magnetic axis may also guide mousing behavior, and is consistent with an axially symmetrical pattern of magnetic input as proposed by [27, 35, 41]. Therefore, SMA in red foxes is thought to result from

the fox aligning components of the visual pattern, providing a targeting system helping to estimate the distance of the unseen prey, increasing the likelihood of successful prey capture [28].

Here, we report the development of magnetic bio-logging techniques for future studies of SMA in free-roaming red-foxes that will likely provide new approaches to study other forms of magnetic behaviors across a range of terrestrial animals. Semi-tamed red foxes trained to exhibit ‘mousing-like’ leaps in outdoor enclosures were used to develop ‘magnetic ethograms’ to provide templates for data collection from free-roaming animals in the wild. Three predetermined behaviors performed in varying magnetic directions were video-taped to serve as ground-truth data. Raw accelerometer data were then used to establish classifiers ‘trained’ to identify these behaviors in unseen datasets recorded from the same individual and from a different individual exhibiting similar behavior. Using a similar machine learning algorithm approach, magnetic classifiers were developed using ground-truth video records and ‘trained’ to distinguish between eight magnetic directions corresponding to the cardinal (i.e. N, S E, W) and anti-cardinal (i.e. NE, SE, SW, NW) magnetic axes. Taken together, the time-synched accelerometer and magnetometer data provide magnetic directional headings for events identified by the behavioral classifier, demonstrating the potential for bio-logging applications in studies of SMA in free-roaming foxes that can be adapted for use in studies of magnetic responses in other mammals.

This work provides the basis for future SMA research in foxes and other free-living mammals equipped with miniaturized tri-axial accelerometer and magnetometer devices, and more generally, makes it possible to improve the accuracy of directional observations for magnetic alignment studies of semi-domesticated and wild animals, and avoid potential biases inherent to observational studies. Such studies have been difficult to conduct following double-blind protocols, are not well-suited for experimental manipulations, and have been criticized for failing

to provide direct evidence for the involvement of magnetic cues underlying SMA responses. We discuss the potential use of magnetic bio-loggers in field-based studies of magnetic behavior in free-roaming animals and propose specific experiments to test for the involvement of light-dependent and magnetite-based magnetic mechanisms underlying magnetic targeting behavior of wild red foxes that would be possible using bio-logging technologies.

Methods

Two adult male red foxes (*Vulpes vulpes*) were used to develop magnetic ethograms and all methods were approved by the Czech University of Life Sciences (SP506051228). Both foxes were rescued from the Bohemian Forest in the Czech Republic as pups and raised in captivity in separate cages. All data were collected within a 20m diameter circular outdoor enclosure located in Prášíly, Czech Republic (49.1033°N 13.3819° E) between February 15, 2014 and May 15, 2014. Both foxes were in good health verified by a veterinarian before the study and were fed commercial dog food supplemented with wild mice. An initial three week period was required to acclimate both foxes to a modified adjustable domestic dog harness (Kong® Comfort Dog Harness). The subject used to collect the majority of behavioral and magnetic alignment data (Fox1) was fitted with a simplified version of the harness in which only the collar portion of the harness was used, securely fastened around the neck (Figure 1A). The second fox (Fox2) wore the complete harness system in which the collar and torso portion of the harness was snugly secured around the fox's neck and torso (Figure 1B). After the acclimation period, the collar was equipped with a bio-logging unit (Gulf Coast Data Concepts, Waveland, MS, USA <http://www.gcdataconcepts.com/contact.html>, model: X8-M3 USB) designed to record simultaneous tri-axial accelerometer and magnetometer data. On Fox1 the device was secured with two plastic zip ties to the ventral side of the collar (Figure 1 A). The device was secured to the

dorsal side of the harness on Fox2 (Figure 1B). Two identical devices were used to collect behavioral and magnetometer data from each of the foxes and were switched every ~five days to recharge the internal battery. The units recorded continuously until the battery was depleted or the device was removed from the animal. On average, two 30min behavioral sessions were recorded each day taking place at various times between 7:00 and 19:00 local time.

Bio-logging Recording Specifications

The X8M-3 USB accelerometer devices provided a continuous stream of time-stamped accelerometer and magnetometer data saved to a 2GB internal flash memory drive. The devices included a +/- 8g accelerometer with a 14-bit analog-to-digital converter yielding 0.001 g measurement resolution on each axis. The magnetometer was programmed to operate over a ± 400 μ T range with measurements approximated to within ± 111 nT on the x-and y-axes and ± 125 nT on the z-axis. For all data collected, tri-axial accelerometer data were recorded at a sampling rate of 6Hz and the magnetometer data were recorded at 3 Hz. An internal lithium-ion polymer battery powered the device and when fully charged would run continuously for ~ 130hrs in these sample rate configurations.

Behavioral Recording Sessions

During the 30min recording sessions all behaviors were videotaped using a digital camera (Nikon Coolpix AW110) mounted on a tripod located approximately 1m outside the observation arena. During each recording session, the fox was released from its home cage directly into a circular open field arena (~25m diameter) where it was allowed to roam freely. At no point were the two foxes in the arena at the same time. The perimeter of the arena was secured using 1.5m tall aluminum mesh fencing, and the top of the arena was covered with plastic mesh to ensure the fox

did not escape during trials. Additional structures were constructed inside the observational arena and used for behavioral and magnetic data collection (described immediately below).

Behavioral data were collected from Fox2 inside a 10m x 10m square enclosure with walls 1m tall constructed of wooden boards located in the center of the observation arena (Figure 2A and see Supplemental Video Files 1, 2). The fox was placed inside the enclosure and allowed to forage for food pellets and live wood mice hidden under small brush piles composed of straw and pine branches. After a foraging bout, typically less than 3min, the fox would jump out of the square enclosure and return to the home cage. Unfortunately, Fox2 was stolen from its home cage shortly after beginning the behavioral recording sessions. Therefore, only a limited amount of behavioral data was obtained from this subject. As a result of the limited number of recording sessions and relatively primitive square enclosure used to collect behavioral data, the behaviors recorded from Fox2 were more variable and erratic relative to those of Fox1.

Most of the behavioral data were collected from Fox1. This fox was trained using two different obstacles built inside the observational arena, both designed to encourage the fox to perform ‘mousing-like’ leaps. One obstacle made of wooden boards and plastic netting stretched across the entire arena at a height of ~1m. An observer inside the arena trained the fox to jump over the obstacle by tossing a food reward (one piece of dog food) on the opposite side of the obstacle. In an attempt to make the jumps mimic natural mousing behavior, in which the fox performs a high vertical jump followed by a rapid deceleration as it lands on top of its prey, a second barrier was placed ~1m beyond the first obstacle so that when the fox jumped over the first obstacle it had to stop immediately after landing to prevent a collision with the second wooden barrier (Figure 2B and see Supplemental Video File 3).

A separate structure was introduced consisting of a 1m central square area (the ‘food reward area’) enclosed with plastic fencing 1m tall. Four corridors were attached to the four sides of the food reward area providing access to one wall of the enclosure from each of the four cardinal compass directions (i.e., North, South, East, West). Fox1 was trained to walk down one of the four corridors toward the food reward area and jump over the 1m tall fence barrier to receive a food reward (Figure 2 C, D and see Supplemental Video Files 4, 5). ‘Mousing-like’ leap data for Fox1 was collected using both of the obstacles described above. Magnetometer data were analyzed from Fox1 only using the arena with the attached corridors aligned along the cardinal compass directions to obtain more precise ground-truth magnetic data from time points when Fox1 was in cardinal (i.e. 0°, 90°, 180°, 270°) and anti-cardinal (i.e. 45°, 135°, 225°, 315°) magnetic alignments.

When the bio-logging unit was removed every ~five days, the accelerometer and magnetometer data were downloaded. Each of the 30min video recording sessions were partitioned into separate data files. The video was then replayed and manually analyzed for three discrete behaviors: trotting, foraging, and ‘mousing-like’ leaps over the barriers described above. These behaviors were chosen a priori with no knowledge about the acceleration signatures underlying each behavior. Mousing, trotting and foraging behaviors are performed with distinct patterns of movement and have been observed in wild foxes (pers. observ.), and therefore were used to develop a behavioral classifier that would satisfy the focus of the current study (i.e., mousing behavior) and identify other functionally relevant behaviors for future bio-logging studies in red foxes. Trotting was defined as moving through the arena at a pace where two of the four paws were not in contact with the ground, but without the rapid horizontal accelerations and high rate of speed associated with sprinting behaviors (see Supplemental Video File 6) [6]. Foraging was defined as the fox slowly moving through the arena (slower pace than a walk) with its head and

snout towards the ground searching for food using olfactory and visual cues (see Supplemental Video File 7). A ‘mousing-like’ leap was defined for Fox1 as jumping over the vertical barrier in either of the obstacles described above (Supplemental Video Files 3, 4), or in the case of Fox2, out of the sides of the square enclosure (see Supplemental Video Files 1, 2). Based on preliminary visual observations, a typical jump lasted ~2 secs (~0.5 Hz) and the predominant oscillations in trotting and foraging behaviors did not exceed 3 Hz. Therefore, in order to fulfill the Nyquist sampling criterion which requires the sampling rate to be greater than twice the highest frequency of the signal components used to characterize the events of interest, the accelerometer sampling rate was programmed to record at 6 Hz after low-pass filtering to minimize aliasing [43].

Statistical Analysis

Accelerometer Data Analysis

All accelerometer and magnetometer data were analyzed in Matlab (MathWorks, Natick, MA). Cross-validation was used to estimate how the classifier would perform on new, unseen accelerometer data. Prior to analysis, individual behaviors (i.e., ‘mousing-like’ leap, foraging, and trotting) were identified using raw video records. For each behavioral event, 15-sample segments, corresponding to 2.5 secs of data given the accelerometer’s sampling rate of 6Hz, were extracted and used for analysis. The 2.5 sec window duration was chosen under the hypothesis that it would be long enough to characterize and distinguish, leaping, foraging, and trotting activity while short enough to minimize errors due to overlapping events and to maintain the practicability of real-time processing. In order to determine if the preselected behaviors could be distinguished based on the acceleration signatures, a 5-nearest neighbor classifier was used, in which unknown (i.e., ‘test’) behaviors are classified by a ‘majority vote’ of their 5 nearest known (training) neighbors in a

feature space. Expanded details of the behavioral classification method are provided in the *Accelerometer Feature Extraction* and *Behavioral Classification* sections below.

Accelerometer Feature Extraction

Each 15-sample data segment was zero-meaned prior to extracting the following four time-domain features: 1) the magnitude of the largest z-axis peak; 2) the time-delay between the two largest z-axis peaks; 3) the energy in the output of a matched filter run on the z-axis; and 4) the energy in the output of a 2 Hz high pass filter, averaged over the x and y axes. The matched filter used for feature 3 was a simple 4-sample rectangular pulse with height 1g. For feature 4, the data on both the x and y axes were first normalized to have unit energy; a 3rd-order Butterworth highpass filter [44] with a -3dB point of 2 Hz, chosen for its maximally flat passband response, was then applied to each axis. Features 1 and 2 were designed to be selective for leaping events, which were expected to have large-magnitude vertical acceleration components; feature 3 was designed to be selective for foraging events, which were expected to have a relatively stable vertical axis acceleration profile; and feature 4 was designed to be selective for relatively high-frequency rhythmic trotting activity. The features were deliberately chosen to have some robustness to differences in accelerometer orientation, which can arise both due to movement and to differences in mounting of the tri-axial accelerometer, requiring only that one axis was known to be at least nominally aligned (at either 0 or 180 degrees) with respect to vertical.

Behavioral Classification

The four features described above were used as inputs to a 5-Nearest Neighbor classifier with the L1 norm as the distance metric (i.e., the distance between any two observations was the sum of the magnitudes of the differences between corresponding feature-values). K-Nearest Neighbors (k-

NN) is a standard nonparametric technique for performing supervised learning tasks such as classification. It can be viewed as an approximation to the optimal but practically unrealizable Bayes classifier, which assigns an observation to the most likely of a predetermined set of classes given its feature measurements. In k-NN, the probability that an unknown observation belongs to a particular class is estimated by the fraction of its k closest training set neighbors belonging to that class. The predicted class label is then the class with the highest probability. Ten-fold cross validation was used to estimate test set error. That is, the entire data set was partitioned into ten randomly chosen disjoint subsets of approximately equal size, nine of which were used for training the classifier and the other for testing on each of ten iterations. Each subset served as the testing data exactly once. The overall estimate of test set error was obtained as an average of the test set errors achieved on each of the ten iterations.

Magnetometer Data Analysis

We defined the animal's magnetic heading (hereafter referred to as heading) as the angle between the posterior to anterior alignment of the spine, assumed to be rigid, and the direction of the Earth's magnetic field when both of these lines are projected onto the plane perpendicular to the gravity vector. A number of uncertainties associated with the free-roaming animal paradigm make it challenging to infer the animal's heading based upon tri-axial magnetometer and accelerometer data. For example, due to the animal's normal movements, all of the following alignments are known only imprecisely: 1) alignment of the sensor relative to the fox's collar; 2) alignment of the collar relative to the fox's neck; and 3) alignment of the fox's neck relative to the rest of its spine. Additionally, it is reasonable to assume that a fox may slightly alter its heading on the timescale of a single magnetometer sample (0.33 sec), leading to the potential measurement of sensor transient responses that add further noise to the data. Traditional tilt-compensation algorithms

[e.g., 45] that attempt to use tri-axial accelerometer data to sense device orientation and apply the appropriate trigonometric corrections to heading estimates are not reliable under these conditions because they assume an unchanging reference mounting orientation; in other words, they assume that the mapping (rotation matrix) between the coordinate frame of the sensor and the coordinate frame of the fox's body remains constant.

To deal with the uncertainties outlined above, we framed the heading estimation problem as a supervised learning task, and in particular, as a classification task. While in principle we could have treated this as a regression, our video-labeling method of ground-truthing had limited resolution, and therefore, we used an 8-way classification task with the four cardinal and four anti-cardinal directions comprising the complete set of eight possible headings. This amounts to binning continuous headings using eight 45° sectors. Specifically, we sought to estimate the fox's heading with this degree of resolution given the acceleration and magnetic field strength measurements along the three orthogonal (x,y,z) axes of the sensor. Inputs to the classifier were thus the six-element vectors formed by concatenating the three accelerometer and three magnetometer measurements. We hypothesized that the optimal boundaries between each of the classes in this six-dimensional input space would be highly nonlinear due to the aforementioned sources of noise, and therefore used random forest classification [46], which is capable of learning nonlinear boundaries while simultaneously mitigating overfitting.

Random forests offer improved predictive accuracy over single decision tree classifiers by smoothing predictions over an ensemble of related trees. Detailed reviews of tree-based classification, and random forests in particular, can be found in [47]. In brief, decision tree classifiers seek to optimally partition input space into a series of non-overlapping hyper-rectangles using labeled training data. Once the partitioning is learned, new observations are classified

according to the region (hyper-rectangle) of input space into which they fall. Specifically, they are assigned the class label most frequently occurring among the training data points falling into the same region.

Because exhaustively searching over all possible unique partitionings of input space is generally computationally intractable, it is standard to use a greedy, top-down approach known as recursive binary splitting. At the start of the procedure (i.e., at the top (root) node of the tree), each training observation belongs to the same region. On each successive iteration, the algorithm chooses the single input feature and cut point (feature value), across all current regions, that leads to the greatest reduction in some objective function. It then forms two new regions by dividing the selected region in accordance with the chosen feature-cut point combination, and continues the splitting procedure until a stopping criterion is met. In this work, we use the Gini index [48] in region m , G_m :

$$G_m = \sum_{k=1}^K \hat{p}_{mk}(1 - \hat{p}_{mk})$$

as the basis for the objective function, where K , the number of classes (headings), is 8 in our case, and \hat{p}_{mk} is an estimate of the probability that an observation in the m^{th} hyper-rectangular region belongs to the k^{th} class. The latter is computed as the fraction of training observations within the m^{th} region having the class label k . G_m can be interpreted as an estimate of what the misclassification rate for observations falling into region m would be if observations were randomly classified according to the distribution of classes in that region. It measures the class-impurity of region m , being smallest (zero) when all observations in the region fall into a single class and largest when the distribution of observations across classes is constant.

The objective at each stage of the binary recursive splitting procedure is to find the region and split that leads to the smallest weighted sum of Gini indices across regions (where the weights are equal

to the number of observations in each region). We stop the binary recursive splitting procedure when no split can be found that decreases the objective. Since this procedure is prone to growing deep trees that overfit the training data and therefore have poor generalization performance, it is typically augmented using some type of statistical method to reduce the variance of the learned model.

Random forests accomplish this variance reduction by learning separate trees on B (here $B = 1000$) bootstrapped data sets [49] of size equal to that of the original training data, formed by randomly sampling with replacement from the original training data. Furthermore, when considering each split for particular tree, only a random subset of j input features (here $j = 2$) are considered as potential candidates for the split. This has the effect of producing B trees that are less correlated than those that would be learned if the full set of input features were considered on each iteration, and hence a final classifier with lower variance and better generalization performance. Specifically, the final random forest classifier, C_{rf} , assigns its class labels according to:

$$C_{rf}(\vec{x}) = \text{mode}\{C_b(\vec{x})\}_{b=1}^B$$

where \vec{x} is the input vector and the right side of the equation denotes a plurality vote among the class predictions made for \vec{x} by each of the B single-tree classifiers learned on a separate bootstrap sample.

Magnetometer Classifier Training

To form a ground-truth data set for training the random forest classifier, a total of 381 samples recorded during 66 distinct heading events were assigned one of eight magnetic heading labels (N, NE,E,SE,S,SW,W,NW) by consensus between two human reviewers. Assignments were made based on reviewing video recordings of Fox1 behaving in the vicinity of the 4-arm maze (Fig. 2C)

aligned along the cardinal compass axes. Therefore, ground-truth heading classifications in the cardinal and anti-cardinal directions could be identified by using the maze as a reference. Distinct heading events were identified as time-separated occasions on which the fox appeared to maintain a consistent heading for at least 0.5 seconds. The duration of the consistent-heading period determined how many samples were collected for each heading event.

Results

Behavioral Classification

A total of 415 events from Fox1 trained to the two obstacles were manually identified using video records and input into the classifier. Of the 415 events, 265 (64%) were ‘mousing-like’ leaps, 100 (24%) were foraging, and 50 (12%) were trotting. Overall classification accuracy was 95.7% (chance performance with a null model of equiprobable classes is 33.3%; chance performance with a null model obtained by assigning each observation to the most frequent class is 63.9%; Table 1). The error rates for each class, leaping, foraging, and trotting, respectively, were 0.015, 0.00, and 0.28. Unsurprisingly, given its relative infrequency, trotting behavior was the most difficult to classify, with 11/50 trotting events misclassified as leaping and 3/50 as foraging (Table 1 and see Discussion). Accelerometer data showed stereotypical acceleration signatures recorded on each axis of the three behaviors used in the classifier (Figure 3). Figure 4 shows the data plotted in the three-dimensional space given by the first three principal components projections after z-scoring (i.e., subtracting the mean and dividing by the standard deviation of each feature), as well as in the two-dimensional spaces defined by all possible pairs of the first three principal components. Z-

scoring and PCA were employed only to facilitate viewing the 4-dimensional feature data in 3-dimensions and were not used as processing steps prior to classification.

Generalizability of the Classifier to New Foxes

To the extent that foxes perform mousing-like leaps, foraging, and trotting in a stereotyped way, one would expect our classifier to accurately distinguish these behaviors in new, free-living foxes. A small amount of data (33 events) from Fox2 were recorded prior to its removal from the study and used to test the classifier's ability to generalize across foxes not used to train the classifier. It should be noted that this fox had much less experience performing the behaviors of interest and was trained using a different type of obstacle compared to Fox1 (see Methods, Behavioral Recording Sessions and Supplemental Video Files 1-5), and therefore, its 'mousing-like' leaps differed from Fox1 used to collect the majority of behavioral data. However, even with the high degree of behavioral variability between Fox1 and Fox2, the accuracy of identifying the three types of behavior was 66.7% (Table 2). The error rates for mousing-like leaps, foraging and trotting respectively, were 0.3, 0.286, and 0.625. This accuracy is significantly better than chance ($\alpha = 0.05$) using a null model that assigns each observation to the most frequently occurring class in this fox's data set (Binomial Test, $p = 0.027$). We also note again that the sensor mounting scheme was different for Fox1 and Fox2. While the features we used were approximately invariant with respect to the 90 degree rotational difference, we did not have a way of quantifying other potential differences in accelerometer orientation between the two device mountings. Any such differences would most certainly negatively impact classification performance in Fox2, though the severity of the impact is difficult to estimate without a quantitative understanding of other orientation differences. No changes were made to the data processing chain to customize the classifier for Fox2 before testing; Fox2 was simply tested using a classifier trained exclusively on data from

Fox1. Results were particularly encouraging in light of the different mounting schemes and will likely improve if mounting can be standardized in future work. See Discussion for other factors that could contribute to decreased classifier performance across individuals and possible solutions to mitigate these sources of error for more accurate and reliable behavioral data in future studies involving wild foxes.

Magnetometer Data

Classification Results

As previously mentioned, the duration of the consistent-heading period determined how many samples were collected for each heading event. The number of samples per event ranged from 2 to 29 with a mean of 5.77 ± 5.16 (mean \pm 1 s.d.). Table 3 shows a detailed breakdown of events and samples for each of the eight heading directions.

We performed two separate classification analyses. The first implicitly assumed that all samples collected from a given heading were independent draws from the same unknown class-conditional probability density function. Each sample was therefore treated as an individual observation (i.e., object for which a heading estimate is desired), giving a total number of observations of 381. Using 10-fold cross-validation to estimate the generalization performance of the random forest classifier, the accuracy achieved was 90.0%. Table 4 gives the complete confusion matrix for the first classifier, which shows performance on a per-heading basis. A Rayleigh test was used to test for non-random clustering of magnetic headings, as predicted by the classifier, relative to ground-truth classifications determined by a human observer [50]. Therefore, data was pooled with respect to ground-truth predictions in each of the eight magnetic directions and plotted as the degree of error for each sample, regardless of the ‘true’ or absolute bearing for a given sample (Fig. 5). All circular

statistics were performed using Oriana 4.0, Kovach Computing Services, and for each analysis, the data were treated as eight equal width groups, each width equal to 45° . Treating each sample as an independent point from the overall dataset resulted in the following; sample size, $n = 381$, mean vector of the distribution, $\mu = 359^\circ$, r -value = 0.95, where r represents the mean vector length of a circle with radius = 1, and $p < 1 \times 10^{-12}$ (Fig. 5A).

The second analysis replaced the assumption that all *samples* from a given heading were class-conditionally independent with the less-stringent assumption that only *events* within a given heading represented independent draws. This accounts for potential time-correlations among the samples within an event that might optimistically bias the measure of generalization performance. Individual observations in this second analysis were therefore heading events rather than samples, and were computed by averaging the samples collected during each event. Collapsing the data set in this way yielded a training set with 66 observations, one for each of the heading events identified by the human reviewers. The 10-fold cross-validated accuracy for the random forest classifier learned in this setting was 74.2% and the complete confusion matrix is shown in Table 5. Testing for non-random clustering of classifier predictions relative to ground-truth classifications when each *event* was treated as an independent point from the overall dataset resulted in the following; sample size, $n = 66$, mean vector of the distribution, $\mu = 2^\circ$, r -value = 0.87, where r represents the mean vector length of a circle with radius = 1, and $p < 1 \times 10^{-12}$ (Fig. 5B).

Discussion

The use of bio-logging technologies to help characterize spatial behavior and the underlying sensory mechanisms mediating magnetic alignment is a promising technique for future studies of

free-roaming animals. In particular, the development of the behavioral ethogram coupled with time-synced recordings of magnetic headings provides a powerful tool to collect unbiased and non-invasive behavioral and magnetic data from wild foxes in the absence of direct observation. These techniques can also be adapted for deployment in magnetic studies of a variety of terrestrial vertebrates, an exciting potential given the growing evidence for SMA responses across diverse taxa [15-17, 25]. Although similar devices (i.e., accelerometer and magnetometer bio-loggers) have been used to characterize spatial behavior in free-roaming animals, extracting magnetic compass headings from animals moving in 3-dimensional space is much more challenging and is rarely reported in behavioral studies. The first attempt to use magnetic sensors to record directional behavior in free-living animals monitored changes in magnetic measurements over time using a fluid-filled ship's compass equipped with Hall sensors to determine activity patterns in sea turtles [51]. A more recent study of flight paths in Andean condors equipped with bio-loggers was able to identify when birds were circulating within thermals using the sine wave signatures of compass measurement readouts, indicating the bird was rotating through 360° in the horizontal plane [52]. However, magnetic compass headings were not reported and only circular vs straight flight path trajectory could be derived from the information provided. Magnetic heading data were reported in studies of pinnipeds that deployed tri-axial sensors to measure changes in magnetic field intensity helping to reconstruct dive paths [53, 54]. However, the accuracy of the heading estimates were not reported or verified by ground-truth data, and it is unclear if the devices were calibrated prior to deployment, as the magnetic output of each axis varies with device orientation and could lead to large errors when calculating magnetic headings [4].

Using a k-NN technique for behavioral classification, we have shown that three distinct behaviors can be identified with a 95.7% rate of accuracy when tested against unseen data from the same

individual (Fox1) that was not used to train the classifier. As shown in Table 1, trotting behavior was by far the most difficult to classify. However, the trots misclassified as leaping represented a false positive rate for leaping of only 4.0%. The rates of misclassification of the three behaviors in the current study are sensitive to relative sample sizes of each behavior and may not be representative of the relative occurrence of behaviors in wild foxes. Therefore, in future studies of free-living foxes, the percentages of misclassifications will be subject to the relative occurrence of each behavior. The low percentage of misclassifications of leaping events may be overly optimistic and the algorithm's assignment of trotting events might be problematic depending upon the cost a particular researcher assigns to a missed trot in other types of studies. However, the precision for declaring a trot (i.e. the likelihood that a trot, as identified by the classifier, was indeed a trot) was 90.0%, and the recall for trotting (i.e. the percentage of total trots identified by the classifier) was 72%, much better than chance performance. Increasing the sample size for trots used to train the classifier would likely increase trotting precision and recall. In addition, implementing automated filters within the feature extraction process (e.g., z-axis max acceleration or peak-to-peak time interval thresholds) could be used to limit the influence of outlying training observations and further 'tune' the classifier for any behavior of interest, e.g., 'mousing'. Additional features that capture pre-mousing behavior (e.g., stalking and slow approach toward prey often accompanied by a brief pause prior to the mousing jump) could help to distinguish between mousing jumps and other non-predatory movements that may resemble mousing behavior. However, the foxes used in the current study did not display this type of pre-mousing behavior, and therefore we were not able to incorporate such techniques into the algorithms.

Importantly, in the context of this study, the classifier was successful at identifying behaviors from data collected from a separate fox (Fox2) not used to train the classifier with an accuracy of 66.7%.

These results are encouraging given the small sample size, the difference in device mounting scheme on Fox2 (see Methods), and much higher behavioral variability relative to Fox1. This variability was due to differences in the design of the enclosure used to elicit mousing-like behavior, resulting in observable differences in jump approach, jump trajectory and landing mechanics (see Supplemental Video Files 1-5). However, even with the differences in sample size, device mounting orientations, and the behavior of Fox2, there were no false positives in identification by the classifier of ‘mousing-like’ leaps (Table 2), i.e., all mousing-like leaps identified in Fox2 were indeed mousing-like leaps.

The observed performance decline for Fox2 reflects not only differences in training and natural behavior between the experimental foxes but also potentially differences in device orientation, as mentioned above, as well as other sensor-related factors, such as temporal drift and calibration parameter differences between devices. All of these sources of error can be mitigated to some degree in future work by protocol standardization (e.g., of behavioral training and device mounting) and enlargement of the sample size of foxes and sensors used to build the training set. But classifier generalization performance will ultimately be governed by how representative any training data is of fox behavior in the wild. Since any wild fox experiment will necessarily involve first capturing subjects in order to instrument them, one possibility would be to use a protocol involving a brief classifier training period during which captive foxes are video-monitored under freely-behaving conditions, perhaps in an enclosure similar to the one used in this study. Though it is unlikely that each fox would exhibit the full set of desired behaviors in this captive setting, data recorded from these sessions could be used to impart some degree of individualized tuning to the classifiers used for each fox, which would in turn result in improved performance for wild fox

classifiers. Furthermore, this approach would help to confirm the generalizability of the current classifier by comparing ground-truth data from the semi-domesticated foxes and wild foxes.

More generally, given the accuracy of the classifier within an individual and its above chance performance on a separate individual not used to train the classifier that exhibited a different set of kinematics, our methods show considerable promise for identifying leaping behaviors in wild foxes. To validate that accelerometer signatures recorded from mousing-like leaps are similar to those of functional mousing behavior in wild foxes, and to confirm the generalizability of the classifier across multiple individuals, ground-truth data from free-roaming foxes equipped with bio-logging devices will be critical for future studies of SMA in red foxes. Moreover, the development of more sophisticated classifiers and using an expanded feature set could allow even greater precision of behavioral identification and provide opportunities to identify more complex behaviors, e.g., predatory from non-predatory leaps, and could be augmented with additional sensors such as jaw accelerometers or onboard video recording devices to identify behavioral outcomes, e.g., prey capture success or foraging habitat type.

In addition to the behavioral classification, we used a supervised learning task, specifically a classification task, to identify the magnetic compass headings of Fox1 during behaviors that parallel the behaviors preceding mousing attempts in wild foxes (e.g., slow, stalking approach). Due to resolution of ground-truth video records, we used an 8-way classification task with the four cardinal and four anti-cardinal directions, and therefore, the classifier could distinguish among eight magnetic directions with a 45° resolution.

We performed two separate random forest classification analyses, the first assumed each *sample* was an individual observation, and therefore contained a total of 381 observations. Using 10-fold cross-validation to estimate the generalization performance of the random forest classifier, the

accuracy achieved was 90.0% (Table 4 and Fig. 5A). Of note, all but 7 (1.8% of all observations) of the errors made by the classifier were “off-by-one”; i.e., the classifier predicted either the correct heading or one of the headings adjacent to the true heading in 98.2% of all cases. However, we recognize that this analysis may be overly optimistic since this approach did not account for potential time-correlations between samples drawn from a given heading. Therefore, the second analysis limited individual observations to heading *events*, defined in this study as periods of time when Fox1 was assigned to a consistent direction by a human reviewer. Heading events were then computed by averaging samples over each such time period. This resulted in a smaller sample size (n= 66 observations) and 10-fold cross-validated accuracy for the random forest classifier learned in this setting was 74.2% (Table 5 and Fig. 5B).

While it is tempting to conclude that the second analysis is more appropriate than the first, it should be noted that some of the observed performance decline is likely attributable to the dramatic reduction in the size of the training set used in the second analysis. It is reasonable to assume that if a larger number of events were available for training, accuracy on unseen data would fall somewhere between the bounds of 74.2% and 90.0% that was achieved (Fig. 5). Of course, even a pessimistic estimate of 74.2% accuracy far outstrips a chance classifier, which would perform at 12.5% on this problem.

Whether a digital compass (i.e., heading-classifier) with the degree of resolution and accuracy we present here would yield conclusive data in a larger field study involving multiple wild foxes depends on the strength and scale of any effect being measured as well as the degree of behavioral similarity across animals. The latter can potentially be managed by training classifiers on individual foxes which participate in field-based studies, or across a representative group of wild and/or captive foxes. In addition, improvements in the sensor fixation and mounting technique, in

the resolution of the apparatus and methodology used to collect and label ground-truth data, and in the size of the training data set would all likely yield improvements in the resolution and accuracy of the classifier. In future studies designed to characterize the biophysical mechanisms mediating SMA, treatment groups (e.g., foxes exposed to radio-frequency fields in the low-MHz range, see below) would be predicted to exhibit magnetic alignment responses indistinguishable from random, similar to the behavioral effects of radio-frequency exposure on the magnetic compass response in migratory birds [55]. The 8-way classifier developed in this study is well-suited to distinguish between the magnetic headings of oriented and random mousing attempts, although the strength of the orientation in control group would determine the sample size needed to confirm any treatment effect. In conclusion, we are encouraged by the performance of the 8-way classifiers in light of the difficulty of the problem, and believe the framework established here is promising and merits further study and development.

The development of these automated behavioral monitoring and classification techniques will make it possible to further investigate magnetic alignment responses exhibited by foraging red foxes whose prey capture success has been shown to be dependent on their orientation with respect to the Earth's magnetic field [28]. Červený et al.'s analysis of prey capture success in habitats where visual cues could not be used to guide mousing behavior (i.e., dense vegetation and snow cover) revealed that foxes were approximately four times more successful when attacks were directed towards magnetic north-northeast. One possible explanation for this type of alignment behavior is the involvement of a light-dependent magnetoreceptor mediated by the so-called 'radical pair mechanism' that could be perceived as a visual pattern superimposed on the animal's visual surroundings [27, 35, 56]. As suggested by Červený et al. (and see Introduction), this visual pattern, fixed in alignment with respect to the magnetic field, could be used as a targeting system

that may allow foxes to initiate their attacks from a fixed distance, increasing the accuracy of the mousing attempt. Consistent with Červený et al.'s findings, the contribution of the proposed magnetic 'range-finder' (i.e. distance estimator) to the accuracy of predatory attacks could be especially pronounced when the fox's view of the prey is obstructed by dense vegetation or snow cover [28].

Although the red fox is considered a generalist species, several studies of central European red foxes suggest that a significant proportion of their diet comes from rodents that varies depending on elevation and season. For example, one study estimates that 65% of the fox's diet comes from rodents throughout the year [57], whereas more recent estimates suggest that >30% of their diet is composed of rodents (and hares), and during the winter months small mammals make up approximately 40% of the fox's diet [58]. Although foxes will use sight to guide the majority of predatory behaviors in habitats with low vegetation and no snow cover, even just two weeks of tall grass or snow would require that foxes 'mouse' to catch prey burrowed under the substrate, and therefore, 'hard' evolutionary selection is considered to underlie the fox mousing phenotype. Given the importance of mousing to fox survival, it's not surprising that multiple cues and sensory systems are involved, helping to increase the success and efficiency of mousing behavior.

Magnetic bio-loggers can provide a valuable tool for future studies of magnetic alignment in free-roaming animals, and in particular foraging wild red foxes. The development of these devices, along with well-developed behavioral classifiers and magnetic alignment data offer a non-invasive technique for collecting robust and unbiased behavioral datasets across multiple individuals. However, it must be confirmed that the bio-loggers themselves, the harness system, or any additional equipment secured to the fox do not introduce unintentional biases or effect the performance of functional behaviors in wild foxes. One advantage of the miniaturized bio-logger

and collar use in the current study is that it offers a light weight and durable approach for external data tag attachment. The mean body mass of western European adult red foxes ranges from roughly 5.5 to 6.5kg (although individual, sexual, and seasonal factors introduce variation) [59], and therefore, the bio-logging equipment used in the current study (total mass = 55.2g) accounts for less than 0.1% of the mean body mass, well below the suggested <10% body mass guidelines recommended by [60]. Since the collars were snugly secured around the fox's neck, it's unlikely that it would hamper the movements involved in wild mousing behavior, and indeed, no impairment in mousing-like leaps or decrease in frequency of leaps were observed in the semi-domesticated foxes when the harnesses were attached compared to when they were removed. However, this was based on general observations of the semi-domesticated foxes inside the behavioral arena, and field-based observations comparing the behavior of free-roaming foxes with and without harnesses will be important to confirm that the equipment is not influencing the quality or frequency of natural behaviors. Furthermore, although the devices did contain small amounts of magnetic material causing a slight deflection ($<5^\circ$) of a compass needle when placed in contact with the device, this effect was eliminated when the device was moved 2cm from the compass. Therefore, it is unlikely that the small magnetic component inherent to the bio-logger would have an effect on perceiving the magnetic field, as the magnetic field strength falls off exponentially with distance, decreasing at a rate to the 3rd power with distance (i.e. inverse cube law) [61], and therefore would produce a much weaker effect, if any, in the eyes and head region (i.e. the proposed site of magneto-receptors [34, 62]). Also, magnetic compass responses in migratory birds exposed to field strengths differing by +/- 30% of the natural field strength showed no effect on compass orientation, suggesting a functional window of magnetic compass responses [63], and if

SMA in red foxes is mediated by a similar sensory mechanism, weak magnetic fields produced by the bio-logging device would not be expected to disrupt magnetic alignment responses.

An exciting possibility is the use of additional technologies in combination with magnetic bio-loggers to perform field-based manipulative experiments on free-roaming animals, which have been difficult to implement in field studies of magnetic alignment to date. For instance, magnetic responses in a variety of animals (e.g., birds, mice, turtles, insects) [18, 55, 64, 65], have been shown to be affected by radio-frequency fields in the low-MHz range, presumably influencing the quantum spin states underlying the light-dependent radical pair mechanism, altering or disrupting the pattern of magnetic input. If a radical pair mechanism mediates the directional component of mousing attacks of red foxes, radio-frequency exposure should disrupt the accuracy (and, therefore, the success) of these attacks. We have developed radio-frequency emitting collars tuned to broadcast in the low MHz range that have been shown to disrupt the magnetic compass orientation of amphibians and birds (sinusoidal frequency sweeps from ~1.0 MHz to 1.8 MHz, at the rate of 10.0 kHz) [55, 66]. The collar is composed of two major units: the transmitter board and the multi-turn loop antenna and the resulting signal is amplified using a Class-C power amplifier to provide greater power efficiency and promote longer battery life for input to the multi-turn antenna. Because the physical size of the antenna was extremely small relative to the wavelength at 1.4 MHz (approximately 215m), multiple loops of wire were stacked vertically to improve the antenna's efficiency and ensure sufficient energy was emitted to the fox. The resulting collar produces a radio-frequency stimulus with a maximal intensity of 88 nT, beyond intensities shown to disrupt migratory compass orientation in birds and SMA responses in hatchling snapping turtles [18, 67]. Integrating the radio-frequency collar with the bio-logging device and harness system will provide a powerful opportunity to test for the involvement of a light-dependent radical-

pair mechanism underlying magnetic alignment responses of mousing red foxes under otherwise natural conditions that can be conducted following double-blind protocols. Importantly, this system can provide further support for, or against, the impact of anthropogenic radio-frequency exposure on wild life [68-70]. Although field observations of wild foxes will be important to confirm that the radio-frequency collars do not affect natural behaviors, it's unlikely that they would impair the use of magnetic cues during mousing attempts. As discussed above, magnetic field strengths fall off exponentially as a function of distance [61], and the radio-frequency collars are only weakly magnetic, making it unlikely that the collar would appreciably affect the perception of magnetic fields. Furthermore, if foxes use a similar magnetoreception mechanism to that used by migratory birds, then magnetic field intensities would need to change by 30% or more to disrupt behaviors relying on magnetic cues [63]. Lastly, non-iron containing loops of wire, like those used in the current radio-frequency collar design, will not manipulate or distort the ambient magnetic field. The radio-frequency intensities proposed for use in future studies of red foxes are well below the guidelines for human exposure adopted by the World Health Organization [71], and are thought to only affect biological processes occurring at the quantum level. Therefore, we do not anticipate the animal to experience any discomfort or long-term effects from radio-frequency exposure.

If however, mousing success is unaffected by radio-frequency exposure, alternative manipulations could be performed, aimed to test for the involvement of a magnetite-based mechanism similar to the one proposed to mediate spontaneous magnetic nest building behaviors in subterranean mole-rats [72-74]. For example, prior to attaching the harness system to wild caught foxes, individuals could be exposed to a brief, high intensity magnetic pulse that re-magnetizes particles of biogenic

magnetite. Similar to the effects of pulse re-magnetization on mole-rats that exhibited a 90° deviation of magnetic nest building orientation after pulse treatments [74], wild foxes would be predicted to exhibit shifted or abolished SMA responses while mousing if this behavior is mediated by a magnetite-based mechanism.

Conclusions

We report the development of ‘magnetic ethograms’ in which the behavior and magnetic alignment of red foxes can be accurately extracted from raw sensor data recorded from tri-axial accelerometer and magnetometer bio-loggers. Three functionally relevant behaviors could be identified using a 5-Nearest Neighbor classifier that performed with an overall accuracy of 95.7% across 415 ground-truth events. To evaluate the generalizability of the classifier, similar behavioral data was recorded from a second fox and resulted in 66.7% performance accuracy when analyzed using identical techniques, suggesting the classifier can extract behaviors across multiple foxes. A similar classification approach was used to identify the fox’s magnetic alignment using two 8-way classifiers with differing underlying assumptions to distinguish magnetic headings in eight equally spaced 45° sectors. The magnetic heading classifiers performed with 90.0% and 74.2% accuracy, suggesting a realistic performance range for a classifier based on an independent set of training events equal in size to our sample.

Given the performance of the behavioral and magnetic classifiers, we argue that ‘magnetic bio-loggers’ are well-suited for use in future studies of SMA in red foxes thought to use the magnetic field as a targeting system, increasing the accuracy of mousing attacks targeting small prey. The deployment of bio-loggers coupled with additional light-weight technologies, e.g., radio-

frequency collars, provide an exciting opportunity to help characterize the adaptive significance and the biophysical mechanisms mediating SMA in free-roaming mammals, both of which remain enigmatic. More generally, these techniques will provide new opportunities for studies of SMA in free-roaming mammals and offer several advantages including the ability to collect large data sets autonomously across multiple individuals, recording data in habitats or locations that may otherwise be inaccessible by observers, observer biases can be avoided, experiments can be conducted following double-blind protocols, and these techniques can be adapted for studies across diverse animals and behaviors. Therefore, we hope that the current study inspires a new approach for future researcher of magnetic alignment in free-roaming animals.

Abbreviations: Spontaneous magnetic alignment (SMA)

Declarations:

Ethics Approval: All methods were approved by the Expert Commission of the Czech Agricultural University (SP506051228).

Consent for Publication: Not applicable

Availability of Data: The authors agree to make all of the raw accelerometer and magnetometer data publically available.

Competing Interests: The authors declare that they have no competing interests.

Funding Sources: This work was funded by the Virginia Tech Doctoral Scholarship Program and Sigma-Xi. The study was also supported by the Grant Agency of the Czech Republic (project. nr. 506/11/2121). JBP was supported by National Science Foundation, IOS 07-48175 and IOS 13-49515.

Author Contributions: MSP contributed to project conception, carried out experimental design, was responsible for data collection, data analysis and interpretation of data, and drafted and edited sections of the manuscript. JAB was responsible for data analysis and interpretation, and drafted and edited sections of the manuscript. MSP and JAB contributed equally to the manuscript and

should be considered co-first authors. EPM contributed to project conception, assisted with experimental design, data analysis and interpretation, and helped draft and edit sections of the manuscript. CRA assisted in experimental design, was responsible for radio-frequency collar conception and electrical design, data analysis and interpretation, and drafted and edited sections of the manuscript. DCS contributed to the experimental design, data collection methodology, contributed to data analysis and interpretation, and drafted and edited sections of the manuscript. CWH contributed to data analysis and interpretation. JC contributed to project conception, helped coordinate experiments with semi-domesticated foxes, and provided logistical support throughout the course of the study. VH contributed to the project conception, assisted with experimental design, helped coordinate experiments with semi-domesticated foxes, and provided logistical support throughout the course of the study. VT helped with construction and design of experimental arenas, gave permission for study of semi-domesticated foxes, assisted with handling of semi-domesticated foxes, and provided logistical support throughout the course of the study. EB provided logistical support throughout the course of the study, and edited versions of the manuscript. HB contributed to project conception, assisted with experimental design, and provided logistical support throughout the study. JBP contributed to project conception, assisted with experimental design, assisted with data analysis and interpretation of data, provided logistical support throughout the course of the study, and drafted and edited sections of the manuscript. All authors read and approved the final manuscript.

Acknowledgments: We are grateful to Štěpánka Topinková and Veronika Hartová for all of their assistance during the study. We thank Paul Youmans, Lukas Landler and Jack Whitehead for their input on project conception and helpful feedback on versions of the manuscript. We also thank the editor for the handling and processing of the manuscript.

Tables:

Table 1. Confusion matrix showing 10-fold cross-validation performance of the 5-nearest neighbor classification algorithm run on Fox1. Correct identifications are in bold. The results displayed in this matrix can be viewed as estimates of how well the classifier, trained on data from Fox1, would perform on new, unseen data from this same fox. Bold values identify the cases where the classifier prediction matches the ground-truth classification.

Accuracy (%):	95.7	<i>True Class</i>			
Cohen's Kappa:	0.92	Leaping	Foraging	Trotting	Precision (%)
<i>Predicted Class</i> Leaping	261	0	11	96.0	
Foraging	0	100	3	97.1	
Trotting	4	0	36	90.0	
Recall (%)	98.5	100.0	72.0		

Table 2. Confusion matrix showing performance of the 5-nearest neighbor classification algorithm trained on data from Fox1 and tested on data from Fox2. Correct identifications are in bold. The results displayed in this matrix can be viewed as estimates of how well the classifier, trained on Fox1, would perform on new, unseen data from a different fox. Bold values identify the cases where the classifier prediction matches the ground-truth classification.

Accuracy (%):	66.7	<i>True Class</i>			
Cohen's Kappa:	0.50	Leaping	Foraging	Trotting	Precision (%)
<i>Predicted Class</i> Leaping	7	0	0	100.0	
Foraging	3	5	6	35.7	
Trotting	0	2	10	83.3	
Recall (%)	70.0	71.4	62.5		

Table 3. Summary of the data set used to train the random forest classifier. An event corresponds to a time interval during which the fox was judged by human reviewers to be maintaining a consistent heading. Samples are 6-element vectors of concatenated x, y, z accelerometer and magnetometer measurements, collected with a 3 Hz sampling rate during each event.

	N	NE	E	SE	S	SW	W	NW
Num. Events	8	12	9	7	11	4	7	8
Samples/event (mean \pm 1 s.d.)	3.50 \pm 1.60	8.17 \pm 6.46	4.20 \pm 1.56	3.10 \pm 0.378	5.90 \pm 2.91	8.50 \pm 10.4	4.10 \pm 2.12	8.40 \pm 8.60
Total Num. Samples	28	98	38	22	65	34	29	67

Table 4. Confusion matrix for the random forest classifier treating each *sample* as an observation. Bold values identify the cases where the classifier prediction matches the ground-truth heading.

Accuracy (%): 90.0	<i>True Class</i>								
	N	NE	E	SE	S	SW	W	NW	
<i>Predicted Class</i>	N	20	0	0	0	0	0	0	2
	NE	2	97	1	2	0	0	0	0
	E	0	1	30	4	1	0	0	0
	SE	0	0	4	15	3	0	0	0
	S	0	0	2	1	58	3	0	0
	SW	0	0	0	0	2	30	1	0
	W	0	0	0	0	0	1	28	0
	NW	6	0	1	0	1	0	0	65

Table 5. Confusion matrix for the random forest classifier treating each *event* as an observation. Bold values identify the cases where the classifier prediction matches the ground-truth heading.

Accuracy (%): 74.2	<i>True Class</i>								
	N	NE	E	SE	S	SW	W	NW	
<i>Predicted Class</i>	N	7	0	0	0	0	1	0	2
	NE	0	9	1	1	0	0	0	1
	E	0	2	8	0	1	0	0	0
	SE	0	0	0	5	1	0	0	0
	S	0	0	0	1	9	1	0	0
	SW	0	0	0	0	0	0	0	0
	W	0	0	0	0	0	1	6	0
	NW	1	1	0	0	0	1	1	5

Figures:

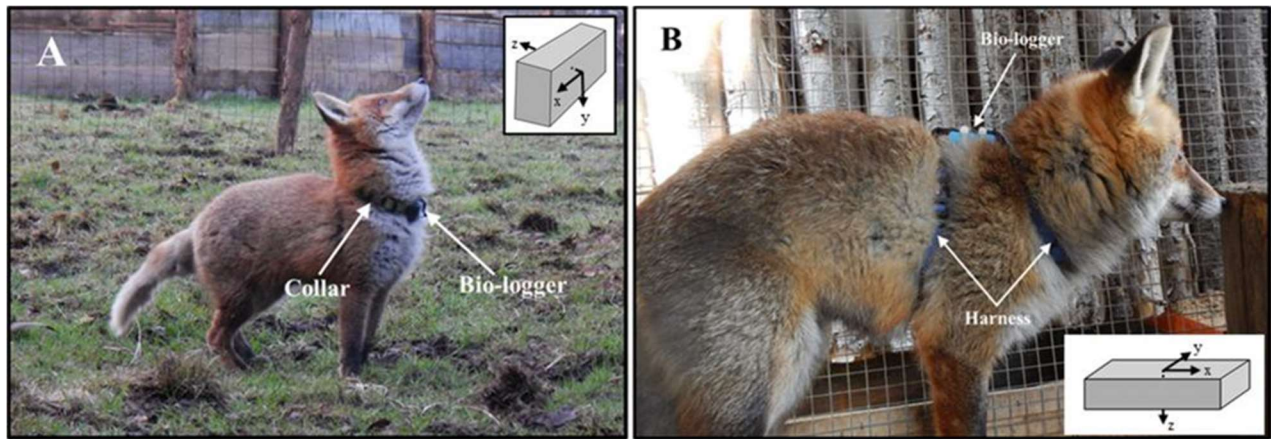


Figure 1. Photos of the two adult red foxes (*Vulpes vulpes*) used to develop magnetic ethograms equipped with tri-axial accelerometer and magnetometer bio-logging devices. A) Fox1 – modified Kong Comfort Dog Harness (collar portion only) equipped with Gulf Coast Data Concept bio-logging device attached to the ventral side of collar beneath the neck. The long axis of the device is aligned perpendicular to the spine. B) Fox2 - Kong Comfort Dog Harness including torso section and bio-logging device attached to dorsal side of fox aligned so the long axis of the device is parallel to the spine. Insets in the upper and lower corners of each photograph show the device orientation for each fox used to collect accelerometer data. The schematic showing the orientation of each device matches the approximate orientation of the device in the photograph. Note that in the photograph of Fox1 (A), the head (and therefore, the bio-logging device) is tilted slightly downward, however, the schematic of the device is shown as leveled with respect to the horizontal for ease of interpretation. Furthermore, there was a total of three different device orientations used to collect data from Fox1 throughout the behavioral recording sessions. The scheme shown above is the orientation used to collect the majority, but not all, of the behavioral data. See Supplemental Table 1 for the number of each behavior recorded from each orientation of the device from Fox1. The device orientation remained unchanged throughout the study for Fox2 and the schematic is an accurate representation of the device orientation during all behaviors as the device was attached to a harness on the fox’s back, and therefore did not experience rotations when the fox moved its head laterally or vertically.

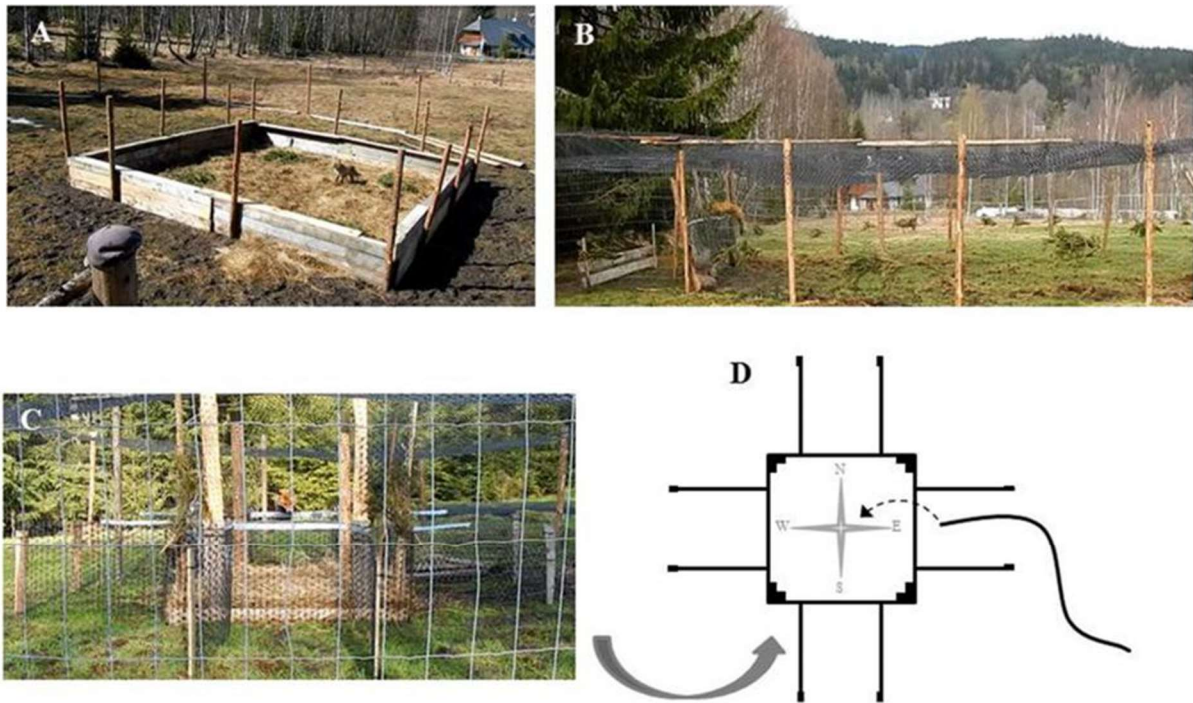


Figure 2. Three types of obstacles used to collect accelerometer (behavioral) and magnetometer (compass) data designed to encourage ‘mousing-like’ leaps. A) Square enclosure (10 x 10 x 1m) made of cut pine planks used to collect foraging and ‘mousing-like’ leap behavior with Fox2. B) Vertical wall obstacle (~1m tall) made of pine boards and plastic mesh that stretched across the entire outdoor arena used to collect ‘mousing-like’ leap behavior with Fox1. The smaller wooden barrier placed ~1m beyond the large vertical wall forced the fox to rapidly decelerate after jumping over the initial wall, similar to natural mousing jumps when a fox will leap through the air and land on top of its prey. C) Four-corridor obstacle with ~1m square ‘food reward area’. A food reward was placed in the center of the obstacle and the fox would walk down one of the four corridors then leap over a ~1m tall mesh gate to obtain the food reward. Each corridor was aligned along the cardinal compass directions (magnetic N, E, S, and W). D) Overhead schematic of four-corridor obstacle. Solid line leading into the East corridor represents the fox’s path towards the food reward area, and dotted line represents the fox’s leap, in this case heading magnetic West, over the mesh gate to obtain the reward.

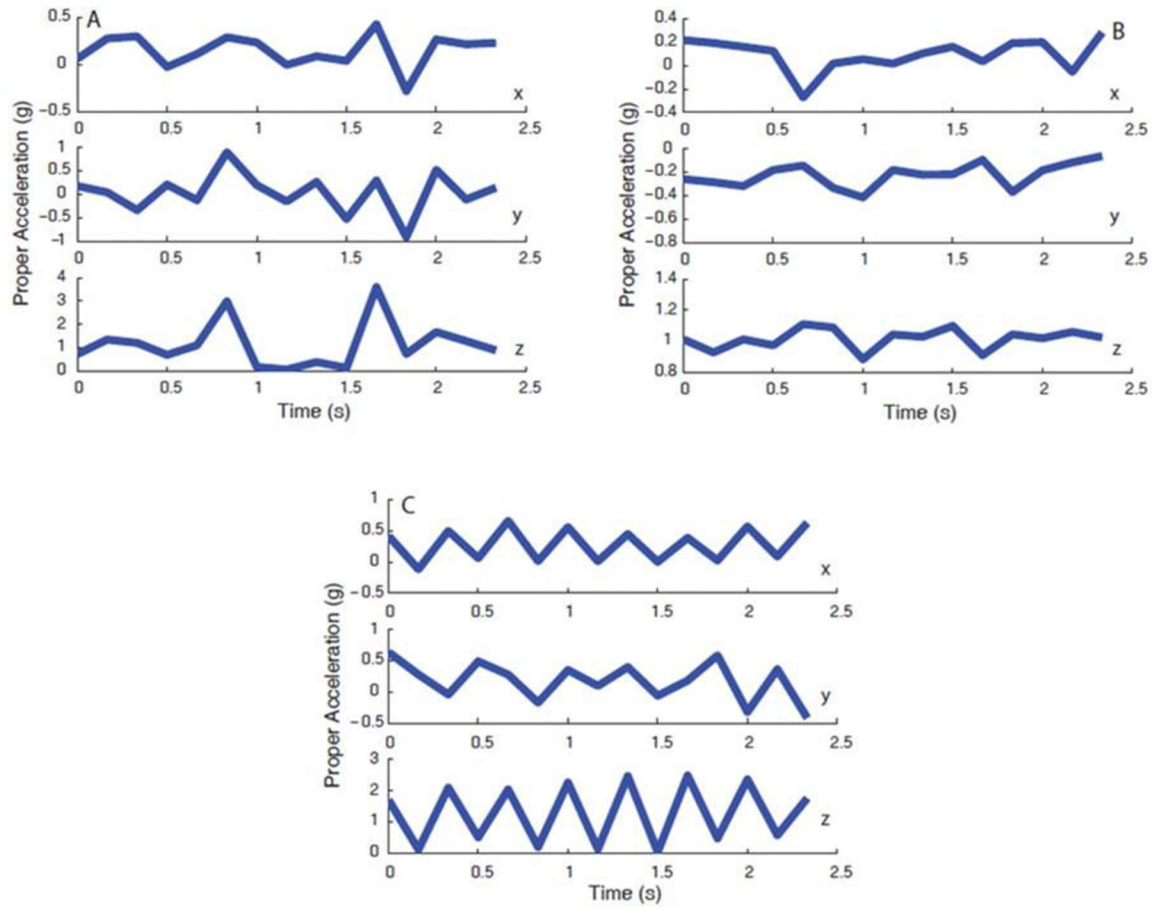


Figure 3. Acceleration signatures on each of the three axes (x, y, and z) for stereotypical leaping (A), foraging (B), and trotting (C) behaviors in Fox1. Note that amplitude scales across both axes and behaviors are made different to facilitate visualization of waveform features. Leaping is in general characterized by two large, positive-going peaks on the z-axis separated by a consistent time-delay; foraging by signals of similar magnitude and irregular morphology on all three axes; and trotting by signals with strong oscillatory components on all three axes.

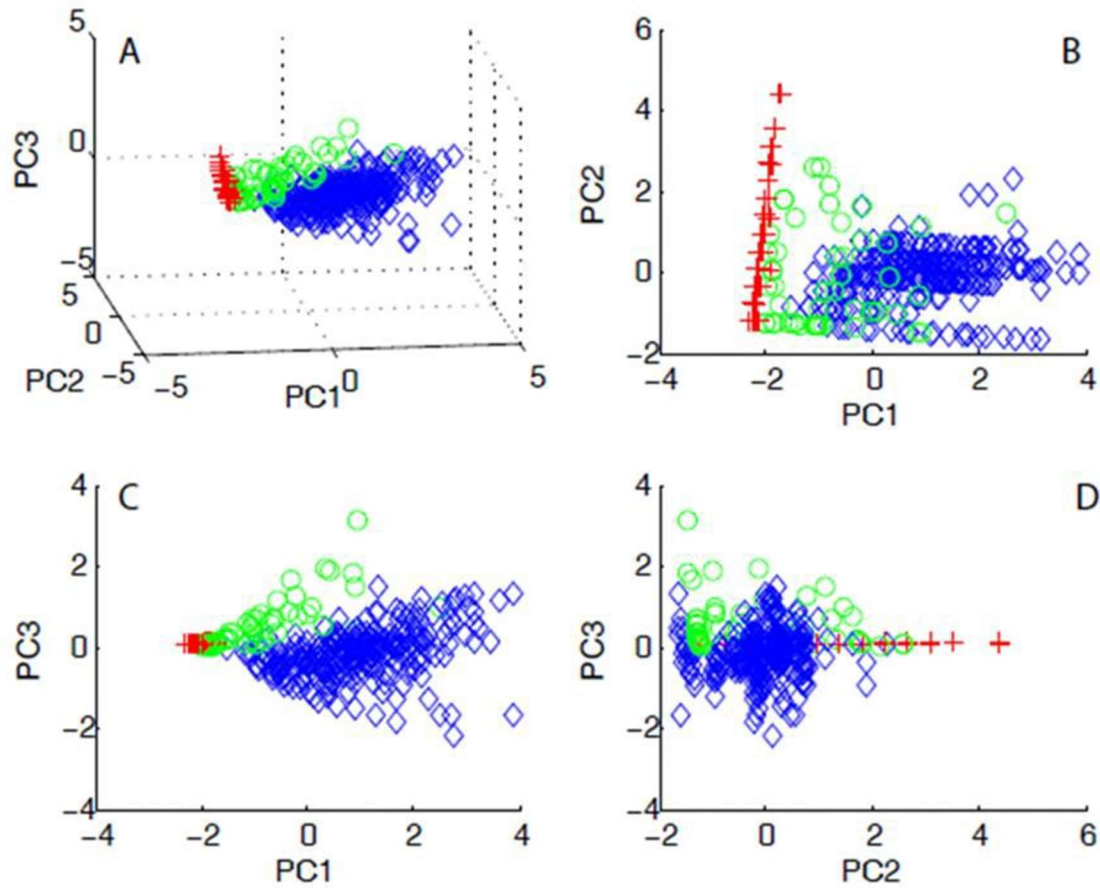


Figure 4. A) Scatter-plot of data collected from Fox1 in the three dimensional space given by the first three principal component projections after z-scoring (i.e., subtracting the mean and dividing by the standard deviation of each feature). Note that z-scoring and PCA were done strictly to facilitate viewing the 4-dimensional feature data in 3 dimensions; they were not employed as processing steps prior to classification. B-D) Two-dimensional projections onto all possible pairs of the first three principle components. Blue = leaping; Red = foraging; Green = trotting.

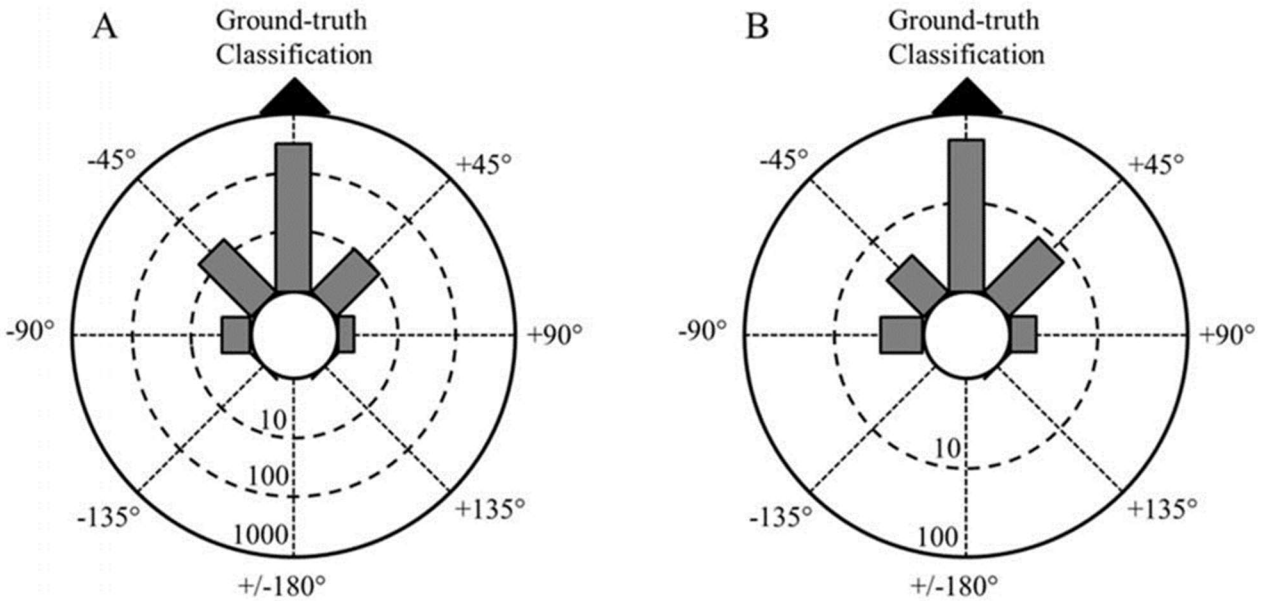


Figure 5. Radial circular plots showing magnetic classifier prediction relative to ground-truth classification made by a human observer. Classifier predictions are pooled relative to ground-truth classification (black triangle at top of circle, i.e., 0°) and the seven other possible classifications headings are shown on the periphery of the circle indicating the degree of error in classifier prediction (positive values indicate clockwise error, negative values indicate counter-clockwise error). The length of each grey bar extending from the center of the circle represents the number of classifications that fall within the 45° bin for that particular direction. The numbers on each dashed circle inside the plot indicate the number of observations (i.e. classification predictions) needed to reach that radius, and note that these are shown on a logarithmic scale. A) Distribution of classifier predictions relative to ground-truth observations when treating each *sample* as an independent data point ($n=381$, $\mu=359^\circ$, $r=0.95$, $p < 1 \times 10^{-12}$). B) Distribution of classifier predictions relative to ground-truth observations when treating each *event* as an independent data point ($n=66$, $\mu=2^\circ$, $r=0.87$, $p < 1 \times 10^{-12}$).

Supplemental Materials:

“SFile1” – Example of Fox2 exhibiting a ‘mousing-like’ leap out of the 10x10x1m arena.



SFile1.mov

“SFile2” - Example of Fox2 exhibiting a ‘mousing-like’ leap out of the 10x10x1m arena.



SFile2.mov

“SFile3” – Example of Fox1 trained to jump over a barrier and immediately come to a stop preventing a collision with a second, smaller barrier. This obstacle was designed to elicit ‘mousing-like’ leaps.



SFile3.mov

“SFile4” – Example of Fox1 trained to approach a ~1m tall barrier by walking down one of four corridors aligned in the four cardinal magnetic directions to receive a food reward in the central square of the arena.



SFile4.mov

“SFile5” – Example of Fox1 exhibiting ‘mousing-like’ behavior using the 4-corridor arena described above.



SFile5.mov

“SFile6” – Example of Fox1 exhibiting behavior defined as ‘trotting’ for the behavioral analysis.



SFile6.mov

“SFile7” – Example of Fox1 exhibiting behaviors defined as ‘foraging’ for the behavioral analysis.



SFile7.mov

“STable1” – Bio-logging device orientations.

Device Orientation	Trotting	Foraging	Mousing-like Leap
1	43	51	209
2	3	0	8
3	4	49	48

Supplemental Table 1. Number of trotting, foraging, and mousing-like leaps recorded from three different device orientations on Fox1. Device orientations are as follows from the perspective of the fox looking straight forward with its head parallel to the horizontal: Device Orientation 1: x-axis 90° to the right, y-axis pointing directly away from the fox, z-axis pointing straight up. Device Orientation 2: x-axis 90° to the left, y-axis pointing directly away from the fox’s body, z-axis pointing straight down. Device Orientation 3: x-axis 90° to the right, y-axis pointing directly towards the fox’s body, z-axis pointing straight down. Note that Device Orientation 1 was used to collect the majority of behavioral data and is shown in the inset in Figure 1 of the main text.

Literature Cited

1. Evans, K., M.-A. Lea, and T. Patterson, *Recent advances in bio-logging science: Technologies and methods for understanding animal behaviour and physiology and their environments*. Deep Sea Research Part II: Topical Studies in Oceanography, 2013. **88**: p. 1-6.
2. Wilmers, C.C., et al., *The golden age of bio-logging: how animal-borne sensors are advancing the frontiers of ecology*. Ecology, 2015. **96**(7): p. 1741-1753.
3. Payne, N.L., et al., *From physiology to physics: are we recognizing the flexibility of biologging tools?* Journal of Experimental Biology, 2014. **217**(3): p. 317-322.
4. Wilson, R.P., E. Shepard, and N. Liebsch, *Prying into the intimate details of animal lives: use of a daily diary on animals*. Endangered Species Research, 2008. **4**(1-2): p. 123-137.
5. Bidder, O.R., et al., *Love thy neighbour: automatic animal behavioural classification of acceleration data using the k-nearest neighbour algorithm*. PLOS ONE, 2014. **9**(2): p. e88609.
6. Gerencsér, L., et al., *Identification of behaviour in freely moving dogs (Canis familiaris) using inertial sensors*. PLOS ONE, 2013. **8**(10): p. e77814.
7. Wiltschko, W. and R. Wiltschko, *Magnetic orientation and magnetoreception in birds and other animals*. Journal of Comparative Physiology A: Neuroethology, Sensory, Neural, and Behavioral Physiology, 2005. **191**(8): p. 675-93.
8. Mouritsen, H. and T. Ritz, *Magnetoreception and its use in bird navigation*. Current Opinion in Neurobiology, 2005. **15**(4): p. 406-414.
9. Lohmann, K.J., C.M.F. Lohmann, and N.F. Putman, *Magnetic maps in animals: nature's GPS*. Journal of Experimental Biology, 2007. **210**(21): p. 3697-3705.
10. Freake, M.J., R. Muheim, and J.B. Phillips, *Magnetic maps in animals: a theory comes of age?* Quarterly Review of Biology, 2006. **81**(4): p. 327-347.
11. Kirschvink, J.L., M.M. Walker, and C.E. Diebel, *Magnetite-based magnetoreception*. Current opinion in neurobiology, 2001. **11**(4): p. 462-467.
12. Deutschlander, M.E., J.B. Phillips, and S.C. Borland, *The case for light-dependent magnetic orientation in animals*. Journal of Experimental Biology, 1999. **202 (Pt 8)**: p. 891-908.
13. Wiltschko, R. and W. Wiltschko, *Magnetoreception*. Bioessays, 2006. **28**(2): p. 157-168.
14. Kishkinev, D. and N. Chernetsov, *Magnetoreception systems in birds: A review of current research*. Biology Bulletin Reviews, 2015. **5**(1): p. 46-62.
15. Begall, S., et al., *Magnetic alignment in mammals and other animals*. Mammalian Biology, 2013. **78**: p. 10-20.
16. Malkemper, E.P., M.S. Painter, and L. Landler, *Shifted magnetic alignment in vertebrates: Evidence for neural lateralization?* Journal of Theoretical Biology, 2016. **399**: p. 141-147.
17. Červený, J., et al., *Magnetic alignment in warthogs Phacochoerus africanus and wild boars Sus scrofa*. Mammal Review, 2016.
18. Landler, L., et al., *Spontaneous magnetic alignment by yearling snapping turtles: rapid association of radio frequency dependent pattern of magnetic input with novel surroundings*. PLOS ONE, 2015. **10**(5): p. e0124728.
19. Červený, J., et al., *Magnetic alignment in warthogs Phacochoerus africanus and wild boars Sus scrofa*. Mammal Review, 2017. **47**(1): p. 1-5.
20. Becker, G. and U. Speck, *Examinations on magnetic field orientation in Dipterans*. Z Vergl Physiol, 1964. **49**: p. 301-340.
21. Wehner, R. and T.H. Labhart, *Perception of the geomagnetic field in the fly Drosophila melanogaster*. Cellular and Molecular Life Sciences, 1970. **26**(9): p. 967-968.

22. Vácha, M., M. Kvalcova, and T. Puzova, *American cockroaches prefer four cardinal geomagnetic positions at rest*. Behaviour, 2010. **147**(4): p. 425-440.
23. Painter, M.S., et al., *Spontaneous magnetic orientation in larval Drosophila shares properties with learned magnetic compass responses in adult flies and mice*. Journal of Experimental Biology, 2013. **216**: p. 1307-1316.
24. Begall, S., et al., *Magnetic alignment in grazing and resting cattle and deer*. Proceedings of the National Academy of Sciences, 2008. **105**(36): p. 13451-13455.
25. Obleser, P., et al., *Compass-controlled escape behavior in roe deer*. Behavioral Ecology and Sociobiology, 2016: p. 1-11.
26. Collett, T.S. and J. Baron, *Biological compasses and the coordinate frame of landmark memories in honeybees*. Nature, 1994. **368**(6467): p. 137-140.
27. Phillips, J.B., R. Muheim, and P.E. Jorge, *A behavioral perspective on the biophysics of the light-dependent magnetic compass: a link between directional and spatial perception?* Journal of Experimental Biology, 2010. **213**(19): p. 3247-3255.
28. Červený, J., et al., *Directional preference may enhance hunting accuracy in foraging foxes*. Biology Letters, 2011. **7**(3): p. 355-357.
29. Phillips, J.B. and S.C. Borland, *Behavioural evidence for use of a light-dependent magnetoreception mechanism by a vertebrate*. Nature, 1992. **359**: p. 142-144.
30. Phillips, J.B. and S.C. Borland, *Wavelength specific effects of light on magnetic compass orientation of the eastern red-spotted newt Notophthalmus viridescens*. Ethology Ecology & Evolution, 1992. **4**(1): p. 33-42.
31. Vácha, M., T. Puzova, and D. Drstková, *Effect of light wavelength spectrum on magnetic compass orientation in Tenebrio molitor*. Journal of Comparative Physiology A: Neuroethology, Sensory, Neural, and Behavioral Physiology, 2008. **194**(10): p. 853-9.
32. Gegear, R.J., et al., *Cryptochrome mediates light-dependent magnetosensitivity in Drosophila*. Nature, 2008. **454**(7207): p. 1014-8.
33. Vácha, M. and H. Soukopová, *Magnetic orientation in the mealworm beetle Tenebrio and the effect of light*. Journal of Experimental Biology, 2004. **207**(7): p. 1241-1248.
34. Mouritsen, H. and P.J. Hore, *The magnetic retina: light-dependent and trigeminal magnetoreception in migratory birds*. Current Opinion in Neurobiology, 2012. **22**(2): p. 343-352.
35. Ritz, T., S. Adem, and K. Schulten, *A model for photoreceptor-based magnetoreception in birds*. Biophysical Journal, 2000. **78**(2): p. 707-718.
36. Wiltschko, W. and R. Wiltschko, *Magnetic compass of European robins*. Science, 1972. **176**(4030): p. 62-64.
37. Phillips, J.B., *Two magnetoreception pathways in a migratory salamander*. Science, 1986. **233**(4765): p. 765-767.
38. Light, P., M. Salmon, and K. Lohmann, *Geomagnetic orientation of loggerhead sea turtles: evidence for an inclination compass*. Journal of Experimental Biology, 1993. **182**(1): p. 1-10.
39. Schulten, K. and A. Windemuth, *Model for a physiological magnetic compass*. Biophysical effects of steady magnetic fields, 1986. **11**: p. 99-106.
40. Cintolesi, F., et al., *Anisotropic recombination of an immobilized photoinduced radical pair in a 50- μ T magnetic field: a model avian photomagnetoreceptor*. Chemical Physics, 2003. **294**(3): p. 385-399.
41. Rodgers, C.T. and P.J. Hore, *Chemical magnetoreception in birds: The radical pair mechanism*. Proceedings of the National Academy of Sciences, 2009. **106**(2): p. 353-360.
42. Skiles, D.D., *The geomagnetic field its nature, history, and biological relevance*, in *Magnetite Biomineralization and Magnetoreception in Organisms*. 1985, Springer. p. 43-102.

43. Chen, K.Y. and D.R. Bassett, *The technology of accelerometry-based activity monitors: current and future*. *Medicine and science in sports and exercise*, 2005. **37**(11): p. S490.
44. Butterworth, S., *On the theory of filter amplifiers*. *Wireless Engineer*, 1930. **7**(6): p. 536-541.
45. STMicroelectronics, *Application note Using LSM303DLH for a tilt compensated electronic compass*. 2010.
46. Breiman, L., *Random forests*. *Machine learning*, 2001. **45**(1): p. 5-32.
47. Hastie, T., R. Tibshirani, and J. Friedman, *Unsupervised learning*. 2009: Springer.
48. Breiman, L., et al., *Classification and regression trees Belmont*. CA: Wadsworth International Group, 1984.
49. Efron, B., *Bootstrap methods: Another look at jackknife*. *Annual Statistics*. **7** (2), 1-2. 1979.
50. Batschelet, E., *Circular statistics in biology*. 1981, New York: Academic Press.
51. Hochscheid, S. and R.P. Wilson, *A new method for the determination of at-sea activity in sea turtles*. *Marine ecology progress series*, 1999. **185**: p. 293-296.
52. Shepard, E.L., et al., *Energy beyond food: foraging theory informs time spent in thermals by a large soaring bird*. *PLOS ONE*, 2011. **6**(11): p. e27375.
53. Mitani, Y., et al., *A method for reconstructing three-dimensional dive profiles of marine mammals using geomagnetic intensity data: results from two lactating Weddell seals*. *Polar Biology*, 2003. **26**(5): p. 311-317.
54. Watanabe, Y.Y., E.A. Baranov, and N. Miyazaki, *Drift dives and prolonged surfacing periods in Baikal seals: resting strategies in open waters?* *Journal of Experimental Biology*, 2015. **218**(17): p. 2793-2798.
55. Ritz, T., et al., *Resonance effects indicate a radical-pair mechanism for avian magnetic compass*. *Nature*, 2004. **429**(6988): p. 177-180.
56. Solov'yov, I.A., H. Mouritsen, and K. Schulten, *Acuity of a cryptochrome and vision-based magnetoreception system in birds*. *Biophysical journal*, 2010. **99**: p. 40-49.
57. Goszczyński, J., *Studies on the food of foxes*. *Acta theriologica*, 1974. **19**(1): p. 1-18.
58. Hartová-Nentvichová, M., et al., *Variation in the diet of the red fox (*Vulpes vulpes*) in mountain habitats: effects of altitude and season*. *Mammalian Biology-Zeitschrift für Säugetierkunde*, 2010. **75**(4): p. 334-340.
59. Iossa, G., et al., *Body mass, territory size, and life-history tactics in a socially monogamous canid, the red fox *Vulpes vulpes**. *Journal of Mammalogy*, 2008. **89**(6): p. 1481-1490.
60. Wilson, D.E.C., et al., *Measuring and monitoring biological diversity standard methods for mammals*. 1996.
61. Michaud, A., *On the magnetostatic Inverse cube law and magnetic Monopoles*. *The General Science Journal*, 2007.
62. Nießner, C., et al., *Cryptochrome 1 in retinal cone photoreceptors suggests a novel functional role in mammals*. *Scientific reports*, 2016. **6**.
63. Wiltschko, W., *Further analysis of the magnetic compass of migratory birds*, in *Animal migration, navigation, and homing*. 1978, Springer. p. 302-310.
64. Vácha, M., T. Puzova, and M. Kvalcova, *Radio frequency magnetic fields disrupt magnetoreception in American cockroach*. *Journal of Experimental Biology*, 2009. **212**(21): p. 3473-3477.
65. Malkemper, E.P., et al., *Magnetoreception in the wood mouse (*Apodemus sylvaticus*): influence of weak frequency-modulated radio frequency fields*. *Sci. Rep.*, 2015. **4**.
66. Thalau, P., et al., *Magnetic compass orientation of migratory birds in the presence of a 1.315 MHz oscillating field*. *Naturwissenschaften*, 2005. **92**: p. 86 - 90.
67. Ritz, T., et al., *Magnetic compass of birds is based on a molecule with optimal directional sensitivity*. *Biophysical Journal*, 2009. **96**: p. 3451 - 3457.

68. Engels, S., et al., *Anthropogenic electromagnetic noise disrupts magnetic compass orientation in a migratory bird*. *Nature*, 2014. **509**: p. 353-356.
69. Balmori, A., *Anthropogenic radiofrequency electromagnetic fields as an emerging threat to wildlife orientation*. *Science of the Total Environment*, 2015. **518**: p. 58-60.
70. Balmori, A., *Radiotelemetry and wildlife: Highlighting a gap in the knowledge on radiofrequency radiation effects*. *Science of the Total Environment*, 2016. **543**: p. 662-669.
71. Protection, I.C.o.N.-I.R., *ICNIRP statement on the "guidelines for limiting exposure to time-varying electric, magnetic, and electromagnetic fields (up to 300 ghz)"*. *Health Physics*, 2009. **97**(3): p. 257-258.
72. Burda, H., et al., *Magnetic compass orientation in the subterranean rodent *Cryptomys hottentotus* (Bathyergidae)*. *Cellular and Molecular Life Sciences*, 1990. **46**(5): p. 528-530.
73. Marhold, S., W. Wiltschko, and H. Burda, *A magnetic polarity compass for direction finding in a subterranean mammal*. *Naturwissenschaften*, 1997. **84**(9): p. 421-423.
74. Marhold, S., et al., *Magnetic orientation in common mole-rats from Zambia*. *Orientation and navigation—birds, humans and other animals*, 1997: p. 5-1.

Chapter IV. Evidence for Plasticity in Nest Building Responses Mediated by Magnetic Cues in Epigeic Mice

Michael S. Painter¹, Madison Davis², Shruthi Ganesh³, Ella Rak⁴, Kelsie Brumet¹, Hunter Bayne¹, E. Pascal Malkemper^{5,6} & John B. Phillips¹

¹Department of Biological Sciences, Virginia Tech, Blacksburg, Virginia, United States of America

²School of Education, Virginia Tech, Blacksburg, Virginia, United States of America

³Virginia-Maryland College of Veterinary Medicine, Blacksburg, Virginia, United States of America

⁴Department of Dairy Sciences, Virginia Tech, Blacksburg, Virginia, United States of America

⁵Department of General Zoology, Faculty of Biology, University of Duisburg-Essen, 45117 Essen, Germany

⁶Department of Game Management and Wildlife Biology, Faculty of Forestry and Wood Sciences, Czech University of Life Sciences, 16521 Praha 6, Czech Republic

This manuscript is in preparation for submission to Animal Behavior

Abstract

The involvement of magnetic cues in spatial behavior has been shown in a range of invertebrates and vertebrates. In mammals, two distinct types of magnetic behaviors have been identified, spontaneous magnetic orientation and learned magnetic compass responses. Although the biophysical mechanisms mediating these responses are not fully characterized, support for a magnetite-based mechanism comes from studies of subterranean mole-rats exhibiting spontaneous magnetic alignment, while magnetic responses shown in epigeic rodents are consistent with the involvement of a photoreceptor-based magnetic compass. It remains to be determined if magnetic responses are species-specific, i.e., species exhibit either learned magnetic compass orientation or spontaneous magnetic alignment, or instead if learned and spontaneous magnetic orientation are context-dependent and expressed in the same species under different circumstances. Using C57BL/6J laboratory mice in an assay adapted from an earlier nest building study, we provide the first evidence that learned magnetic compass orientation and spontaneous magnetic alignment can be studied in the same experimental system, which will facilitate future studies to characterize the magnetoreception mechanism(s) that underlie these behaviors. Moreover, these findings show that the use of magnetic cues is more flexible than previously recognized. Determining the factors that elicit different forms of magnetic behavior may shed light on the functional significance of spontaneous magnetic alignment responses in mammals, which to date, remains poorly understood.

Introduction

Use of magnetic cues for spatial orientation has been demonstrated in multiple classes of vertebrates, as well as in a variety of invertebrates [for review see 1]. In mammals, two types of magnetic responses have been reported; spontaneous magnetic alignment, and goal-directed compass orientation. Until recently, most of the evidence for magneto-sensitivity in mammals has come from spontaneous (i.e. non-learned, non-goal oriented) magnetic nest building responses of subterranean mole rats (Genus *Fukomys*), typically positioning nests in locations corresponding to the magnetic south-east sector of circular arenas [2-4, but see 5]. However, over the past decade a growing number of studies of other mammalian groups have provided support for spontaneous magnetic alignment. For example, a spontaneous preference for nest construction along the ~north-south magnetic axis was found in wood mice (*A. sylvaticus*) and bank voles (*C. glareolus*) in ambient and experimentally rotated magnetic fields [6, 7]. In addition, several field-based observational studies have reported spontaneous body alignment along the ~north-south magnetic axis in a variety of free-roaming mammals [8-11]. Although direct evidence for the involvement of magnetic cues in spontaneous magnetic alignment responses in free-roaming mammals is currently lacking, the alignment of cattle and deer was shown to be disrupted in proximity to high voltage power lines, and data collected from high latitudes where there is considerable variation in magnetic declination revealed that magnetic north was a better predictor of north-south alignment than geographic north [8]. These findings are consistent with the involvement of magnetic cues underlying spontaneous body alignment in mammals. Surprisingly this behavior appears to be widespread in mammals, its functional significance remains enigmatic [9].

In addition to spontaneous magnetic alignment, evidence for a well-developed magnetic compass has come from studies showing that the C57BL/6J strain of laboratory mice readily learn to orient

relative to the magnetic field; in nest building and modified 'Plus' Morris watermaze assays, mice learned the magnetic compass direction of a sheltered refuge or submerged platform (respectively) [12, 13]. What remains to be determined, however, is whether the types of responses exhibited by mammals are species-specific, i.e., species show either learned magnetic compass orientation or spontaneous magnetic alignment, or instead if learned and spontaneous magnetic orientation are contextually-dependent magnetic responses and can be expressed in the same species in different circumstances.

The available evidence points to the involvement of two separate magnetoreception mechanisms relying on different biophysical processes in terrestrial vertebrates: a magnetite-based mechanism (MBM) and a light-dependent mechanism (LDM). A MBM involves single domain or superparamagnetic crystals of biogenic magnetite (Fe_3O_4) thought to influence the opening and closing of membrane channels depending on the local magnetic environment [14, 15]. Properties consistent with a MBM (i.e., functional in absolute darkness, sensitive to the polarity of the magnetic field, unaffected by exposure to low-level radio frequency fields in the nT-range, disrupted by high intensity magnetic pulses in the T-range) have been shown in studies of the spontaneous magnetic nest building responses of subterranean mole rats [3, 16]. In contrast, a LDM is thought to rely on specialized photopigments that form radical pair intermediates, where the product yield is sensitive to the alignment of the magnetic field axis [17, 18]. Spontaneous magnetic nest-building behavior in wood mice has been shown to be sensitive to radio-frequency fields in the low-MHz range [6], consistent with involvement of a LDM [17, 19-22]. In addition, learned magnetic compass orientation by laboratory mice was obtained reliably only after the radio-frequency field background noise was lowered to less than 1 nT by electromagnetically shielding the training and testing facilities [12, 13], and therefore, was suggested to be mediated

by a LDM. Interestingly, the fine structure in the distribution of responses exhibited by mice in the learned nest building assay, like that of photoreceptor-based magnetic responses in other animals, is consistent with a complex, axially symmetrical visual pattern of magnetic input like that proposed to underlie a LDM [see 23].

In the present study, we provide the first evidence that magnetic compass orientation and spontaneous magnetic alignment can be studied in the same experimental system, which will facilitate future studies to characterize the magnetoreception mechanism or mechanisms that underlie these behaviors. Furthermore, determining the factors (e.g. environmental, physiological) which elicit different types of magnetic behavior will help to shed light on the functional significance of magnetic alignment behavior in mammals.

Methods

General Methods:

Training

Male C57BL6/J mice used in this study were reared in a laboratory colony from stock obtained from the Jackson Laboratory. Pups were weaned 23 ± 4 days after birth and raised in same sex sibling groups until transported to the Behavioral Testing Facility where mice were trained and tested. All mice were tested between 65 and 80 days of age. In the initial experiments reported here (Series 1), training was carried out in an outer ('control') room in the building housing the testing enclosure used in the original nest building experiments [12]. For series 2-4, the training shelves were moved into the inner 'testing' because the electromagnetic shielding was more effective, and testing was carried out in a separate building located at the Behavioral Testing Facility. Male mice were trained for a minimum of four days and a maximum of 10 days in translucent polycarbonate cages with wood shavings as substrate. Food pellets and water were

provided *ad libitum*, and an opaque plastic nestbox containing two 5 x 5cm pressed cotton fiber nestlets (Ancare) was positioned at one end of the cage. Training cages were placed on one of four sets of enclosed non-magnetic wooden shelves with the nestbox at the sheltered end facing out. The shelves with the open ('light') end facing in four different compass directions at 90° intervals [See 12 for additional details]. A full spectrum 20 Watt halogen light source (Premium MR16/BAB 21V, 20W) was centered above the four corridors and set on a 12:12 L:D cycle (in synch with the main colony light cycle). The nestlets were placed at the back (dark end) of the training cage. Food pellets and water were placed at the front of the cage (i.e., light end). All mice were trained in the local geomagnetic field (51,000nT, -65°). An A/C unit, two 1500 W oil-filled heaters, and a dehumidifier were used to maintain environmental conditions during training between 18.0 - 20.5°C and 20-50% RH and were all located in the outer room of the training building. Mice were initially trained in the outer room in enclosures shielded with two layers of grounded brass screening. After bursts of RF noise from the heaters and AC were detected inside the shielded enclosures, training shelves were moved into the shielded inner room previously used for testing [12] where the RF noise bursts not detected.

Air was circulated between the two rooms by means of an in-line fan connected to a 20 cm dia air duct that circulated air between the 'control' room and the training room. After the training shelves were moved into the inner room (Series 2-4), they were positioned below the inflow of the air duct with a 90° elbow that directed air flow and fan noise down towards the center of the training corridors. The location of the training shelves in the inner room also minimized exposure of the mice to directional sound and vibrational cues, and electromagnetic fields produced by the equipment used to maintain environmental conditions. Additionally, the training room was

shielded from electromagnetic noise with grounded aluminum screening. See below and Table 2 for summary of training conditions.

Testing

Mice were tested in a separate building located approximately 70m NE (53°) relative to the training building. Underground air ducts connecting the training and testing buildings made it possible to mix air from the two buildings. In the testing building, mice were tested individually in a circular plastic arena (50 cm top dia, 37 cm bottom dia x 32 cm high), fitted with a circular PVC floor that provided a level surface in the bottom of the arena. Prior to testing, the arena floor was covered with a uniform (~1 cm thick) layer of wood shavings. Four pressed cotton fiber nestlets identical to those provided in the training cages were positioned at the four cardinal compass directions at the edge of the arena. A circular food and water dish constructed from a single piece of round Plexiglas was fastened to the arena floor in the center of the arena. The arena was covered with a white frosted Plexiglas diffuser and equally spaced supports (~1/16" deep) around the top edge of the arena edge provided a series of symmetrical gaps between the diffuser and the arena to allow air circulation. Before transporting a mouse from the training building to the testing building, the frosted Plexiglas diffuser which transmitted light, but prevented mice from seeing visual cues outside the arena was placed off center, leaving a small opening along one edge of the area to provide an access point to release the mouse in the arena.

A 3 Watt (30 Watt equivalent) 48 LED array 'full-spectrum' testing light source (SuperBright LEDs INC, MR16-CW48SMD 9-14.8V 120° viewing angle) was centered directly overhead of the testing arena (132 cm above the arena floor) to provide a broad band light source and passed through two white frosted, 0.6 cm thick Plexiglas diffusers (one resting on top of the coil frame

and the other on top of the testing arena), before reaching the arena floor. Light levels with and without the Plexiglas diffuser resting directly on top of the arena were recorded in Lux before each test. The test light ran continuously throughout each test trial (i.e. 24:0 L:D).

The testing arena was surrounded by an orthogonal pair of horizontal cube surface coils wrapped on a wooden frame that were used to rotate the alignment of the geomagnetic field so that magnetic north was at geographic North, South, East or West; in Series 1 and 2, only two alignments of the field were used with mN at North or West. The outer surface of the wooden frame was covered with brass screening connected to the building ground to shield the testing arena from ambient radio-frequency interference.

Tests began between 9:00am and 10:30am local time each day and were ended 22 to 23 hr later, typically before 9:00am the following morning. Prior to each test, a mouse was removed from the training cage by hand and placed into an opaque porcelain transport container (9.5 cm dia x 10 cm high) fitted with an opaque plastic lid. The experimenter walked the transport device containing the mouse from the training building to the testing building while continuously rotating (~5-6 times/min) the transport container to deprive mice of route-based cues during transport. Once inside the test building, the transport container was lowered into the arena and, after removing the lid, gently tilted until the mouse crawled out onto the arena floor. Mice were always released at the outer edge of the arena, at approximately 315° relative to geographic north for all conditions. Immediately after release, the frosted Plexiglas diffuser was centered so that it completely covered the top of the arena. Temperature and humidity were recorded at the beginning and end of each test.

At the end of each test (approximately 22 to 23hr after test start), the mouse was removed from the arena and placed back in its training cage, which was held in a separate building until it was

transported back to the main colony. After removing the mouse, a wooden marker was positioned at geographic north and a handheld compass was placed in the center of the arena. The location and appearance of the nest was then recorded with a handheld digital camera, along with the number of nestlets used to construct the nest and the percentage of nestlets chewed. The arena contents (bedding, food, water, nestlets) were then discarded. The arena, PVC floor, food and water dish, and arena diffuser were rinsed with water, and cleaned first with a 4ml/1L concentration of Bioquat 20 (Biosentry); the recommended concentration for research and veterinary use), and then with 70% ethanol. All testing equipment was allowed to air dry for at least a 24hr period before use in another test. See below and Table 2 for summary of testing conditions.

All data were analyzed using Oriana Statistical Software 4.0. A Rayleigh test was performed to determine if the distributions of nest bearings were distinguishable from random at the $p < 0.05$ significance level. In Series 1, a test for significant bimodal magnetic orientation was performed by doubling each magnetic bearing (modulo 360deg) and the analyzing the resulting distribution using a Rayleigh test [24].

Series 1

An initial series of data were collected between September 19, 2014 and February 2, 2015. All mice tested during this period were trained on training shelves identical to those described above aligned along the anti-cardinal compass axes. Therefore, individual mice were trained to the northeast, southeast, southwest, and northwest magnetic directions. Training shelves were located in the outer ‘control’ room containing the A/C unit, oil-filled heaters and dehumidifiers. Training shelves were positioned inside aluminum screened enclosures. The light source, light cycle,

training period, and environmental conditions were consistent with those described in *the General Training Methods*. However, after the initial training period, mice were tested overnight (i.e. 17:00 – 9:00 local time) in an on-going magnetic compass nest building assay located in an adjacent room within the same building. After the initial testing, mice were placed back in their cages and returned to their original training shelf in the control room. Mice were then re-tested within 24hr of returning to their training shelf using the methods described above (e.g. placed inside a transport device and walked to the testing arena located in a separate building) with magnetic north aligned to north or west. Importantly, although the individual training shelves were enclosed in aluminum screening to intended to shield against radio-frequency noise, intermittent RF noise bursts were detected inside the training enclosures as a consequence of their close proximity to strong sources of radio-frequency noise (i.e. A/C unit and oil-filled heaters), as well as grounding of the training enclosures to a common earth ground also connected to the heaters and AC unit. Therefore, mice in *Series 1* were exposed to some level on RF noise during their training period (Table 2).

Series 2

Data were collected between May 31, 2015 and July 17, 2015. Mice were trained in one of four magnetic directions, i.e., 20°, 110°, 200°, and 290° following the protocol described in *General Training Methods*. No electromagnetic noise was detected during *Series 2, 3* and *4* when the training shelves were located in the shielded inner room that was the site of testing in earlier nest-building experiments [12]. The training and testing building air supplies were uncoupled (i.e. no mixing of air between the training and testing buildings) (Table 2). As in *Series 1* mice were tested in one of two magnetic field alignments with magnetic north at geographic north and west. An A/C unit located in a room adjacent to the testing room was used to keep the temperature at the

start of each test between 18.5 and 22.0°C, however the equipment was turned off before mice were transported to the testing building, and therefore, the temperature steadily increased during the test; tests could not be conducted on consecutive days because the test building needed approximately 12hrs of cooling before reaching suitable starting temperatures before each test.

Series 3

Data were collected between September 5, 2015 and December 2, 2015. Mice were trained in one of four magnetic directions corresponding to geographic and magnetic 0°, 90°, 180°, and 270°. The air flow between the training and testing buildings was uncoupled. Mice were tested in one of four magnetic field alignments with magnetic north at geographic North, South, East, and West. In the testing building, a 20 cm dia air duct with an in-line fan was installed to mix air between the outer room containing the A/C unit and inner testing room. The fan and air duct were identical to those used in the training building to mix air between the control room and training room. During testing, the A/C unit in the testing building was left on, so the testing room temperature remained within range. Additionally, the noise generated from the in-line fan was similar in acoustic quality and intensity between the training and testing environments. Leaving the A/C unit on during each test day allowed for the option to test mice on consecutive days, and therefore, a second testing arena, floor platform, food and water dish, and arena diffuser were constructed and used on alternative testing days so each arena had at least 24hr to air dry before each use. As discussed in more detail below, *Series 3* was 'interrupted' by a change in protocol (i.e., *Series 4*) and therefore, the data analysis is partitioned into two data sets, (i.e. *Series 3a, 3b*) that were separated in time, but conducted following identical protocols.

Series 4

Data were collected between October 6, 2015 and October 27, 2015. Data collected during this period followed all procedures and experimental conditions outlined in *Series 3* with the exception that the air supplies of the training and testing buildings were coupled by means of ~50 m of underground air ducts (20 cm dia), which allowed mixing of the air between the two buildings by means of in-line fans (Table 2). Mice in training and testing were not exposed to direct air flow from the circulating fans, however, olfactory cues from each building were mixed so that mice experienced olfactory cues from the test building while in training, and mice in testing were exposed to olfactory cues in the training building.

Results

The topographic distributions of bearings in all four *Series* were indistinguishable from random, indicating that there were not non-magnetic cue (s) in the testing arena or surrounding environment that had a significant effect on nest positioning (Table 1).

Series 1

When bearings were pooled with respect to magnetic north, nest positions exhibited a highly significant axially symmetrical distribution along the northeast-southwest magnetic axis ($\mu = 36^\circ - 216^\circ$, $r = 0.72$, $p < 0.0001$) (Table 1, Figure 1B). When nest bearings were pooled relative to the trained magnetic direction, however, the distribution was indistinguishable from random (Figure 1C), suggesting that mice were exhibiting spontaneous (i.e. non-learned) magnetic nest positioning, rather than a learned compass response, like that shown in earlier studies by Oliveriusová et al. [7] and Malkemper et al. [6].

Series 2

In contrast to *Series 1*, the distribution of magnetic bearings was indistinguishable from random (Table 1, Figure 2B). However, when bearings were pooled with respect to the trained magnetic direction, nest orientation was significantly clustered in the magnetic direction corresponding to the light end of the training cage (i.e. ~opposite the magnetic direction toward the nest box and dark end of the trained axis), providing evidence that mice were exhibiting learned magnetic compass orientation ($n = 13$, $\mu = 182^\circ$, $r = 0.79$, $p < 0.0001$) (Figure 2C).

Series 3

Data for *Series 3* was collected in two series separated in time by a modification in the circulation of air between the training and testing building (i.e. *Series 4*). Therefore, data from *Series 3* was analyzed in two groups, *Series 3a* and *Series 3b*, providing independent replications for this condition. The distribution of magnetic bearings in *Series 3a*, *Series 3b*, as well as the two distributions combined (i.e. *Series 3a + Series 3b*), was indistinguishable from random (Table 1, Figure 3B). In *Series 3a*, when the bearings were pooled relative to the trained magnetic direction, the distribution did not reach significance ($\mu = 340^\circ$, $r = 0.41$, $0.05 < p < 0.10$) however, the mean bearing for this distribution coincided with the trained magnetic direction (i.e. towards the nest box) (Table 1) and was consistent with mean orientation in *Series 3b* (Table 1). In *Series 3b*, the distribution did reach significance with the mean vector towards the nest box ($n = 23$, $\mu = 359^\circ$, $r = 0.59$, $p < 0.0002$) (Table 1). When the bearing from *Series 3a and 3b* were combined, the nest positions were strongly clustered in the direction towards the dark end of the trained axis (i.e. towards the nestbox refuge) ($n = 31$, $\mu = 355^\circ$, $r = 0.54$, $p < 0.0001$) (Table 1) (Figure 3C).

Series 4

Data for *Series 4* was collected during a ~ 3-week period in the middle of the *Series 3*. The distribution of magnetic bearings is indistinguishable from random (Table 1, Figure 4B), while the distribution of bearings pooled relative to the trained magnetic direction revealed a significant clustering of nest bearings coinciding with the light end of the training cage (i.e. orientation opposite the nest box) ($n = 9$, $\mu = 169^\circ$, $r = 0.57$, $p = 0.049$) (Figure 4C). The distributions of bearings relative to the dark end of the trained axes in *Series 3* (*3a* and *3b* combined) versus those in *Series 4* were significantly different (Watson $U^2 = 0.502$, $p < 0.005$)

Discussion

Findings from the present experiments show that nest positioning by male C57BL/6J mice can exhibit both spontaneous magnetic alignment and learned magnetic compass orientation. Although both responses have previously been reported in mammals [2, 3, 6, 12, 13], this is the first evidence that the two responses can be exhibited by the same species. Furthermore, relatively minor changes in environmental conditions caused the learned magnetic compass orientation of mice to reverse, i.e., switching from orientation towards the dark end of the trained axis to orientation towards the light end of the trained axis, suggesting that magnetic cues can be used for a variety of context-dependent spatial behaviors.

In *Series 1*, mice were held in cages in the room adjacent to the testing room used in earlier nest building studies [12]. Mice were tested in a separate nest building experiment the night prior to being tested in the current assay. Although the training cages were housed in a shielded enclosure, radio-frequency noise generated by equipment used to control the building environmental

conditions was detected inside the training cages (Table 2). Low-level radio-frequency fields have been shown to disrupt magnetic compass orientation in a variety of organisms [6, 19, 25-27]. Consistent with previous findings of radio-frequency effects on magnetic compass orientation, the distribution of nests from mice tested on the night prior to use in these experiments were indistinguishable from random when pooled relative to the trained magnetic direction (data not shown). Previous studies of magnetic compass orientation in laboratory mice have shown that electromagnetic shielding of both training and testing environments is necessary to obtain consistent learned magnetic compass responses [12, 13].

After the initial tests, mice were returned to the training shelf and re-tested within 24hr in the new testing building located approximately 70m northeast of the training building. Re-tested mice (*Series 1*) also failed to exhibit magnetic compass orientation relative to the trained magnetic axis (Table 1, Figure 1C), and instead positioned nests bimodally along the NE-SW magnetic axis (Figure 1B). Because the distribution of nests was independent of the trained axis (i.e., the alignment of the cages on the training shelves), and coincided with the north-northeast ↔ south-southwest alignments observed in a variety of vertebrate groups not engaged in goal-directed orientation [for review see 9], this response appears to have been an example of spontaneous (i.e., unlearned) magnetic alignment.

Although the functional significance of spontaneous magnetic responses remains poorly understood, a variety of possibilities have been suggested, including: (1) increasing the accuracy of magnetic measurements used to derive geographic position (i.e., magnetic map information) [28], (2) simplifying the encoding and recognition of landmarks, analogous to honeybees' use of the magnetic field to standardize the viewing angle when approaching a visual landmark [29], (3) helping to encode spatial relationships among local landmarks [8], and (4) helping to place

multiple local maps of space into register [30]. Clearly further research will be needed to characterize the biological relevance of spontaneous magnetic alignment. None-the-less there is growing evidence that in addition to its well-established role in long-distance migratory orientation and homing, the magnetic field plays an important role in organizing spatial behavior over a range of spatial scales [8, 11, 28-30]. Interestingly, the spontaneous magnetic alignment of mice in the present experiment, as has been shown in a variety of other vertebrates, was shifted clockwise of the magnetic north-south axis, which has been discussed to be a consequence of lateralized neural processing of magnetic information [31].

In the present experiments, exposure to intermittent bursts of radio-frequency noise in the training enclosure may have prevented the mice from learning/encoding the location of their nests relative to the magnetic field because it prevented the magnetic compass from operating, or caused the pattern of magnetic input to differ between training and testing or to vary unpredictably [26], making directional input from the magnetic compass unreliable. In the absence of a learned response, spontaneous magnetic alignment may reflect a more fundamental response to magnetic cues that helps to integrate magnetic and non-magnetic information when the animal finds itself in novel surroundings [30]. As discussed above, previous studies have shown similar spontaneous magnetic responses in wood mice and bank voles that had no prior training and were tested in visually symmetrical circular arenas [6, 7]. It is important to emphasize, however, that we cannot rule out the possibility that re-testing mice in *Series 1*, after they had been tested in the original nest-building testing arena, may have caused mice to switch to a spontaneous magnetic response. However, this seems unlikely since subjects were not re-tested in either of the earlier nest-building studies of epigeic rodents that exhibited spontaneous magnetic alignment.

In *Series 2-4*, mice were moved to a fully shielded training room (the room used for testing in earlier mouse nest-building experiments; [12] where radio-frequency interference was below detectable levels (~ 0.05 nT from 0 to 15 MHz). The training shelves and procedures were identical to those used in *Series 1*, however, mice were tested only once in the same test building used in *Series 1*. The distributions of nests in *Series 2-4* were unimodally distributed along the trained magnetic axis with the mean vector bearing pointing either in the direction of the nest box at the dark end of the training cage (Figure 3C), or towards the light ('open') end of the cage in the direction opposite the nest box (Figure 2C, 3C). Thus, in contrast to *Series 1*, mice learned magnetic compass orientation. These findings are consistent with earlier studies showing that consistent compass orientation by epeigic rodents were only observed after screening out electromagnetic noise from both training and testing environments [12, 13].

Variation in the direction of orientation along the trained magnetic axis in *Series 2 – 4*, suggests that minor changes in the training and/or testing environment can alter the type of learned magnetic response exhibited by mice. For example, in *Series 2* when daytime temperatures and humidity in testing exceeded the upper limit established in previous experiments for mice to exhibit orientation towards the dark end of the trained magnetic axis ($<23^{\circ}\text{C}$, $<50\%$ R.H.) [12, 13], mice instead exhibited compass orientation towards the light end of the trained axis. This is consistent with mice reversing their learned response to disperse from an unsuitable nesting site, i.e., away from the nest box. Indeed, in *Series 3*, maintaining the testing room temperature and humidity within the limits established in the earlier experiments (Table 2) resulted in mice exhibiting magnetic compass orientation toward the dark end of the trained axis, i.e., toward the nest box, as shown in the earlier experiments in which mice were tested under similar environmental conditions.

Although the behavioral responses in *Series 3* are consistent with orientation toward the dark end of the learned magnetic axis occurring within a relatively narrow range of temperatures, an alternative possibility is that the difference in temperature between the training and testing environments in *Series 2* was responsible for triggering the reversal in the direction of orientation. To test this, we further increased the consistency of environmental conditions in the training and testing building by coupling the air supplies of the two buildings (*Series 4*) (Table 2). Surprisingly, mice exposed to the mixture of air from the training and testing building reversed their direction of orientation, i.e. orienting toward the light end of the trained magnetic axis (Figure 4C). Uncoupling the air systems caused the response to revert to the original direction, i.e., towards the dark end of the magnetic axis (Table 1). Although the reason for the effect of mixing the air supplies between the two buildings is by no means clear, we include these findings to: (1) show that the use of magnetic compass cues by mice appears to be quite flexible [see also 13], and (2) to provide further evidence that the success of attempts to replicate learned magnetic compass orientation by epigeic rodents depends on careful attention to a variety of environmental factors, including background levels of electromagnetic noise, environmental conditions in testing and/or training, and, possibly also, the degree of similarity or difference between cues present in training and testing environments (e.g. olfactory cues including those from other mice in training).

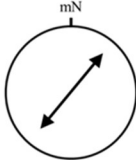
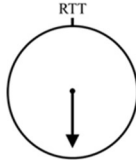
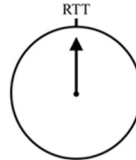
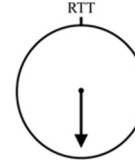
In summary, these findings show that that reliance on magnetic cues for nest positioning by laboratory mice can be influenced by a variety of factors. Moreover, the ability to study spontaneous magnetic alignment and learned magnetic compass orientation in the same behavioral assay and strain of mice should facilitate future studies to characterize the biophysical mechanism(s) that mediate these responses and will likely provide insight as to the biological significance of spontaneous magnetic alignment behaviors.

Tables:

Table 1. Nest building orientation in male C57BL6J male mice. For each *Series*, the first order statistics are provided for nest bearings pooled relative to geographic north (‘Topographic’), relative to magnetic north (‘Magnetic’), and relative to the magnetic direction of the dark end of the training cage toward the nest box (‘Relative to Trained’). In *Series 1* ‘Magnetic’ bearings were first doubled (modulo 360°) and the resulting distribution analyzed and presented in the table below [24]. All other data were analyzed as unimodal distributions.

	Series 1				Series 2				Series 3a/3b				Series 3 (a + b)				Series 4			
	n	μ	r	p	n	μ	r	p	n	μ	r	p	n	μ	r	p	n	μ	r	p
Topographic	18	104°	0.28	n.s.	13	8°	0.46	n.s.	8/23	245°/327°	0.16/0.05	n.s./n.s.	31	284°	0.06	n.s.	9	115°	0.49	n.s.
Magnetic	18	36-216°	0.72	<0.0001	13	71°	0.35	n.s.	8/23	129°/330°	0.51/0.02	n.s./n.s.	31	126°	0.12	n.s.	9	289°	0.23	n.s.
Relative to Trained	18	204°	0.14	n.s.	13	182°	0.79	< 0.0001	8/23	340°/359°	0.41/0.59	n.s./<0.0002	31	355°	0.54	<0.0001	9	169°	0.57	0.049

Table 2. Summary of training and testing conditions. Each column shows training and/or testing conditions and the type of magnetic responses elicited in each *Series*. Note that the orientation in *Series 1* is plotted relative to magnetic north ‘mN’ and the double-headed arrow represents the bimodal distribution along the ~northeast-southwest magnetic axis. All other distributions are plotted as unimodal distributions relative to trained (‘RTT’) direction corresponding to the dark end of the training cage containing the nest box.

	Series 1	Series 2	Series 3	Series 4
Mice-RE-tested	Yes	No	No	No
Exposure to RF Noise in Training	Yes	No	No	No
Testing Room Environmental Conditions Continuously Controlled	No	No	Yes	Yes
Training and Testing Building Air Supply Mixed	No	No	No	Yes
Nest Building Orientation				

Figures:

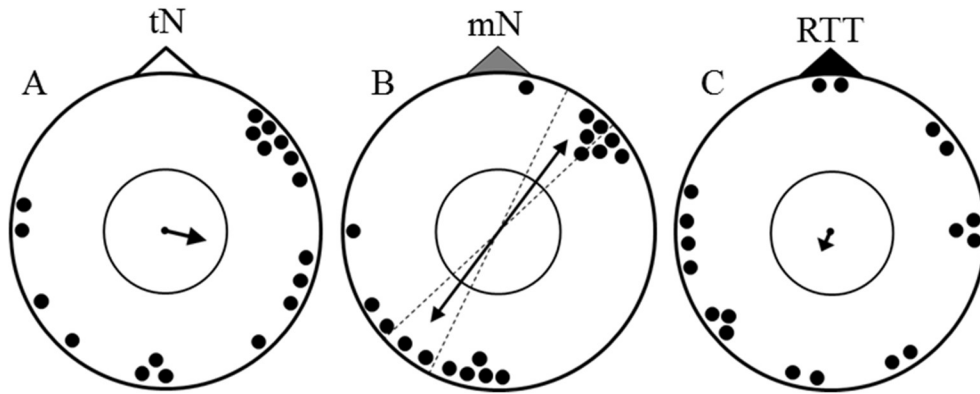


Figure 1. *Series 1* (A) Topographic bearings (tN), (B) magnetic bearings (mN), and (C) bearings relative to the dark end of the trained magnetic axis (RTT). Black arrows show mean vectors calculated by vector addition where the length of the arrow is proportional to the strength of response (circle radius = 1). Inner circle shows the 0.05 significance level for mean vector length calculated by the Rayleigh's test. Distributions that are significant at the $p = 0.05$ significance level include 95% confidence intervals (dashed black lines). White triangle labeled tN = topographic north. Grey triangle labeled mN = magnetic north, black triangle labeled RTT = magnetic of dark end of trained magnetic axis.

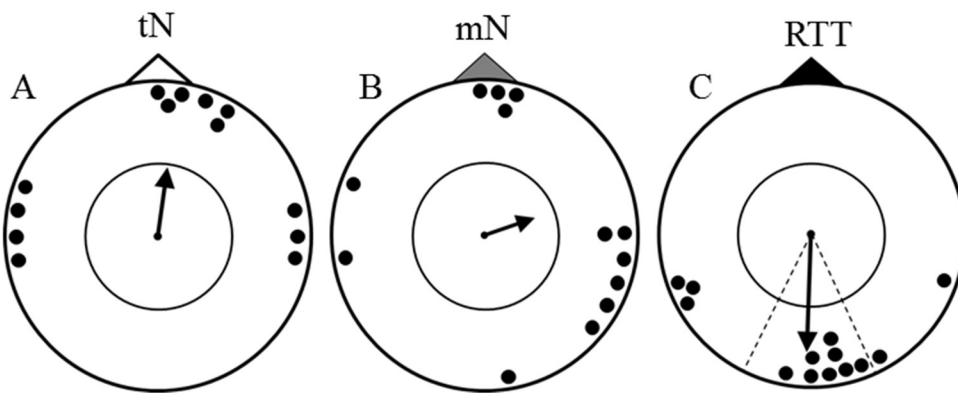


Figure 2. *Series 2*. All symbols are the same as in Figure 1.

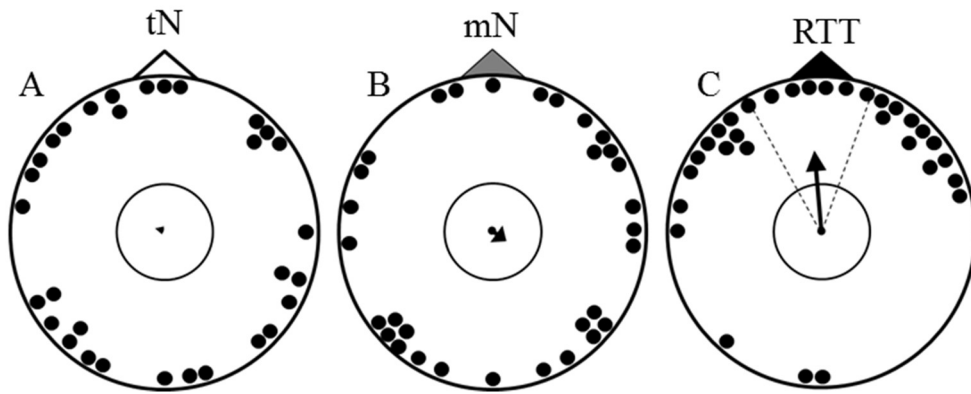


Figure 3. *Series 3*. All symbols are identical to those described in Figure 1.

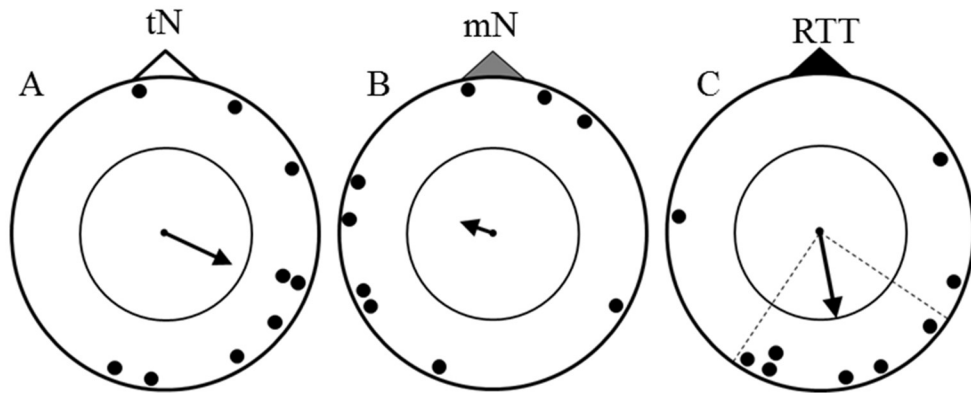


Figure 4. *Series 4*. All symbols are identical to those described in Figure 1.

Literature Cited

1. Wiltschko, W. and R. Wiltschko, *Magnetic orientation and magnetoreception in birds and other animals*. Journal of Comparative Physiology A: Neuroethology, Sensory, Neural, and Behavioral Physiology, 2005. **191**(8): p. 675-93.
2. Burda, H., et al., *Magnetic compass orientation in the subterranean rodent *Cryptomys hottentotus* (Bathyergidae)*. Cellular and Molecular Life Sciences, 1990. **46**(5): p. 528-530.
3. Marhold, S., W. Wiltschko, and H. Burda, *A magnetic polarity compass for direction finding in a subterranean mammal*. Naturwissenschaften, 1997. **84**(9): p. 421-423.
4. Thalau, P., et al., *The magnetic compass mechanisms of birds and rodents are based on different physical principles*. Journal of The Royal Society Interface, 2006. **3**(9): p. 583-587.
5. Oliveriusová, L., et al., *Magnetic compass orientation in two strictly subterranean rodents: learned or species-specific innate directional preference?* Journal of Experimental Biology, 2012. **215**(20): p. 3649-3654.
6. Malkemper, E.P., et al., *Magnetoreception in the wood mouse (*Apodemus sylvaticus*): influence of weak frequency-modulated radio frequency fields*. Sci. Rep., 2015. **4**.
7. Oliveriusová, L., et al., *Spontaneous expression of magnetic compass orientation in an epigeic rodent: the bank vole, *Clethrionomys glareolus**. Naturwissenschaften, 2014. **101**(7): p. 557-563.
8. Begall, S., et al., *Magnetic alignment in grazing and resting cattle and deer*. Proceedings of the National Academy of Sciences, 2008. **105**(36): p. 13451-13455.
9. Begall, S., et al., *Magnetic alignment in mammals and other animals*. Mammalian Biology, 2013. **78**: p. 10-20.
10. Červený, J., et al., *Magnetic alignment in warthogs *Phacochoerus africanus* and wild boars *Sus scrofa**. Mammal Review, 2017. **47**(1): p. 1-5.
11. Červený, J., et al., *Directional preference may enhance hunting accuracy in foraging foxes*. Biology Letters, 2011. **7**(3): p. 355-357.
12. Muheim, R., et al., *Magnetic compass orientation in C57BL/6J mice*. Learning & Behavior, 2006. **34**(4): p. 366-373.
13. Phillips, J.B., et al., *Rapid Learning of Magnetic Compass Direction by C57BL/6 Mice in a 4-Armed 'Plus' Water Maze*. PLOS ONE, 2013. **8**(8): p. e73112.
14. Kirschvink, J.L., M.M. Walker, and C.E. Diebel, *Magnetite-based magnetoreception*. Current opinion in neurobiology, 2001. **11**(4): p. 462-467.
15. Winklhofer, M. and J.L. Kirschvink, *A quantitative assessment of torque-transducer models for magnetoreception*. Journal of the Royal Society Interface, 2010. **7**(Suppl 2): p. S273-S289.
16. Kimchi, T. and J. Terkel, *Magnetic compass orientation in the blind mole rat *Spalax ehrenbergi**. Journal of Experimental Biology, 2001. **204**(Pt 4): p. 751-8.
17. Ritz, T., S. Adem, and K. Schulten, *A model for photoreceptor-based magnetoreception in birds*. Biophysical Journal, 2000. **78**(2): p. 707-718.
18. Schulten, K., C.E. Swenberg, and A. Weller, *A biomagnetic sensory mechanism based on magnetic field modulated coherent electron spin motion*. Zeitschrift für Physikalische Chemie, 1978. **111**: p. 1-5.
19. Ritz, T., et al., *Resonance effects indicate a radical-pair mechanism for avian magnetic compass*. Nature, 2004. **429**(6988): p. 177-180.
20. Ritz, T., et al., *Magnetic compass of birds is based on a molecule with optimal directional sensitivity*. Biophysical Journal, 2009. **96**: p. 3451 - 3457.
21. Thalau, P., et al., *Magnetic compass orientation of migratory birds in the presence of a 1.315 MHz oscillating field*. Naturwissenschaften, 2005. **92**: p. 86 - 90.

22. Wiltschko, R., et al., *Orientation of migratory birds under ultraviolet light*. Journal of Comparative Physiology A, 2014: p. 1-9.
23. Painter, M.S., et al., *Spontaneous magnetic orientation in larval Drosophila shares properties with learned magnetic compass responses in adult flies and mice*. Journal of Experimental Biology, 2013. **216**: p. 1307-1316.
24. Batschelet, E., *Circular statistics in biology*. 1981, New York: Academic Press.
25. Engels, S., et al., *Anthropogenic electromagnetic noise disrupts magnetic compass orientation in a migratory bird*. Nature, 2014. **509**: p. 353-356.
26. Landler, L., et al., *Spontaneous magnetic alignment by yearling snapping turtles: rapid association of radio frequency dependent pattern of magnetic input with novel surroundings*. PLOS ONE, 2015. **10**(5): p. e0124728.
27. Schwarze, S., et al., *Weak broadband electromagnetic fields are more disruptive to magnetic compass orientation in a night-migratory songbird (Erithacus rubecula) than strong narrow-band fields*. Frontiers in behavioral neuroscience, 2016. **10**.
28. Phillips, J.B., et al., *'Fixed-axis' magnetic orientation by an amphibian: non-shoreward-directed compass orientation, misdirected homing or positioning a magnetite-based map detector in a consistent alignment relative to the magnetic field?* Journal of Experimental Biology, 2002. **205**: p. 3903-3914.
29. Collett, T.S. and J. Baron, *Biological compasses and the coordinate frame of landmark memories in honeybees*. Nature, 1994. **368**(6467): p. 137-140.
30. Phillips, J.B., R. Muheim, and P.E. Jorge, *A behavioral perspective on the biophysics of the light-dependent magnetic compass: a link between directional and spatial perception?* Journal of Experimental Biology, 2010. **213**(19): p. 3247-3255.
31. Malkemper, E.P., M.S. Painter, and L. Landler, *Shifted magnetic alignment in vertebrates: Evidence for neural lateralization?* Journal of theoretical biology, 2016. **399**: p. 141-147.

Chapter V. Conclusions

Findings from the previous Chapters provide evidence for the involvement of magnetic cues in various forms of spatial behavior spanning diverse taxonomic groups. We show 1) that spontaneous quadramodal alignment in a model organism, *Drosophila melanogaster* 2nd instar larvae, is mediated by magnetic cues, 2) that the development of bio-logging techniques to further characterize spontaneous magnetic alignment responses in mousing red foxes provides a novel approach that will make it possible to collect behavioral and magnetic alignment data in free-living animals without direct observation, and 3) evidence for plasticity in the magnetic nest building responses in another model organism, C57BL/6J laboratory mice. We argue that the responses in larval *Drosophila*, red foxes, and some forms of nest building orientation in laboratory mice are consistent with a light-dependent magnetic mechanism where the response/sensitivity of specialized photopigments is influenced by the alignment of the magnetic field. Input from a light-dependent photoreceptor-based mechanism is thought to provide more than ‘simple’ directional information, and may provide an omnipresent coordinate system or reference frame that is fixed in alignment with respect to magnetic north that plays a more fundamental role in organizing spatial behavior [1]. These possibilities are consistent with the variety and complexity of magnetic responses reported here, as well as in previous studies of magnetic orientation [2-11]. Of course, the next step is to obtain direct evidence for the involvement of a light-dependent mechanism, or an alternative (e.g. magnetite-based) mechanism, and the assays discussed in Chapters II-IV are well-suited to further characterize the functional properties underlying magnetic sensitivity in vertebrate and invertebrate groups.

We provide evidence that magnetic cues mediate spontaneous quadramodal orientation from three strains of wild-type 2nd instar *Drosophila melanogaster* larvae. These findings were confirmed in a double-blind experiment where the horizontal component of the magnetic field could be cancelled, resulting in a distribution of responses indistinguishable from random.

Although direct evidence that a light-dependent mechanism underlies spontaneous magnetic orientation in larval *Drosophila* is lacking, a previous study of adult *Drosophila* shows that magnetic compass responses are indeed, light-dependent [12]. Adult flies trained under UV (365 nm) light to one of four cardinal compass directions exhibited learned magnetic compass responses when tested under UV light. However, when tested under long-wavelength (500 nm) of equal quantal flux, flies exhibited a 90° clockwise shift in compass orientation, providing the first evidence to date showing light-dependent magnetic orientation in an invertebrate. These findings make the possibility of a light-dependent mechanism mediating spontaneous magnetic alignment in *Drosophila* larvae all the more compelling.

We also provide additional support for the involvement of a light-dependent mechanism in larval spontaneous quadramodal orientation by performing a reanalysis of an earlier study showing learned magnetic compass orientation in adult *Drosophila* and the C57BL/6 strain of laboratory mice [12, 13]. Orientation from mice and flies trained along the north-south axis resulted in a unimodal distribution of bearings clustered in the expected (i.e., north or south) magnetic direction. In contrast, mice and flies trained along the east-west axis, exhibited a split around the trained direction, resulting in distributions clustered at $\pm 45^\circ$ of east (i.e., magnetic 45° and 135°) and west (i.e., magnetic 225°-315°), similar to the spontaneous magnetic quadramodal responses exhibited by larval flies. These responses are consistent with theoretical models of magnetic input from a light-dependent mechanism that exhibit a complex, axially symmetrical pattern of response. Not

only might these responses reflect the pattern of magnetic input underlying trained compass responses, but also may reflect the same pattern that underlies the quadramodal orientation exhibited in invertebrates aligned along the cardinal (adult) or anti-cardinal (larvae) magnetic axes [11, 14]. The difference in alignment preferences between adult and larval insects may parallel developmental changes in phototaxis when responding to a light-dependent mechanism. For example, if the magnetic field alters the response of photoreceptors, resulting in a quadramodal pattern of increased and decreased brightness, adult flies (positively phototactic) may orient to brighter components of the pattern, while larval flies (negatively phototactic) may orient to darker component of the pattern. More generally, such a visual pattern superimposed on the visual field and fixed in alignment with respect to magnetic north, may not only provide a stable compass reference, but also a reference frame or coordinate system with which to structure more fundamental forms of spatial behavior [1].

Additional support for the magnetic field's role in structuring multiple forms of spatial behavior comes from Chapter IV involving laboratory mice. In a nest building assay modified from Muheim et al., 2006 [13], small changes in the training and testing protocols caused mice to switch from spontaneous magnetic alignment to learned magnetic compass orientation. Briefly, mice exhibited magnetic orientation along a fixed north-northeast – south-south-southwest magnetic axis, independent of the trained directions, when held in training cages exposed to intermittent radio-frequency (RF) noise bursts produced from nearby laboratory equipment. The north-northeast – south-southwest alignment of this response is consistent with spontaneous magnetic alignment responses published for a variety of mammals, including two nest building assays involving wood mice and bank voles. Importantly, when training was relocated to a shielded enclosure that screened out all sources of RF interference, learned magnetic compass

orientation emerged. These findings suggest that intermittent bursts of RF noise in training prevented the mice from learning/encoding the location of their nests relative to the magnetic field, either because it prevented the magnetic compass from operating, or because it caused the pattern of magnetic input to vary unpredictably, making directional input from the magnetic compass unreliable. This is consistent with earlier studies of magnetic compass orientation in mice that required electromagnetic shielding of both the training and testing enclosures to establish learned magnetic compass responses, supporting involvement of a radical-pair mechanism underlying light-dependent magnetic compass orientation. Spontaneous magnetic alignment in mice and other mammals may help to simplify the use of magnetic and non-magnetic information when the animal finds itself in novel surroundings [1]. Other possibilities for the functional relevance of spontaneous magnetic alignment include 1) increasing the accuracy of magnetic measurements used to derive geographic position (i.e., magnetic map information) [15, 16], (2) simplifying the encoding and recognition of landmarks by standardizing the viewing angle [17], (3) helping to encode spatial relationships among local landmarks [1, 3], and (4) helping to place multiple local maps of space into register [1, 3].

In subsequent nest building experiments, mice trained and tested in electromagnetically shielded enclosures exhibited learned magnetic compass orientation, however the type of response was affected by seemingly minor changes in environmental conditions. For example, when mice were exposed to temperatures in the testing enclosure that exceeded those established in a previous nest building assay, mice exhibited magnetic compass orientation in the direction corresponding to the light end of the trained axis, i.e., away from the nest box refuge. This reversal of the learned magnetic orientation may reflect responses consistent with dispersal from unstable and/or unsuitable environmental conditions. In contrast, when temperatures were maintained within

ranges established *a priori*, mice oriented toward the dark end of the trained magnetic axis, i.e., towards the nest box refuge. These findings indicate that learned magnetic compass orientation in mice may be context-dependent. More generally, these findings show that the magnetic sense in mice is more flexible than previously demonstrated and that the spontaneous magnetic alignment and learned magnetic compass responses can be expressed in the same species. Determining the factors which elicit different types of magnetic behavior is likely to shed light on the functional significance of spontaneous magnetic alignment responses in mammals, which to date, remains poorly understood.

Another example of spontaneous magnetic alignment that highlights the utility of magnetic cues underlying various forms of spatial behavior comes from alignment responses of ‘mousing’ red foxes. Visual observations of mousing red foxes, in which a fox is attracted to the sounds produced by small rodents, and then performs an arching leap to land on the prey from above (‘mousing’), showed a strong tendency for mousing attacks to be directed towards magnetic north-northeast [4]. Interestingly, when attacks were performed in habitats with high vegetation and/or snow cover that prevented the use of visual cues to help guide prey capture, there was a 4- fold increase in successful attacks when the fox was facing north-northeast in comparison to mousing attempts in other directions. The authors propose that the magnetic field could serve as a ‘targeting system’ used to estimate distance from the location of hidden prey. A light- dependent mechanism that produces a visual pattern superimposed on the animal’s surroundings that is fixed in alignment with respect to magnetic north, could provide the basis for a targeting system to increase the success of mousing attacks when the fox is positioned in a particular magnetic alignment (i.e., aligns such that components of the visual pattern are superimposed on the location of the prey providing a visual ‘target’).

However, as with the majority of observational studies providing evidence for spontaneous magnetic alignment in mammals, direct evidence for magnetic cues mediating the behavior is lacking and experimental manipulations to 1) confirm the involvement of magnetic cues, and 2) characterize the sensory mechanisms mediating spontaneous magnetic alignment are difficult to implement in free-roaming animals. In Chapter III, we describe the development of a new approach for studying magnetic alignment in red foxes that can be adapted for a variety of terrestrial mammals. Bio-loggers attached to semi-domesticated red foxes were used to create ‘magnetic ethograms’ in which the behavior and magnetic alignment of foxes can be extracted from raw sensor data. The advantages of these techniques are manifold and include 1) identifying the behavior and alignment of an animal without direct observation, 2) recording behavioral and alignment data continuously in habitats or during times when visual observations are not possible, 3) greatly reducing the time and effort typically associated with observational studies, 4) eliminating potential biases in field-based measurements or descriptions of behavior by human observers necessarily located at some distance from the animal, and 5) ease of coupling bio-loggers with additional sensors/technologies to perform experimental manipulations in free-roaming animals.

‘Magnetic ethograms’ were constructed from data collected from two semi-domesticated red foxes fitted with harnesses equipped with tri-axial accelerometer and magnetometer bio-loggers. The foxes were trained to exhibit three distinct behaviors (i.e., trotting, foraging, and mousing-like leaps). Raw acceleration signatures were then used to train the behavioral classifier. A similar approach using raw magnetometer data extracted from the fox in known magnetic directions were used to create a magnetic classifier that could distinguish between eight (i.e. N, NE, E, SE, S, SW, W, NW) magnetic alignments. Accelerometer and magnetometer data were time-synched so

that the magnetic alignment of behaviors identified by the classifier could be determined. Across all three behaviors, the behavioral classifier performed with an accuracy of 95.7% when predicting unseen and independent behavioral events not used to train the classifier. Overall performance dropped to 66.7% when tested against unseen data from a second individual not used to train the classifier. Although there was a sharp drop in accuracy, the classifier performed well above chance levels (33%), and the small sample size of total number of behaviors recorded from the second fox, different bio-logger mounting schemes, and the differences in the kinematics of behaviors between the two foxes certainly reduce performance. These issues can be overcome by training classifiers from large numbers of observations collected from multiple individuals, and standardizing the mounting schemes for each bio-logger. Nevertheless, these preliminary findings demonstrate the generalizability of the classifier across multiple subjects. Two magnetic classifiers with different underlying assumptions performed with 90.0% and 74.2% accuracy, suggesting a realistic performance range somewhere between these two values and far outstrips the accuracy of a chance classifier, which would perform at 12.5% on this problem. Furthermore, of the errors in each classifier, only seven (1.8%) and six (10%) were ‘off-by-more-than-one’ (i.e. when the predicted heading was not classified as the sector immediately adjacent to the ground-truth heading), and therefore, each classifier predicted either the correct heading or one of the headings adjacent to the true heading in 98.2% and 90.0% of all cases. Given the performance of the behavioral and magnetic classifiers, and the potential to combine these techniques with additional technologies offers a powerful new approach for studying spontaneous magnetic alignment in mousing foxes and other free-roaming mammals.

For example, we have developed radio-frequency emitting collars sized to fit around a fox’s neck and tuned to broadcast in the low-MHz range that have been shown to disrupt the magnetic

orientation in a range of animals [18-23]. Integrating the radio-frequency collar with the bio-logging device will provide a powerful opportunity to test for the involvement of a light-dependent radical-pair mechanism underlying magnetic alignment responses of mousing red foxes under otherwise natural conditions that can be conducted following double-blind protocols. Importantly, this system can provide further support for, or against, the impact of anthropogenic radio-frequency exposure on wild life.

In summary, the findings discussed in the previous Chapters show that magnetic cues mediate a variety of behaviors across diverse taxonomic groups and that input from a light-dependent magnetoreception mechanism may provide more than ‘simple’ directional (‘compass’) information. The complex pattern(s) of magnetic input based on theoretical modeling is consistent with the complexity of some forms of magnetic responses (e.g. quadramodal orientation, splitting in trained response), and therefore, the magnetic field has been proposed to play a more general role in organizing and structuring spatial behavior and cognition. Future experiments using both the *Drosophila* and inbred mouse nest building assays are well-suited to characterize the functional properties of learned and spontaneous magnetic orientation in invertebrates and mammals, and further development on bio-logging technologies will provide new opportunities to study magnetic orientation in free-roaming animals.

Literature Cited

1. Phillips, J.B., R. Muheim, and P.E. Jorge, *A behavioral perspective on the biophysics of the light-dependent magnetic compass: a link between directional and spatial perception?* Journal of Experimental Biology, 2010. **213**(19): p. 3247-3255.
2. Malkemper, E.P., M.S. Painter, and L. Landler, *Shifted magnetic alignment in vertebrates: Evidence for neural lateralization?* Journal of theoretical biology, 2016. **399**: p. 141-147.
3. Begall, S., et al., *Magnetic alignment in grazing and resting cattle and deer.* Proceedings of the National Academy of Sciences, 2008. **105**(36): p. 13451-13455.
4. Červený, J., et al., *Directional preference may enhance hunting accuracy in foraging foxes.* Biology Letters, 2011. **7**(3): p. 355-357.
5. Hart, V., et al., *Magnetic alignment in carps: evidence from the Czech christmas fish market.* PLoS ONE, 2012. **7**(12): p. e51100.
6. Begall, S., et al., *Magnetic alignment in mammals and other animals.* Mammalian Biology, 2013. **78**: p. 10-20.
7. Hart, V., et al., *Directional compass preference for landing in water birds.* Frontiers in Zoology, 2013. **10**(1): p. 38.
8. Obleser, P., et al., *Compass-controlled escape behavior in roe deer.* Behavioral Ecology and Sociobiology, 2016: p. 1-11.
9. Vácha, M. and H. Soukopova, *Magnetic orientation in the mealworm beetle Tenebrio and the effect of light.* J Exp Biol, 2004. **207**(Pt 7): p. 1241-8.
10. Vácha, M., T. Puzova, and D. Drstková, *Effect of light wavelength spectrum on magnetic compass orientation in Tenebrio molitor.* Journal of Comparative Physiology A: Neuroethology, Sensory, Neural, and Behavioral Physiology, 2008. **194**(10): p. 853-9.
11. Vácha, M., M. Kvicalova, and T. Puzova, *American cockroaches prefer four cardinal geomagnetic positions at rest.* Behaviour, 2010. **147**(4): p. 425-440.
12. Phillips, J.B. and O. Sayeed, *Wavelength-dependent effects of light on magnetic compass orientation in Drosophila melanogaster.* Journal of Comparative Physiology A Sensory Neural and Behavioral Physiology, 1993. **172**(3): p. 303-8.
13. Muheim, R., et al., *Magnetic compass orientation in C57BL/6J mice.* Learning & Behavior, 2006. **34**(4): p. 366-373.
14. Painter, M.S., et al., *Spontaneous magnetic orientation in larval Drosophila shares properties with learned magnetic compass responses in adult flies and mice.* Journal of Experimental Biology, 2013. **216**: p. 1307-1316.
15. Fischer, J.H., et al., *Evidence for the use of magnetic map information by an amphibian.* Animal behaviour, 2001. **62**(1): p. 1-10.
16. Phillips, J.B., et al., *'Fixed-axis' magnetic orientation by an amphibian: non-shoreward-directed compass orientation, misdirected homing or positioning a magnetite-based map detector in a consistent alignment relative to the magnetic field?* Journal of Experimental Biology, 2002. **205**: p. 3903-3914.
17. Collett, T.S. and J. Baron, *Biological compasses and the coordinate frame of landmark memories in honeybees.* Nature, 1994. **368**(6467): p. 137-140.
18. Ritz, T., et al., *Resonance effects indicate a radical-pair mechanism for avian magnetic compass.* Nature, 2004. **429**(6988): p. 177-180.
19. Thalau, P., et al., *Magnetic compass orientation of migratory birds in the presence of a 1.315 MHz oscillating field.* Naturwissenschaften, 2005. **92**: p. 86 - 90.
20. Malkemper, E.P., et al., *Magnetoreception in the wood mouse (Apodemus sylvaticus): influence of weak frequency-modulated radio frequency fields.* Sci. Rep., 2015. **4**.

21. Engels, S., et al., *Anthropogenic electromagnetic noise disrupts magnetic compass orientation in a migratory bird*. *Nature*, 2014. **509**: p. 353-356.
22. Schwarze, S., et al., *Weak broadband electromagnetic fields are more disruptive to magnetic compass orientation in a night-migratory songbird (*Erithacus rubecula*) than strong narrow-band fields*. *Frontiers in behavioral neuroscience*, 2016. **10**.
23. Vácha, M., T. Puzova, and M. Kviclova, *Radio frequency magnetic fields disrupt magnetoreception in American cockroach*. *Journal of Experimental Biology*, 2009. **212**(21): p. 3473-3477.